DESIGN AND SYNTHESIS OF PEPTIDE-BASED NANOFIBERS FOR IMAGING AND THERAPY OF CANCER

A Dissertation
Submitted to the Graduate Faculty
of the
North Dakota State University
of Agriculture and Applied Science

By

Ruchi Malik

In Partial Fulfillment
for the Degree of
DOCTOR OF PHILOSOPHY

Major Department:
Pharmaceutical Sciences

August 2012

Fargo, North Dakota

North Dakota State University
Graduate School

Title

Design and synthesis of peptide-based nanofibers for imaging and therapy of cancer

By

Ruchi Malik

The Supervisory Committee certifies that this ***disquisition*** complies with North Dakota State University's regulations and meets the accepted standards for the degree of

DOCTOR OF PHILOSOPHY

SUPERVISORY COMMITTEE:

Dr. Benedict Law
Chair

Dr. Jagdish Singh

Dr. Steven Qian

Dr. Katie Reindl

Approved:

May 6, 2013
Date

Dr. Jagdish Singh
Department Chair

ABSTRACT

Nanotechnology has been the subject of significant scientific and biomedical development efforts over the past decades. Improvement in biomarker discovery, targeting approaches and conjugation chemistries has led to the development of many novel nanomaterials for individualized therapy. In this thesis, we investigate a new class of nanomaterial called "nanofiber precursor" (NFP). The NFP is composed of multiple self-assembling peptides *via* electrostatic and non-covalent interactions. Each peptide consisted of β-sheet sequence attached to a methoxypolyethylene glycol (mPEG) *via* a linker. By conjugating either near infrared fluorophore or therapeutic antibodies, we demonstrate the application of NFP in diagnosis and therapy of cancer respectively. The main objectives of this thesis are: (1) To design and synthesize a near infrared nanofiber for imaging urokinase plasminogen activator (uPA) activity (2) To develop a Herceptin-conjugated nanofiber as multivalent targeted system for increasing therapeutic efficacy of Herceptin, a monoclonal antibody used for breast cancer treatment. We were successful in conjugating near infrared dye NIR664 to the nanofiber as well as Herceptin on the surface of nanofiber. (1) The NIR-NFP conjugate could detect recombinant uPA activity with sensitivity of 3 ng. (2) The Herceptin-conjugated nanofiber (HER-NFP) was more than two fold effective in inhibiting growth of HER-2 positive cells. In the second half of the thesis, we have also investigated tumorigenic role of 15-LOX-1, a lipid peroxidizing enzyme in prostate cancer. The aim of this study was: (3) To investigate the role of 15-lipoxygenase-1 (15-LOX-1) in upregulation of uPA in PC-3 prostate cancer cells. As a whole, the research presented in this thesis is aimed at designing new strategies and understanding molecular mechanisms that lead to prevention and treatment of cancer.

ACKNOWLEDGEMENT

I would like to begin by thanking my advisor Dr. Benedict Law for his valuable advice and guidance throughout the course of my research. I am grateful to my other committee members Dr. Jagdish Singh, Dr. Steven Qian, and Dr. Katie Reindl for their constant encouragement and support. I would like to thank the Graduate School, NDSU for awarding me a Doctoral Dissertation Fellowship. I appreciate the Department of Pharmaceutical Sciences, NDSU for providing me the funding for my research.

I would also like to thank Dr. Steven Qian for his valuable comments and discussion during weekly lab meetings. I appreciate Dr. Katie Reindl, Dr. Estelle Leclerc and Dr. Stefan Vetter for allowing me to use their labs and chemical reagents, especially for my experiments in third chapter. I am grateful to all staff members, especially Jean and Janet for their constant support and helping me with ordering daily laboratory supplies. I am pleased to thank my friends and all present and past members for being very cooperative and helpful. I would also like to thank my lab mate Anil Wagh and former labmate Vipin Saxena who have made my research worthwhile and memorable. Finally and most importantly, I owe special gratitude to my parents and sister for their love, support, and encouragement.

TABLE OF CONTENTS

LIST OF TABLES

LIST OF FIGURES

LIST OF ABBREVIATIONS

15-LOX-1……15-Lipoxygenase-1

AA…….....Arachidonic acid

ADCC……..Antibody-dependent cellular cytotoxicity

ADCs……Antibody-drug conjugates

ATCC……....American type culture collection

BCA……...Micro-bicinchoninic acid

CHF….....Congestive heart disease

COX……Cyclooxygenase

DHA……...Docosahexaenoic acid

CT……..……..X-ray computed tomography

DGLA……..Di-homo-gamma-linolenic acid

DHA……...Docosahexaenoic acid

DIEPA…….……..N,N-Diisopropylethylamine

DLGA…….….Dihomo-gama-linolenic acid

DMEM……...Dulbecco's modified eagle's medium

DMF……..Dimethylformamide

DMSO……..Dimethylsulfoxide

DNA…….. Deoxyribonucleic acid

ECD……..Extracellular domain

ECL……Enhanced chemiluminescence system

ECM…….. Extracellular matrix

EFA……Essential fatty acids

EGF…….Epidermal growth factor

EGFR……Epidermal growth factor receptor

ELISA……Enzyme-linked immunosorbent assay

EPA……Eicosapentaenoic acid

EPR…….Enhanced permeability and retention

ERK…….Extracellular signal-regulated kinase

ETA……..……Eicosatetranoic acids

FBS……..Fetal bovine serum

FDA……...US food and drug administration

FGF-2……...Fibroblast growth factor-2

FITC……Fluorescein isothiocyanate

FRET……...Fluorescence resonance energy transfer

GLA……Gamma-linolenic acid

HBSS……..Hank's balanced salt solution

HBTU…….2-(1H-benzotriazole-1-yl)-1,1,3,3,-tetramethylaminium hexafluorophosphate

HER-2……...……Human epidermal growth factor receptor type 2

HER-NFP……..Herceptin-conjugated nanofibers

HETE……..Hydroxyeicosatetraenoic acid

HOBt……..N-Hydroxybenzotriazole

HODE…….Hydroxyoctadecadienoic acid

HPETE……Hydroperoxyeicosatetraenoic acid

HPLC…….High pressure liquid chromatography

HPODE……...Hydroperoxyoctadecadienoic acid

HRP…….Horse radish peroxidase

HUVEC……Human umbilical vein endothelial cell

ICAM1……..Intercellular adhesion molecule 1

ICG……...Indocyanine green

IFN…….Interferon

IGF-1…….…….Insulin-like growth factor 1

IGF-IR…….…….Insulin-like growth factor-I receptor

IHC…….. .Immunohistochemistry

IL……..Interleukin

JNKs……c-Jun amino-terminal kinases

kDa……..Kilo Dalton

LA…….Linoleic acid

LNA……...Alpha-linolenic acid

LOX……...Lipooxygenase

LT……...Leukotriene

M……..Molar

mAb…….Monoclonal antibody

MALDI-TOF……...Matrix assisted laser desorption/ionization-time of flight

MAPK……...Mitogen-activated protein kinase

MBC…….. Metastatic breast cancer

mM……Millimolar

MMP……..Matrix metalloproteinase

mPEG……..Methoxy polyethylene glycol molecule

MRI……..Magnetic resonance imaging

mRNA……Messenger ribonucleic acid

MS……...Mass spectrometry

mTOR…….Mammalian target of rapamycin

NDGA…….Nordihydroguaiaretic acid

NF-kB……Nuclear factor kB

NFP……Nanofiber precursor

NIR……...Near-infrared

NIR-NFP……..Near infrared nanofiber

NK……Natural killer cells

nM……Nanomolar

NMP…….N-Methylpyrrolidinone

NMR…….Nuclear magnetic resonance

NP…….Nanoparticle

PAI1…….Plasminogen activator inhibitor-1

PBS…….. Phosphate buffer saline

PCR……..Polymerase chain reaction

PDGF……Platelet derived growth factor receptor

PET……Positron emission tomography

PF……...Peptide nanofiber

PG……Prostaglandin

PI3K…….. Phosphatidylinositol 3-kinase

PLA2…….Phospholipase A2

PPAR……Peroxisome proliferator-activated receptors

PSA……Prostate-specific antigen

PTEN……....Phosphatase and tensin homolog deleted on chromosome ten

PUFA……..Polyunsaturated fatty acids

RES……Reticuloendothelial system

RIA……Radioimmunoassay

RNA……Ribonucleic acid

ROS……Reactive oxygen species

rp-HPLC……...Reverse phase high performance liquid chromatography

RT-PCR……Reverse transcription polymerase chain reaction

siRNA……Small interfering RNA

SPECT……..Single photon emission computer tomography

TBS……... Tris buffer saline

TEM……Transmission electron microscopy

TFA……Trifluoroacetic acid

TGF……...Transforming growth factor

TGF-β……Transforming factor-β

TNBSA……..2,4,,6-Trinitrobenzenesulfonic acid

TNF……...Tumour necrosis factor

uPA……Urokinase plasminogen activator

UV……Ultraviolet

VEGF……Vascular endothelial growth factor

CHAPTER 1. STATEMENT OF PROBLEM AND RESEARCH OBJECTIVES

Cancer is the second most common cause of death in the US, exceeded only by heart disease, accounting for nearly 1 of every 4 deaths [1]. According to the American cancer society, about 577,190 Americans are expected to die of cancer in the year 2012. Among all strategies explored, use of nanotechnology has been proven to useful in many aspects of cancer treatment and prevention [2, 3].

Today, nanomaterial are extensively used in designing sensors [4], imaging contrast agents [5, 6], platforms for localized delivery and therapy [7, 8], and development of research tools for understanding the biology of cancer [9, 10]. The primary objective of this thesis is to investigate the potential applications of new type of peptide based nanomaterial known as "nanofiber precursor" for diagnosis and treatment of cancer [11-13]. This thesis is divided into three chapters, in which the first two chapters are focused on the application of peptide nanofiber precursor (NFP) for either imaging or therapy via conjugation of near infrared fluorophore and, therapeutic antibodies respectively. The third chapter focuses on a different study in which we discuss a new role of a lipid oxidizing enzyme 15-lipoxygenase-1 (15-LOX-1) in tumorigenesis of prostate cancer mediated by upregulation of uPA. The detailed description of individual chapters is discussed below:

In the first chapter, we discuss the application of nanofiber for imaging urokinase plasminogen activator (uPA) [8]. uPA is a clinically validated biomarker for predicting patient prognosis as it is found to be overexpressed in various cancers [14] including breast [15], prostate [16], renal [17], ovarian [18], cervical [19], pancreatic [20], glioma [21], colorectal [22], and gastric cancers [23]. Since a majority of cancer deaths are due to metastasis, determining level of uPA in tumors is important for predicting metastatic potential of the tumor and helps us

in identifying the subset of patients requiring chemotherapy [15, 24, 25]. Unfortunately, the currently available methods such as ELISA and IHC for determining uPA level in tumors rely on biopsy or surgical invasion [26-29]. Therefore, there are efforts needed towards in vivo protease imaging which will be convenient for patients as they do not have to undergo invasive surgeries. Moreover, current technologies rely only on determining levels of uPA, instead of activities. My work is extension of previously designed a peptide-based, self-assembly nanofiber precursor (NFP) for detecting uPA activity [12, 13]. In the previously described NFP, FITC was employed as an optical reporter [30]. However, the fluorescence emission in the visible wavelength (at 485 nm) limits its use for in vivo imaging [31]. In order make NFP applicable for in vivo imaging, an important feature would be to utilize a near infrared fluorophore in the construction of this probe. Near infrared dyes provide better contrast as they fluoresce in region where there is no interference from biological tissues [32, 33]. To this end, the first chapter in this thesis is focused on the design and synthesis of near infrared nanofiber (NIR-NFP) for imaging uPA. We believe that results obtained from this study will help in designing biomarker based strategies and ultimately be beneficial in prognosis, prediction, screening of disease, and monitoring therapy in patients.

In chapter 1, we proposed the following hypotheses:

1. A near infrared nanofiber (NIR-NFP) can be successfully designed and synthesized.
2. The NIR-NFP will have nanoscale dimensions and its fluorescence intensity will be quenched due to close placement of near infrared dyes on its structure.
3. Due to the presence of methoxy polyethylene glycol molecules (mPEG), the nanofiber will be homogeneous preparation.

4. Upon incubation of recombinant uPA activity in vitro, the nanofiber will increase near infrared fluorescence signal. The increase in fluorescence signal will be accompanied by conversion of nanofiber into interfibril network.
5. The nanofiber can detect uPA secreted from cancer cells. The increase in fluorescence signal will correlate to level of uPA level in the cell lines, which can be further confirmed using commercial uPA activity assay kit.

The proposed hypotheses were tested by designing the following specific aims:

- To design, synthesize and perform in vitro characterization of NIR-NFP. In order to achieve this, the previously reported peptide construct (mPEG-BK(FITC)-SGRSANA-$[kldl]_3$) will be modified by replacing the FITC with a near infrared fluorophore (NIR664).
- To characterize the NIR-NFP by UV spectroscopy, fluorescence spectroscopy and transmission electron microscopy (TEM).
- To investigate whether NIR-NFP can detect cell-secreted uPA and, whether NFP is able to differentiate cancer cell lines based on different expression of uPA.

This study is intended to answer the following questions:

1. Can NIR-NFP detect recombinant and cell-secreted uPA? If so, is it sensitive enough to detect clinically relevant levels of uPA?
2. Does the increase in fluorescence intensities correlate with structural changes in nanofiber?

In chapter II, we discuss the application of nanofiber for increasing the therapeutic efficacy of Herceptin, a monoclonal antibody used in the treatment of breast cancer [34]. Monoclonal antibodies have entered an era in which they are increasingly becoming the

treatment of choice for cancer because of advantages such as less side-effects and higher specificity as compared to chemotherapeutic drugs [35, 36]. However, their clinical response rate is modest and development of resistance occurs in some cases [37-40]. Therefore, new formats of antibodies with modified properties have been generated to improve the therapeutic efficacy of monoclonal antibodies [41]. Among all strategies investigated, multivalency approach has provided meaningful improvements in clinical activity over unconjugated antibodies [42, 43]. "Multivalency" means essentially means a state of having valency of more than two. Multivalent antibodies are known to have higher functional affinity [44], lower dissociation rates when bound to cell-surface antigens, and enhanced biodistribution and pharmacokinetic profiles [45]. In the present study, we employed a previously described nanofiber precursor (NFP) [12, 13] as a multivalent platform to improve the cytotoxicity of a monoclonal antibody against epidermal growth factor receptor 2 (HER-2), a receptor that is overexpressed in 20 to 30% of breast cancer patients [46-48]. NFP was a two-dimensional monolayer assembled from multiple self-assembling peptides via electrostatic and non-covalent interactions [49, 50].

In chapter two, we proposed the following hypotheses:

1. Herceptin-conjugated NFP (HER-NFP) will be more effective in inhibiting cell growth as compared to Herceptin alone.
2. The mechanism of cell growth inhibition will be accompanied by downregulation of signal transduction pathway associated with HER-2 receptor.

The proposed hypotheses were tested by designing the following specific aims:

- Design and synthesis of Herceptin-conjugated nanofibers (HER-NFP). Each peptide will consist of β-sheet sequence (kldlkldlkldl, where k, l, and d were in D-configurations)

attached to a methoxypolyethylene glycol (mPEG) via a linker (SGASNRA) to prevent aggregation.

- To perform covalent conjugation of Herceptin antibodies on the surface of nanofibers by sodium periodate method [51]. Multiple antibodies against HER-2 (Herceptin) will be conjugated to the NFP surface at the surface -NH_2 functional groups contributed by the side chains of the lysine residues.
- To characterize the HER-NFP loading by UV spectroscopy, electrophoreses and transmission electron microscopy (TEM).
- To investigate the influence of different loading density of Herceptin on rate and intensity of cellular uptake of HER-NFP in HER-2 overexpressing SKBr-3 cells
- To determine specificity of HER-NFP in cancer cells exhibiting different levels of HER-2 receptor.
- To investigate the mechanism involved in increasing the therapeutic efficacy of Herceptin by activation status of proteins of cell survival pathways, mainly phosphatidylinositol 3-kinase (PI3K) and mitogen activated protein kinase (MAPK) pathways.

This study was intended to answer the following questions:

1. Is HER-NFP is more efficacious in inhibiting cell growth as compared to Herceptin alone in HER-2 overexpressing cancer cells?
2. Will there be changes in cellular uptake, cellular distribution and HER-2 receptor signaling when multiple Herceptin antibodies are conjugated to nanofiber? If so, how will it compare to unconjugated Herceptin?

In the third chapter, we are investigated the role of a lipid-peroxidizing enzyme, 15-lipoxygenase-1 (15-LOX-1), in the expression of urokinase plasminogen activator (uPA) in prostate cancer. It is known that metastases mediated by proteases are one of the main causes of death due to prostate cancer [52, 53]. Several epidemiologic studies have revealed that there may be association between dietary lipids and progression of prostate cancer [54-58]. However, there is no published data on the relationship between lipid metabolism and metastatic progression mediated by proteases among prostate cancer patients. Among the large families of lipid peroxidising enzymes, 15-LOX-1 is particularly interesting enzyme, which has been implicated to have a strong tumorigenic role in prostate cancer [59-62]. In this study, our aim was to study the relationship between 15-LOX-1 and urokinase plasminogen activator, a validated marker for metastasis [63, 64]. We believe that this study is important because it provides understanding how diet control may prevent onset for metastatic progression of cancer.

In chapter three, we proposed the following hypotheses:

1. 15-LOX-1 in PC-3 prostate cancer cells is involved in the upregulation of uPA level. Normal prostate cancer cells (PC-3 cells) transfected with 15-LOX-1 (15-LOX-1/PC-3 cells) will lead to upregulation of uPA as compared to their parental controls. On the other hand, knockdown of 15-LOX-1 using siRNA transfection in 15-LOX-1/PC-3 cells may lead to downregulation of uPA.
2. 15-LOX-1/PC-3 cells will demonstrate enhanced migratory potential and wound healing ability as compared to parental PC-3 cells.
3. 15-LOX-1/PC-3 cells will demonstate higher levels of activated forms of members of MAPK family as compared to PC-3 cells. Since MAPK pathway is central mechanism that regulates the level of uPA, we hypothesize that it may serve as an intermediatory

pathway involved in the signaling between 15-LOX-1 and uPA. We also hypothesize that incubation with specific inhibitors of MAPK subfamilies will decrease the levels of uPA in both PC-3 cells and 15-LOX-1/PC-3 cells.

The proposed hypotheses were tested by designing the following specific aims:

- To investigate whether overexpression of 15-LOX-1 may lead to upregulation of uPA in PC-3 cells
- To investigate whether mitogen-activated protein kinase (MAPK) pathway is involved in the upregulation of uPA in 15-LOX-1/PC-3 cells.
- To investigate whether increases migratory ability and wound healing ability of 15-LOX-1/PC-3 cells

This study is intended to answer the following questions:

1. Does there any relationship exist between 15-LOX-1 and uPA in prostate cancer?
2. Can induction of 15-LOX-1 in prostate cancer cells lead to enhanced migration and wound healing ability?

CHAPTER 2. DESIGN AND SYNTHESIS OF A NEAR-INFRARED FLUORESCENT NANOFIBER PRECURSOR FOR IMAGING UROKINASE ACTIVITY

2.1. Abstract

Abnormal proteolysis is often observed during disease progression. Up-regulation of certain tumor-associated proteases such as urokinase plasminogen activator (uPA) can be a biomarker of malignant transformation. In this chapter, we report the design and synthesis of a near infrared (NIR) nanofiber precursor (NIR-NFP) for detection of uPA activity. NIR-NFP, which is optically silent in its native state, is composed of multiple self-assembled peptide units (PEG_{54}-BK(*NIR664*)SGRSANA-kldlkldlkldl-$CONH_2$). Upon uPA activation, NIR-NFP releases peptide fragments that contribute to significant fluorescence amplifications at 684 nm. The NIR-NFP was able to detect uPA activity in culture media obtained from uPA-overexpressing cancer cell lines (SKOV-3, MCF-7, MDA-MB-231, PANC-1, PC-3, and HT-1080). Fluorescence changes were uPA dependent, and the results were as comparable with both western blot analysis and enzyme activity assay. Our data suggests that the optimized NIR-NFP preparation may be useful for imaging uPA activity in vivo.

2.2. Introduction

2.2.1. Biomarkers for cancer

Biomarkers are increasingly becoming important tools for understanding a wide range of diseases through randomized clinical trials, epidemiology studies, screening, diagnosis and prognosis [65-67]. In cancer research, there is ongoing research to identify new biomarkers that can be used for early screening and/or detection, designing personalized therapies, and understanding mechanisms that are involved in the progression of disease [68, 69]. Examples of some clinically relevant biomarkers are summarized in Table 1.

Table 1. Examples of clinically relevant biomarkers.

Biomarker	Cancer	Reference
Alpha-foetoprotein	Hepatocellular carcinoma	[70]
APC gene	Adenocarcinoma	[71]
HER-2/neu gene	Breast cancer	[72]
Prostate specific antigen (PSA)	Prostate cancer	[73]
Urokinase plasminogen activator (uPA)	Breast cancer	[15]
S100 protein	Melanoma	[74]
CA-125	Ovarian cancer	[75]
Heat shock proteins (Hsp27& Hsp27)	Prostate cancer	[76]
Human chorionic gonadotrophin (hCG)	Ovarian cancer	[77]

Biomarkers can be constituents of tissues or body fluids, and their levels detected help clinicians in discriminating disease condition versus normal condition [78]. For example, urokinase plasminogen activator (uPA), a serine protease and its inhibitor PAI1 are validated diagnostic and prognostic biomarkers for breast cancer [79]. Likewise, another serine protease PSA (prostate-specific antigen), has been the major diagnostic marker for prostate cancer [80]. The levels of these biomarkers are normally found to be low in their serum, however become increased in cancer conditions. By determining the exact level of biomarker, clinicians are able to select optimal adjuvant treatment for therapy on the basis of the nature and stage of disease. Biomarkers are identified from epidemiological investigation [81, 82]. Advancement in genomics and proteomic technologies allows large number of survival pathways to be screened simultaneously. For example, simultaneous analyses of genes can be achieved by microarray- or sequencing-based technologies in same sample set [83]. Likewise, different protein expressions in the sample set can be analyzed by MALDI-MS maintenance [84]. Such information is useful

for understanding of complex mechanisms that play important role in cancer development [85, 86]. The successful discovery and validation of biomarkers also depends on factors such as data handling, sample processing, statistical analysis, and therefore is a colloaborative effort which is contributed by clinicians, statisticians, scientists.

2.2.2. Proteases as biomarkers

Proteases are an important class of enzymes which regulate a variety of functions and can be classified into six groups: serine, cysteine, aspartate, glutamic acid, threonine, and metalloproteases, depending on the structure of catalytic site and presence of amino acid essential for activity [87-91]. They are vital for maintaining normal physiological processes such as cell proliferation, cell replication and apoptosis, tissue wound healing, coagulation and respond to specific stimuli. For example, proteases such as pepsin and trypsin are secreted to improve digestion in the stomach [92]. Likewise, proteases such as plasmin and thrombin play important role in blood clotting [93]. Other proteases such as cathepsins are located in the leukocytes and contribute to regulation of immune response [94]. Given their roles in various conditions, proteases have emerged as prognostic or diagnostic marker diseases such as digestion disorders, inflammatory conditions, and immunity and blood flow disorders [95]. There are several new technologies being developed to detect proteases for early screening of deseases, drug targeting, and therapeutics.

2.2.3. Existing technologies for detecting biomarkers

Various types of assays are used to measure proteins in complex biological samples [96]. Current techniques for protein biomarkers discovery and profiling include mass spectroscopy, electrophoreses, and immunological assays such as enzyme-linked immunosorbent assay (ELISA), and western blotting are described in the following sections:

2.2.3.1. Polyacrylamide gel electrophoresis

One- or two-dimensional sodium dodecyl sulfate polyacryamide gel electrophoresis (1D or 2D SDS PAGE) has been available for several decades for the quantitation and identification of proteins. This method relies on separation of proteins on the basis of isoelectric point (pI) and molecular weight [97-99], and allows different proteins in complex biological system can be resolved and compared. However, the only limitation of 2D SDS PAGE is that it cannot resolve proteins in conditions when proteins are smaller than 10 kDa or too basic [100].

2.2.3.2. Mass spectroscopy

Mass spectrometry (MS) based assays have been available for several decades for biomarker identification and characterization. The main advantages of this technique over antibody-based methods are its less cost, time-effective, and specific [101], and is therefore an attractive alternative to antibody based assay when desired antibody is not available. This method has advantage that it requires minimal sample processing and that it can analyze a large number of samples in a short time [102, 103]. However, one limitation of MS is that only small proteins can be analyzed using this method [104].

2.2.3.3. Western blot

Western blot is widely used for assessing protein levels in in serum, tissues, and organs and commonly used in laboratory practices [105]. Its main advantage is that it is relatively inexpensive procedure; however not FDA is approved methods for clinically determining biomarker levels [106]. Few limitations of western blot are its semi-quantitative nature, time-consuming and resource-intensive nature and cannot practically be undertaken for many proteins [107].

2.2.3.4. Immunohistochemistry (IHC)

Immunohistochemistry (IHC) is the method of choice for tissues, especially when a protein is the target [108]. It is FDA approved method and widely used in clinics and relatively inexpensive. It is especially advantageous when the proteins undergo posttranslational modification such as phosphorylation [109]. However, this method is semiquantitative in nature, and requires well trained pathologists to interpret grading of tumor.

2.2.3.5. Enzyme-linked immunosorbent assay (ELISA)

ELISA has been traditional method for biomarker discovery and validation, and it still considered to be a "golden standard" for detection of protein in clinical tests and multicenter prospective and randomized studies [110-112]. It is highly sensitive method for detecting proteins; however, its limitation is that sometimes desired antibodies are not available for the target under investigation.

2.2.4. Optical imaging

Various molecular techniques have been used to image proteases including magnetic resonance imaging (MRI), positron emission tomography (PET), and single photon emission computer tomography (SPECT) [113-117]. Imaging of proteases is becoming an important strategy for developing new anti-cancer therapies [118-120]. Proteases play crucial roles in the progression of cancer by facilitating invasion of the extracellular matrix, cell proliferation, and angiogenesis. Therefore, imaging protease activity may be a useful tool in biomedical applications such as detection of early-stage tumors and metastases [121-123].

Majority of the probe used for optical detection of proteases rely on the change of their optical properties after protease cleavage, and thus are commonly referred as "smart probes" or "activatable probes" [124, 125]. In native stage, the probe is typically designed to be maximally

quenched by placement of fluorophore and quencher (same or another fluorophore dye) in close proximity because of fluorescence resonance energy transfer (FRET). [126-128]. Cleavage of the protease substrate separates the fluorophore and the quencher resulting in the enhancement of fluorescent signal. Therefore, "activatable probes" can be designed which have little or no optical signal in the inactive state but generate signal after interacting with molecular target [122, 129, 130]. More than a decade ago, the first in vivo optical imaging probe was developed for detecting activity of cathepsin B in in a xenograft lung carcinoma [131]. The probe consisted of multiple near-infrared fluorophores conjugated to long circulating graft copolymer consisting of poly-L-lysine and methoxypolyethylene glycol succinate. Due to their close proximity, the fluorophores were optically quenched. Following intravenous injection, the probe accumulated in tumor as a result of enhanced permeability and retention effect (EPR). In vivo imaging revealed a 12-fold increase in the NIRF signal, allowing the detection of submillimeter-sized tumors [131].

Recently, near infrared imaging has been valuable for non-invasive detection of proteases and other molecules. Biological tissues such as water, lipids, and hemoglobin, generate auto fluorescence because they absorb in the visible range (350-700 nm) [31, 132]. NIR probes offer higher sensitivity and efficiency because they absorb light in near-infrared part of the spectrum (700-1000 nm). They offer higher target to background ratio, and optical signal at depths of 7-14 cm may be achieved using NIRF probes. In small animals, a variety of NIRF dyes such as Cy5.5, indocyanine green, and Alexa dyes have been used [133-135]. Besides using dye molecules, near infrared imaging has also been performed using nanomaterial such as quantum dots; however, their potential toxicity may limit their applications in patients [136, 137].

2.2.5. Near infrared dyes for optical imaging

The synthesis of NIR dyes is gaining a great deal of attention due to their wide application in various fields such as biomedical research and material sciences [138-141]. The NIR dyes can be broadly classified according to their core structures and include phthaocyanines, cyanines, and squarine dyes [142, 143]. Several modifications are being performed in the structure of NIR dyes to improve their photochemical and photophysical properties. For example, functional groups such as sulfonate, carboxylate, and pyridinium have been conjugated to the core structure of the NIR dye to increase solubility [144, 145]. Cyanine dye fluorophore belongs to a family of dyes which contain a heterocyclic ring such as an indole, quinolone, or isoquinoline and benzooxazole as well as an unsaturated carbon chain.

The structure and positions of functional groups the heterocyclic rings and the length of the carbon chain govern the photochemical and photophysical properties of the dye [146], such as fine tuning the excitation wavelength, emission wavelength, solubility, and stability [147, 148]. For example, the color of the dye and the emission wavelength can be changed by modification of the polymethine moieties bridging the heterocyclic ring system [149]. Furthermore, these dyes can be further modified with succinimidyl esters as reactive functional groups to allow the conjugation to biologically active moieties such as antibodies, DNA, and proteins [150, 151]. Till now, the only FDA approved dye is iodocyanine green, a water soluble cyanine dye, which is clinically used in applications such as ophthalmic angiography, determination of cardiac output and liver function [152-154]. Some of the examples of the currently used near infrared dye molecules are shown in Fig. 1.

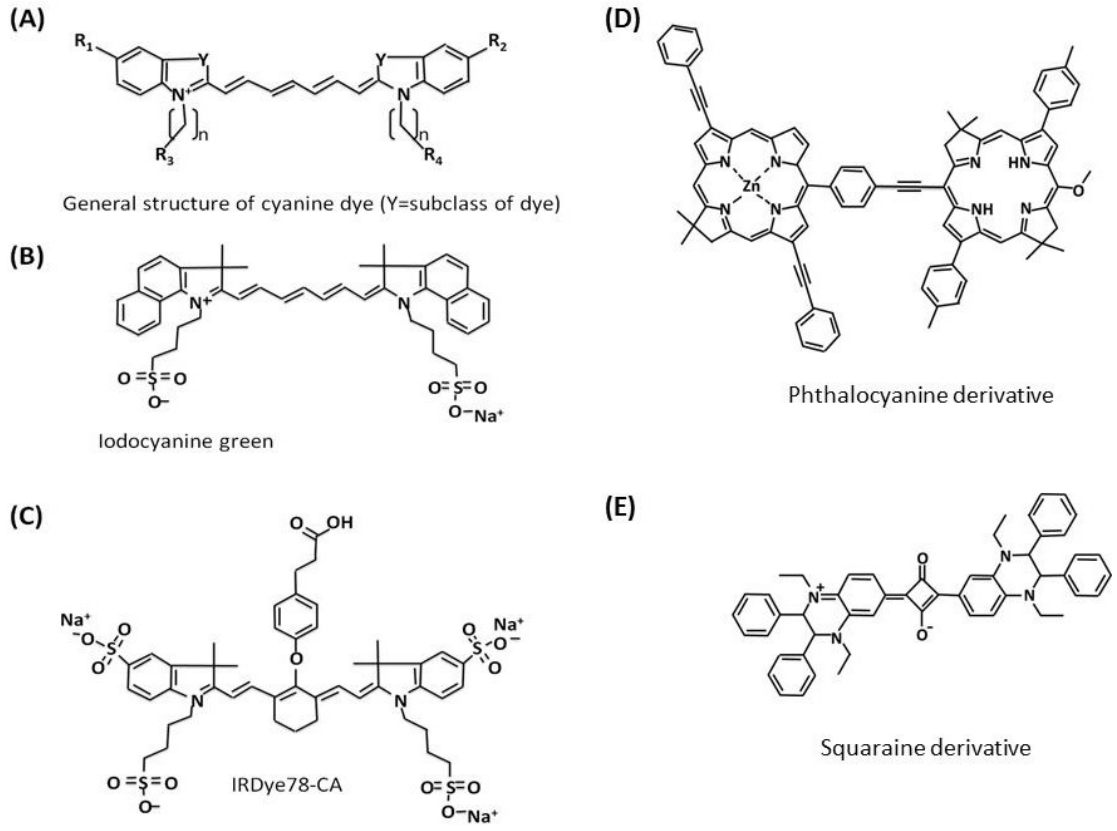

Fig. 1. Structures of commonly used near infrared dyes**.**

2.2.6. Nanomaterial for near infrared imaging

Various nanomaterials are used for near infrared imaging [140, 155-158]. The dyes may be encapsulated in the core of the nanoparticle or conjugated on its surface. Encapsulation of dyes in the core of the nanoparticle or surface conjugation may be advantageous for the purpose of in vivo imaging due to the following reasons. Firstly; the dye is protected from the outside environment which may lead to either degradation of the dye or quenching of the fluorescence. Secondly, a high payload of dye may be encapsulated within the core of the nanomaterial which may boost the fluorescence signal and sensitivity for detection. [159-161]. Examples of nanoparticles used for various imaging applications are listed in Table 2.

Table 2. Various nanomaterials used as probes for near infrared imaging.

NPs	Core material	Synthesis	Properties	Reference
Silica NPs	Amorphous Silica	Microemulsion	Biocompatible and amenable to conjugation	[162, 163]
Calcium Phosphate NPs	Calcium Phosphate	Double emulsion	Effective for targeted drug and gene delivery, safe and stable	[164, 165]
Lipoprotein NPs	Low Density Lipoprotein (LDL)	Microemulsion	Biodegradable and high payload capacity	[166]
Quantum Dots	Semi-conductor Elements	Organic synthesis Aqueous synthesis	Broad absorption spectrum, high extinction coefficient, resistant to photobleaching	[167, 168]
Upconversion NPs	Rare Earth Elements	Thermal decomposition	Can be excited by IR radiation due to upconversion	[169, 170]

Furthermore, biologically reactive moieties may be conjugated to the surface of the nanomaterial through reactive functional groups of the shell which may improve in targeting For example, various ligands such as antibodies [171, 172], peptides [173], folic acid [163], polysaccharides [174], and oligonuclides have been conjugated to dye containing nanoparticles. ICG has been commonly employed dye for purpose of encapsulation since it is approved by FDA [175-177]. Poly (D, L-lactic-co-glycolic acid) (PLGA) nanoparticles entrapping ICG increased the deposition of ICG in organs upto 2-8 as compared to free ICG [178].

Silica nanoparticles are also commonly used for fluorescence imaging [175, 179]. Dye containing silica nanoparticles, also commonly referred as “nanodot” have been used for imaging of metastatic progession to lymph nodes has been investigated in clinical trials for diagnosis and staging of advanced melanoma [180]. Besides imaging, several nanoparticles are also used for intracellular sensing [181-183].

2.2.7. Optical imaging of protease activity

One unique feature of fluorescence imaging is that probes can be designed to be optically quenched in their native state and can be activated by interacting with the target [184, 185]. Therefore, activatable probes can be designed which have little or no optical signal in the inactive state but generate signal after interacting with molecular target [122, 129, 130]. Some examples of optical imaging of proteases are summarized below (Table 3):

Table 3. Examples of proteases used for optical imaging of various diseases.

Target protease	Disease	Substrate	Reference
Cathepsin B	Cancer	KK	[131]
Cathepsin D	Breast cancer	PICFF	[186]
MMP-2	Metastases	PLGVRG	[187]
Caspase-3	Apoptosis	DEVD	[188]
Thrombin	Cardiovascular	F(Pip)RS	[189]
uPA	Cancer	GGSGRSANAKC-NH_2	[12]
MMP-3	Arthritis	Polymeric probe	[190]
MMP-13	Osteoarthritis	GPLGMRGLGK	[191]

2.2.8. Urokinase as biomarker

The urokinase plasminogen activator (uPA) is a serine protease that plays an important role in tumor-associated proteolysis. The enzyme initiates the catalytic conversion of inactive

zymogen plasminogen to the active plasmin [192]. This conversion can further (1) facilitate cancer metastasis by degrading the extracellular matrix and basement membrane [193] and (2) activate certain MMP's precursors [194] as well as specific growth factors, such as transforming factor-β (TGF-β), fibroblast growth factor-2 (FGF-2), and insulin-like growth factor 1 (IGF-1) [195] (Fig. 2).

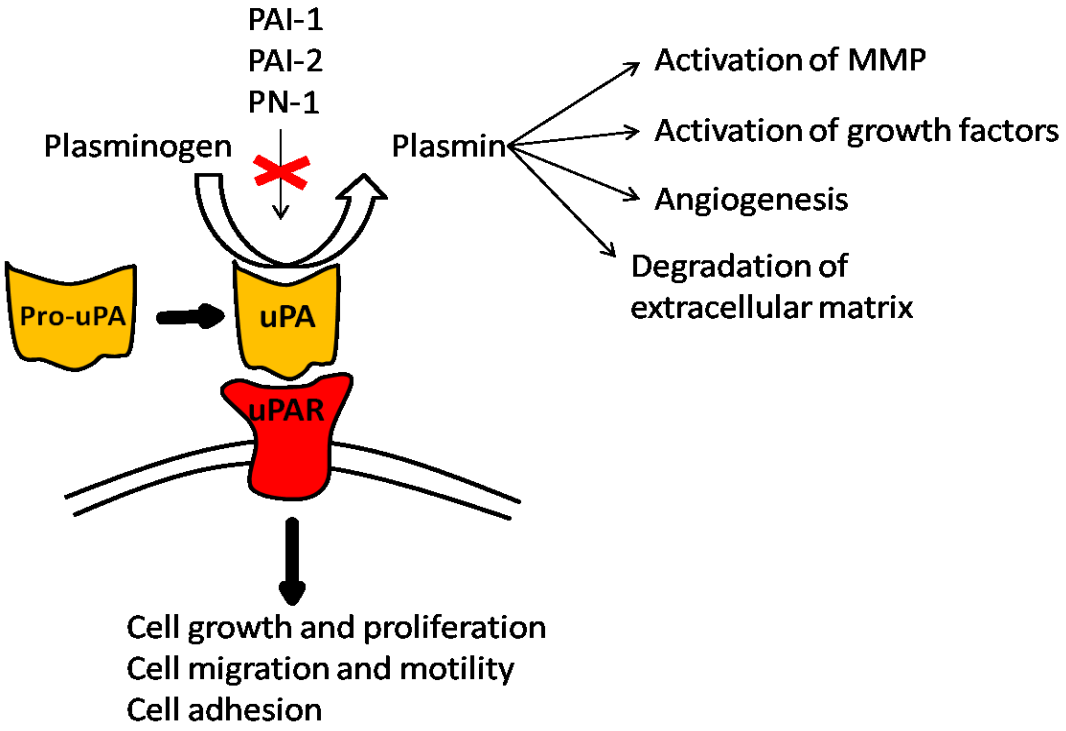

Fig. 2. Various pathological roles of urokinase plasminogen activator (uPA).

Overexpression of uPA can be found in various types of cancers [14] including breast [15], prostate [16], renal [17], ovarian [18], cervical [19], pancreatic [20], glioma [21], colorectal [22], and gastric cancers [23]. Particularly in breast cancer, the overexpression of uPA and its natural inhibitor urokinase plasminogen activator inhibitor-1 (PAI-1) is associated with poor patient prognosis [15]; this has been studied in multicenter prospective clinical trials, meta-analysis and both retrospective and prospective studies [24, 196, 197].

2.2.9. Optical imaging of tumor-associated uPA activity

2.2.9.1. Using grafted polymer

The development of the first uPA-activatable NIRF imaging probe was reported in year 2004 [12]. The probe consisted of a uPA cleavable motif (GGSGRSANA) terminally capped with NIR fluorophores and a polymethylene glycol (PEG) poly-L-lysine grafted co-polymer (Fig. 3). As shown in the figure, upon addition of recombinant human uPA, there was 680% amplification of fluorescence signal observed. The probe was able to discriminate cancer cell lines based on the high level (HT-1080) and low level (HT-29) of uPA. In vivo studies performed in nude mice indicated that there were up to three-fold increases in uPA-overexpressing tumors as compared to the control tumors [12].

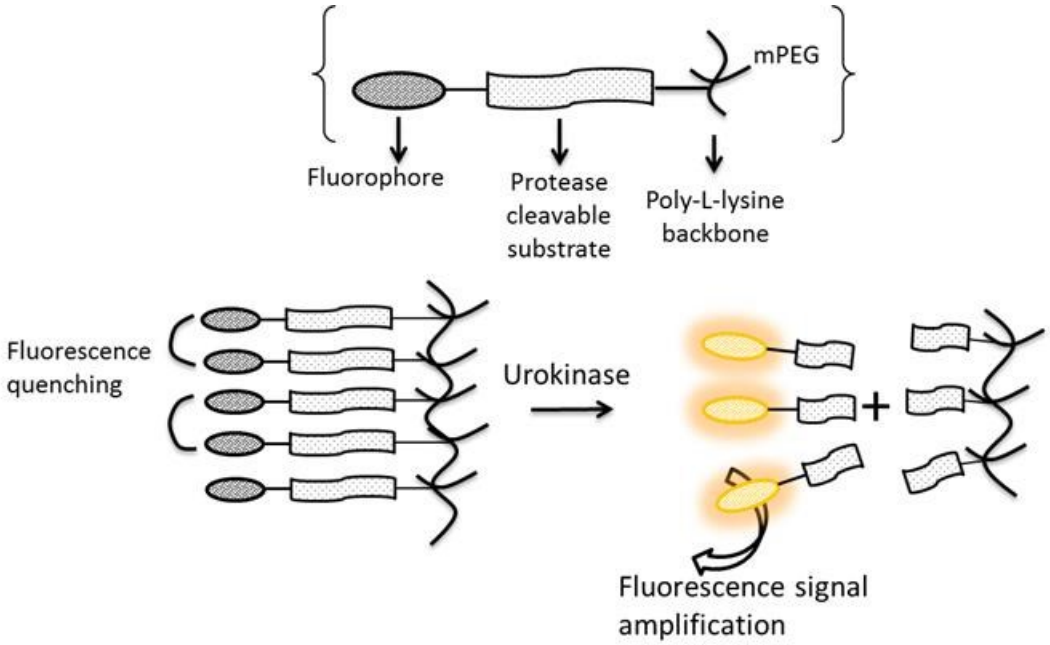

Fig. 3. Schematic diagram showing the design of an uPA-sensitive grafted polymer probe. The probe consisted of a peptide substrate (GGSGRSANA) terminally conjugated to fluorophore and a polymethylene glycol (PEG) poly-L-lysine backbone. The close proximity of fluorophores resulted in fluorescence quenching.Upon the addition of uPA, the enzyme digests the probe, subsequently releasing the free dye-conjugated fragments, resulting in fluorescence amplification.

2.2.9.2. Peptide-based matrix

Protease-responsive peptide matrices have been used for the detection of uPA [26, 198]. The backbone of the peptide matrix is essentially composed of the self-assembly peptide KLDL-12 (Ac-KLDLKLDLKLDL) which is able to form a self-assembled matrix via β-sheet interaction molded in a casting frame [199, 200]. In the presence of uPA, cleavage of the peptide substrate in the matrix takes place, resulting in weakening of the matrix. The degradation of matrix could be monitored by release of fluorescence which was covalently conjugated to the N-terminus of the peptide. Additionally, a cytotoxic peptide (r7-kla) was incorporated into the matrix which could be triggered to release by uPA.

2.2.9.3. Using protease sensitive nanofiber

Nanomaterial may alternately used for detection of proteases. A modification of previous strategy was performed by the same group in which self-assembly sequence $(kldl)_3$ [201] was conjugated to a uPA clevable substrate (SGRSANA) [202], hydrophilic polyethylene glycol (PEG), and a fluorophore (FITC). The sequence of individual peptide construct was mPEG-BK(FITC)-SGRSANA-$[kldl]_3$ [13]. In aqueous solution, the presence of PEG prevented the formation of inter-fibril networking and resulted in the formation of homogeneous nanofibers. Upon exposure to uPA, there was cleavage of substrate and release of fluorescence signal [203].

2.2.10. Imaging uPA activity

The amount of uPA in tumor extract can be determined by enzyme-linked immunosorbent assay (ELISA) [27, 28] or by immunohistochemistry (IHC) [29]. Commercial ELISA kits are available for identifying the subgroup of cancer patients who will benefit from adjuvant therapy [25]. A clinical cut-off value (3 ng of uPA per mg of protein) found in the

tumor extract is normally utilized for classifying the at-risk patient groups [204]. For example, lymph-node-negative patients with low uPA levels (<3 ng/mg) are candidates for avoiding the burden of adjuvant chemotherapy [204]. On the other hand, patients with high uPA levels (>3 ng/mg) can be benefit from the treatment [25]. Although ELISA is a golden standard for determining uPA levels, this technique is confined to *in vitro* analysis. Moreover, it detects only the level of uPA, instead of its activity.

2.2.11. What are the advantages of using near infrared (NIR) nanofiber?

Nanomaterials derived from self-assembly peptides can provide a high degree of flexibility to be modified into bioresponsive materials [205]. These materials are normally constructed with β-sheet peptides, and can be self-assembled to form hydrogels *via* ionic and non-covalent interaction [206], which has been used for tissue engineering [207] and drug delivery [208]. A peptide-based self-assembled nanofiber precursor (NFP) for detecting uPA activity was previously described [13]. FITC was employed as an optical reporter. However, the fluorescence emission in the visible wavelength (at 485 nm) limits its use for *in vivo* imaging [115]. Our aim in this study was to design a second generation NFP. The previously reported peptide construct (mPEG-BK(*FITC*)-SGRSANA-$[kldl]_3$) could be modified by replacing the FITC with a near infrared fluorophore (NIR664). In addition, two homogeneous polyethylene glycols (PEG), instead of one heterogeneous methoxyl PEG (mPEG) could be conjugated at the peptide N-terminus. As a result, the peptide could be synthesized as a homogenous moiety.

2.3. Experimental procedures

2.3.1. Chemicals

All amino acids used for peptide synthesis were purchased from Protein Technologies (Tucson, AZ). Fmoc-NH-$(PEG)_{27}$-COOH and Boc-NH-$(PEG)_{27}$-COOH were purchased from

Novabiochem (San Diego, CA). Thioanisole and ethanedithiol were acquired from Alfa Aaeser (Ward Hill, MA). Anisole was purchased from TCI America (Portland, OR). NIR-664-N-succinimidyl ester (NIR-664-NHS) was purchased from Fluka (Milwaukee, WI). uPA (urokinase from human urine) and PSA (prostate specific antigen) were purchased from Sigma Aldrich (St. Louis, MO). Caspase-3 and cathepsin L were obtained from Biovision (San Francisco, CA). MMP-2 was purchased from Calbiochem (Gibbstown, NJ).

2.3.2. Peptide elongation

All peptides were synthesized on an automated solid phase peptide synthesizer (PS3, Protein Technologies, Tucson, AZ), employing the traditional N-α-Fmoc methodology on rink amide resin (0.1 mmol), as previously described [12]. Side-chain protections were Arg(Pbf), Asn(Trt), Lys(Boc), Ser(tBu), and Lys(ivDde). The coupling agent was 2-(1H-benzotriazole-1-yl)-1,1,3,3,-tetramethylaminium hexafluorophosphate (HBTU), N-hydroxybenzotriazole (HOBt), and N,N-diisopropylethylamine (DIEPA) in N-methylpyrrolidinone (NMP) .

2.3.3. Pegylation

A mixture of Fmoc-NH-$(PEG)_{27}$-COOH (308 mg, 0.2 mmol) and DIEPA (1 mL) dissolved in DMSO (4 mL) was added to the resin, followed by gentle shaking for 3 hr at room temperature. The Fmoc was removed by 20% (v/v) piperidine in DMF. Using the same protocol, Boc-NH-$(PEG)_{27}$-COOH (285 mg, 0.2 mmol) was finally attached to the peptide N-terminus.

2.3.4. Conjugation of NIR-664 to the peptide

Prior to NIR-664 conjugation, the side-chain deprotecting group, ivDde (4,4-dimethyl-2,6-dioxocyclohex-1-ylidene)-3-methylbutyl), was removed with 2% (v/v) hydrazine monohydrate in DMF (10 mL) [12]. The resin was washed three times with DMF. NIR-664-N-succinimidyl ester (25 mg, 0.03 mmol) dissolved in DMSO (4 mL) was added to the resin (0.02

mmol). DIEPA (1 mL) was used as the catalyst. The reaction was allowed to react for 3 hr at room temperature.

2.3.5. Peptide cleavage

The resin was dried in methanol. A cleavage cocktail (2 mL) containing TFA/thioanisole/ethandithiol/anisole (90/5/3/2) was added to the resin for 3 hr at room temperature. The peptide was then precipitated in methyl-tert-butyl ether at 4°C and purified by reverse phase high performance liquid chromatography (rp-HPLC). The molecular weight of all peptides was confirmed by MALDI-TOF mass spectrometry (Tufts Medical School, Core Facility, Boston, MA). Peptide concentrations were determined by UV absorbance, according to the pre-determined extinction coefficient of NIR-664 (ε = 200,700 $M^{-1}cm^{-1}$ at 672 nm) in 80% (v/v) DMSO in water.

2.3.6. NFP synthesis

To synthesize NFP, either uPA-cleavable (PEG_{54}-BK(NIR664)SGRSANA-kldlkldlkldl-$CONH_2$) or non-cleavable (PEG_{54}-BK(NIR664)SGSARNA-kldlkldlkldl-$CONH_2$) peptide-conjugate (5 mg) was added to a mixture of 50% (v/v) acetonitrile in water (5 mL). The solution was allowed to sit at room temperature overnight. The resulting NFP were then purified using Sephedex G-75 (GE Healthcare, Piscataway, NJ). The concentrations of all NFP were determined by UV absorbance, according to the extinction coefficient of NIR-664 (ε = 200,700 $M^{-1}cm^{-1}$ at 672 nm) in 80% (v/v) DMSO in PBS. To make NFP of various lengths, the NFP solution was passed through a mini-extruder (Avanti polar lipids Ltd., Alabaster, AL) with polycarbonate membrane (Whatman, Florham Park, NJ) of different pore sizes (0.1 or 0.4 μm), which were then purified by size exclusion chromatography (GE Healthcare, Piscataway, NJ).

2.3.7. Transmission electron microscopy

A solution of uPA (5 μg, 100 μL) was added to the NFP (4 μM, 100 μL) in a PBS buffer (10 mM, pH 7.4). The samples were allowed to incubate for 24 hr at room temperature. A small amount of NFP (20 μL) were then transferred onto the formvar/carbon-coated grids. Excess NFP were blotted off using a filter paper. The NFP were further stained with a 2% (v/v) uranyl formate solution [13]. The grids were allowed to dry and then examined under the TEM (JEOL 100CX, Peabody, MA). For the inhibition study, the uPA was pre-incubated with amiloride (1 mM) for 5 min prior to incubation with NFP.

2.3.8. Fluorescence activation

Different amounts of uPA (0, 6.25, 12.5, 25, and 50 μg, 100 μL) were added to the NIR-NFP (4 μM, 100 μL) in the PBS buffer. Their fluorescence intensities were measured in a submicro cuvette (Starna cells, Atascadero, CA) by a fluorescence spectrometer (Cary eclipse, Varian, Palo Alto, CA) at different time points. All samples were excited at 665 nm, and their emissions were recorded at 684 nm. For the inhibition study, amiloride (1 mM) was added to the uPA prior addition to the NFP. For specificity studies, the NIR-NFP was incubated with other tumor-associated proteases including cathepsin L (12.5 μg/mL), prostate specific antigen (12.5 μg/mL), caspase-3 (0.3 μg/mL), and MMP-2 (12.5 μg/mL).

2.3.9. Cell lines

Human cancer cell lines, SKBr-3, PANC-1, MCF-7, SKOV-3, MDA-MB-231, PC-3, and HT-1080 were purchased from ATCC. The non-cancerous cells (primary vascular smooth muscle cells and glial cells from rat) were supplied as generous gifts from Dr. Chengwen Sun (NDSU, Fargo, ND). HEK-293 cells were provided as a generous gift from Dr. Jagdish Singh (NDSU, Fargo, ND). All cell lines were cultured in their respective culture media as

recommended by ATCC. All culture media were supplemented with 10% FBS and antibiotics (100 U/mL penicillin G and 0.1 mg/mL streptomycin). All cells were cultured in incubators at 37^{o}C with 5% CO_2 under humidified conditions.

2.3.10. Western blot

To determine the expression of uPA, all cells were grown to 80% confluency. The old media was discarded, and the remaining cells were rinsed twice with Hank's balanced salt solution (HBSS). Cells were then incubated with serum-free McCoy's 5A medium at 37^{o}C with 5% CO_2 under humidified conditions. After 24 hr, the conditioned media was collected and then centrifuged at 1500 rpm for 5 min. The supernatants were collected, centrifuged at 15,000 rpm, and concentrated with an Amicon Ultra-4 10k filter (Millipore, Billerica, MA). Micro-BCA assay (Pierce, Rockford, IL) was used to normalize the protein levels in all cell lines. The media (5 μL) was mixed with equal volumes of Laemmli buffer (BioRad, Hercules, CA) and then loaded onto 4-15% SDS-PAGE ready gel precast gels (BioRad, Hercules, CA). Electrophoresis was carried out at 80 V using Tris/glycine/SDS (25 mM Tris, 192 mM glycine and 0.1% (w/v) SDS, pH 8.3). Purified uPA (5 ng) was used as the positive control. After electrophoresis, the separated proteins were transferred to a polyvinylidene fluoride membrane (Hybond^{TM}-P, Amersham, Piscataway, NJ). The membrane was then blocked with 5% (w/v) nonfat dry milk (BioRad, Hercules, CA) in 0.1% (v/v) Tween 20 in a Tris buffer saline (TBS) buffer, which was then incubated with primary mouse antibody against human urokinase (1:1000 dilution, American Diagnostica, Stamford, CT) in 0.1% (v/v) Tween 20-TBS, containing 1% (w/v) nonfat dry milk. After 4 hr, the membrane was washed with 0.1% (v/v) Tween 20-TBS (3 × 20 min) and allowed to incubate with secondary goat antimouse IgG (H+L) HRP conjugate (1:20,000 dilution, ImmunoPure®, Pierce, Rockford, IL) for 1.5 hr. The membrane was washed again with

0.1% (v/v) Tween 20-TBS (3 × 20 min), and uPA was detected with ECL™ Western Blot Detection Reagents (Amersham, GE Healthcare Bio-Sciences, Piscataway, NJ) on Blue Ultra Autorad Film (BioExpress® Kaysville, UT).

2.3.11. Ex vivo activation of NIR-NFP

The supernatants were prepared as described in western blot. Stock concentration of NIR-NFP (1 μM) was prepared by diluting the NIR-NFP with PBS (10 mM, pH 7.4). The diluted NIR-NFP (60 μL) was added to the conditioned cell culture medium (60 μL). A similar procedure was followed for the scrambled substrate control NIR-NFP. The samples (100 μL) were transferred to a fluorescence cuvette, (Sub micro fluorometric cell, Starna cells, Atascadero, CA). Fluorescence emissions (at 684 nm) were recorded at 24 hr after incubation. Excitation wavelength was set at 665 nm. The enzyme activities secreted from individual cell lines were further quantified by interpolating the data from a standard curve. To generate a standard curve, different amounts of uPA (15-5000 μg/mL, 50 μL) (0.0625-10 μg/mL, 50 μL) of known activities, (where 1U = 2 μg), as determined by the supplier) were added to the NIR-NFPs (1 μM, 50 μL).

2.3.12. uPA activity assay

The supernatants were prepared as described in the Western Blot section. The uPA activity was measured using the AssaySense Human uPA Chromogenic Activity Assay Kit (ASSAPRO, St. Charles, MO), according to the manufacturer's instructions. Briefly, all samples were pre-diluted in assay buffer, followed by addition to the uPA substrate. The supernatant containing substrate solutions (100 μL) were then transferred to 96-well polystyrene microplate. The enzyme activities were monitored by absorbance at 405 nm at 4 hr after incubation. A standard curve of known uPA activities (between 0.015 and 2.5 U/mL) was generated at the time

the assay was performed. The activities of supernatants were interpolated from the standard curve. Each reaction was performed in triplicate.

2.4. Results and discussion

2.4.1. The design of an NIR nanofiber precursor (NIR-NFP)

To design an NIR-NFP for *in vivo* application, a previously reported NFP peptide construct was modified to comprise (1) a β-sheet peptide sequence (kldlkldlkldl, where k, l, and d are in *D*-configurations) for NFP assembly [201, 209] (2) a uPA substrate motif (SGRSANA) for enzyme cleavage [12, 13, 202, 210], (3) a polyethylene glycol (PEG_{54}) to prevent inter-fibril aggregation, and 4) a conjugated NIR664 fluorophore as the optical reporter [211, 212] (Fig. 4).

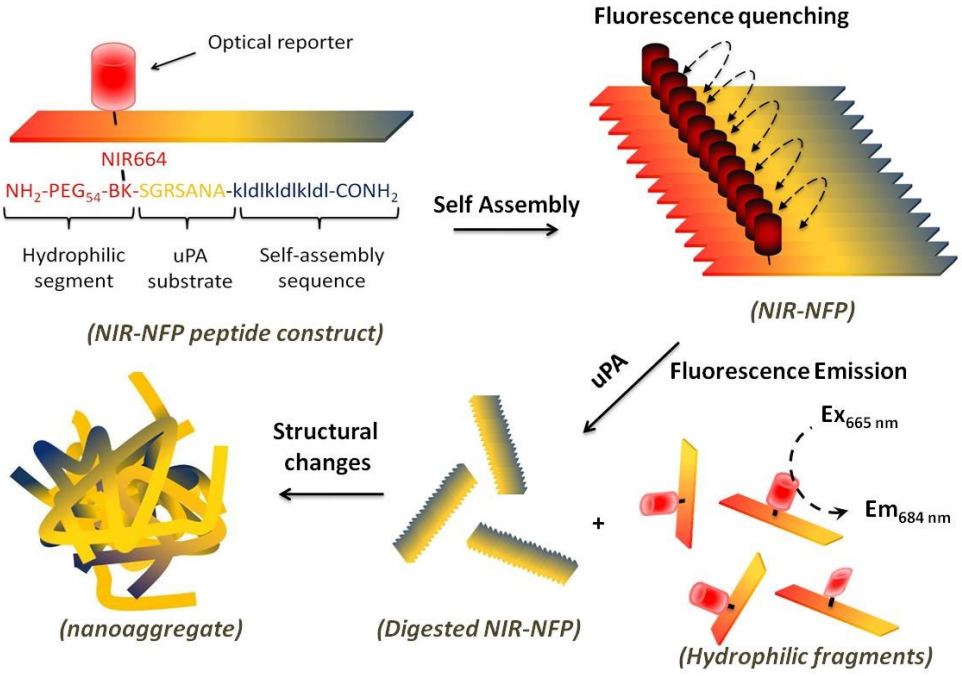

Fig. 4. Schematic presentation showing the design of an uPA-sensitive, near-infrared nanofiber precursor (NIR-NFP). The basic peptide construct of NIR-NFP is composed of a self-assembly peptide sequence (kldlkldlkldl), an uPA substrate motif (SGRSANA), a hydrophilic polyethylene glycol (PEG_{54}), and a NIR reporter (NIR664). In an aqueous buffer, multiple NIR-NFP peptides (PEG_{54}-BK(*NIR664*)SGRSANA-$[kldl]_3$-NH_2) spontaneously self-assembled to form an optically quenched NIR-NFP platform. Upon the addition of uPA, the enzyme digests the NIR-NFP, subsequently releasing the free NIR664-conjugated hydrophilic fragment (NH_2-PEG_{54}-BK(NIR664)SGR-COOH), which results in fluorescence amplification.

In an aqueous buffer, multiple NFP constructs are expected to self-assemble to form a 2-dimensional fiber via hydrophobic and electrostatic interactions [206, 213]. In the native state, the multiple NIR664 molecules attached to the NIR-NFP are orientated in a closed proximity; thus they become optical silent *via* static quenching. Upon activation with uPA, NIR664-conjugated hydrophilic fragments (NH_2-PEG_{54}-BK(*NIR664*)SGR-COOH) can be released from the NIR-NFP, which in turn cause a significant increase in NIR fluorescence emission. The uniqueness of this NFP platform is that in simultaneous response to uPA digestion, the NIR-NFPs will interact and transform into inter-fibril networks of micrometer size [214], which may potentially be used for protease-mediated drug delivery [215-220].

2.4.2. Synthesis and characterization of NIR-NFP

The entire NIR-NFP (NH_2-PEG_{54}-BK(*NIR664*)SGRSANA-kldlkldlkldl-$CONH_2$) and control NIR-NFP (PEG_{54}-BK(NIR664)SGSARNA-kldlkldlkldl-$CONH_2$) peptide constructs were synthesized in rink-amide resin (Fig. 5). We employed two homogeneous PEGs (Fmoc-NH-$(PEG)_{27}$-COOH and Boc-NH-$(PEG)_{27}$-COOH) for pegylation, which was performed at the peptide N-termini by stepwise elongation. This method allowed NIR-NFP peptide to be synthesized as a homogenous moiety. NIR664, a cyanine dye, was introduced to the N-terminal lysine as the optical reporter. We found that NIR664, similar to some cyanine derivatives, displayed high chemical stability in TFA [221]. After cleavage, the NIR-NFP peptide was purified by rp-HPLC to > 90% purity (Fig. 6) and then lyophilized. MALDI-TOF MS analyses showed the expected molecular weight of the NIR-NFP peptide (Fig. 7, $[M + H]^+$= 5487.77, calculated = 5486.45) (Fig. 7).

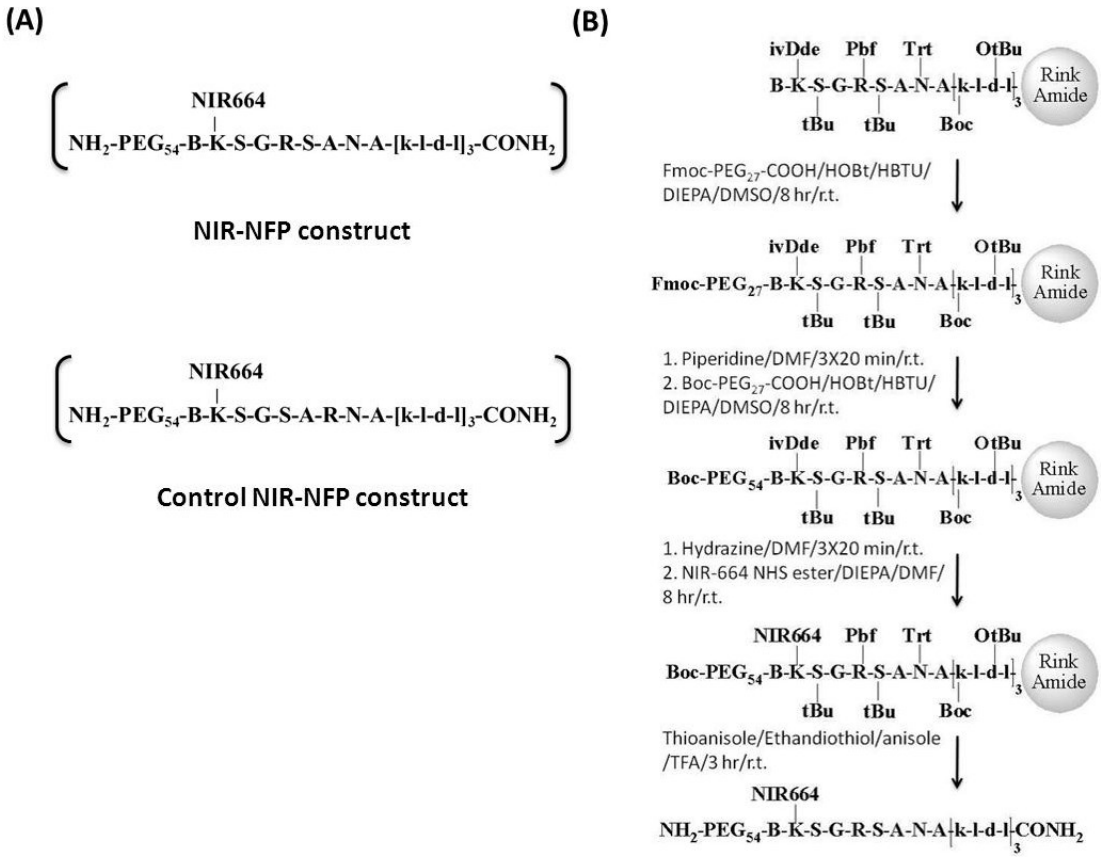

Fig. 5. NIR-NFP peptide synthesis. (A) The amino acid sequences of the NIR-NFP peptide construct and its control. (B) Synthetic scheme of the NIR-NFP peptide.

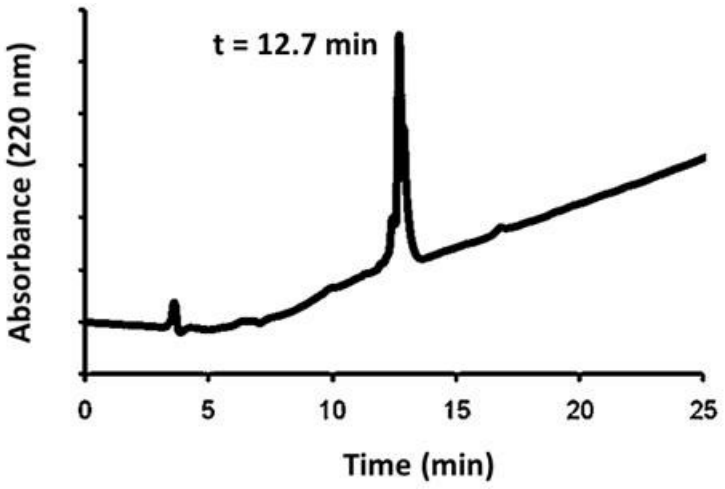

Fig. 6. Analytical C-18 rp-HPLC chromatogram of the purified NIR-NFP peptide construct. The sample was eluted using a linear gradient (30 min) starting from 0 min with 20 % (v/v) of acetonitrile in 0.1 % (v/v) TFA in water and ending at 30 min with 80 % (v/v) of acetonitrile in 0.1 % (v/v) TFA in water.

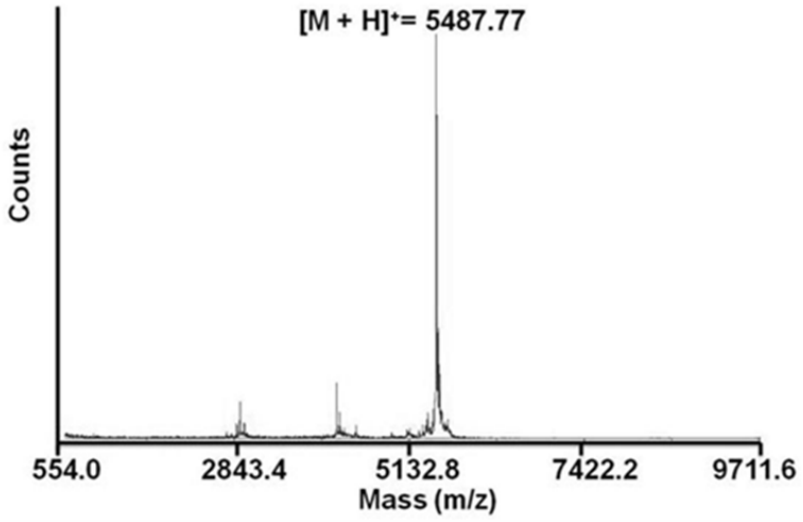

Fig. 7. The MALDI-TOF spectrum of the NIR-NFP peptide.

To synthesize the NIR-NFP, the peptide was dissolved in a mixture of acetonitrile and PBS. Self-assembly was induced by solvent evaporation and it was allowed to be homogenized, as previously described [13]. The formation of NIR-NFP was confirmed by transmission electron microscopy (TEM). The as-prepared formulations were imaged as discrete fiber-like structures, spanning 1- 2 μM in length. The width of the NFP was extremely narrow (4 nm) depicting its 2-dimensional structure. NIR-NFPs of various lengths (30 to 400 nm) could be fine-tuned by passing the samples through a mini-extruder, depending on the sizes of the pore filters employed.

The fragmented fibers' physical properties were similar to those of as-prepared fibers. Unlike previous studies, which showed that various self-assembling peptides were able to form fiber-like networks [201, 222], NIR-NFPs are individual fibers with no cross-linking (Fig. 8). This suggests that the incorporation of a hydrophilic PEG at the peptide N-termini can prevent the formation of 3-dimensional networks as a hydrogel.

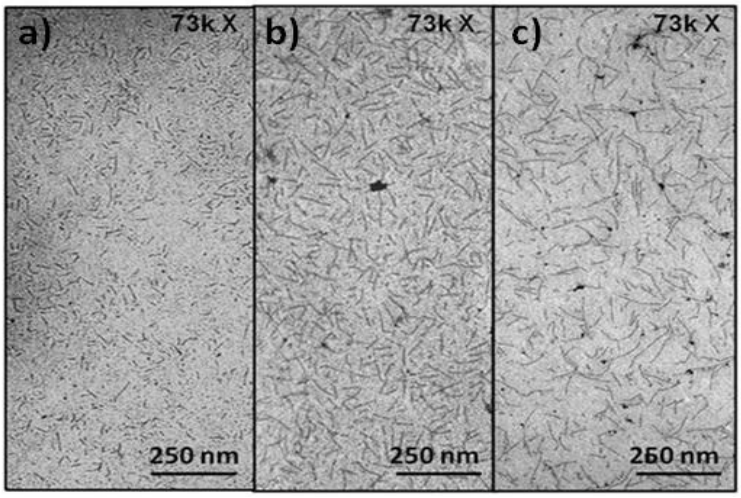

Fig. 8. TEM images of a) 30 nm, b) 100 nm, and c) 400 nm NIR-NFPs. Images magnifications were 73k X.

2.4.3. Fluorescence activation

To study the fluorescence activation, 100 nm NIR-NFP (2 μM) was incubated with various amounts of uPA (μg/mL). The NIR-NFP concentration in all experiments was determined by UV absorbance (Fig. 9), according to our determined extinction coefficient (extinction coefficient = 200, 700 $M^{-1}cm^{-1}$ at 672 nm) of NIR-664 in 80% (v/v) DMSO in PBS.

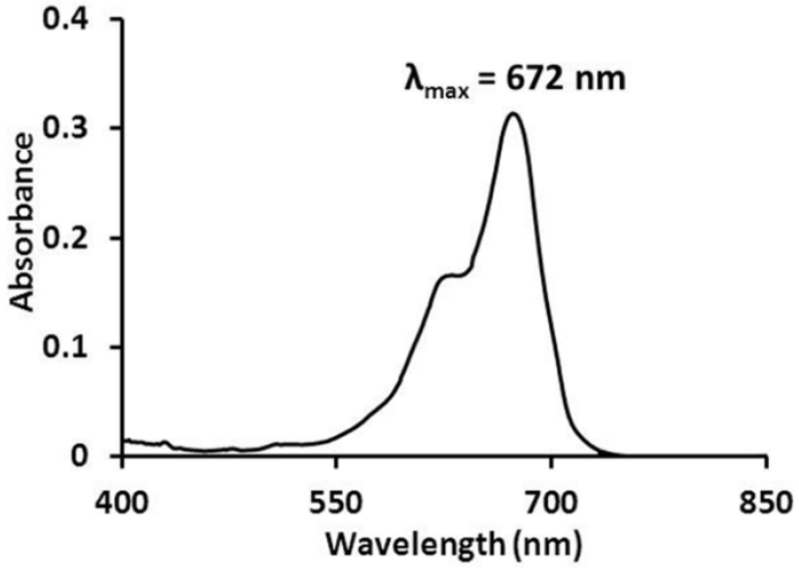

Fig. 9. The absorbance spectrum of NIR-NFP in 80% (v/v) DMSO in PBS.

Fluorescence emissions were measured at different time points (hr). We found that NIR-NFP activation was uPA dependent. After 24 hr, up to 19.6-fold signal amplification was observed in samples incubated with a higher uPA level (Fig. 10A).

To evaluate the specificity of NIR-NFP, we compared the activation kinetic level of NIR-NFP with its control as well as in the presence of amiloride inhibitor. The control NIR-NFP consisted of a scrambled substrate sequence (SGSARNA) that is not recognized by uPA. With the addition of uPA, the fluorescence intensity of NIR-NFP increased with time, whereas the control did not show any changes (Fig. 10B). Fluorescence amplification was also significantly inhibited by amiloride inhibitor, confirming that NIR-NFP activation is specific to uPA.

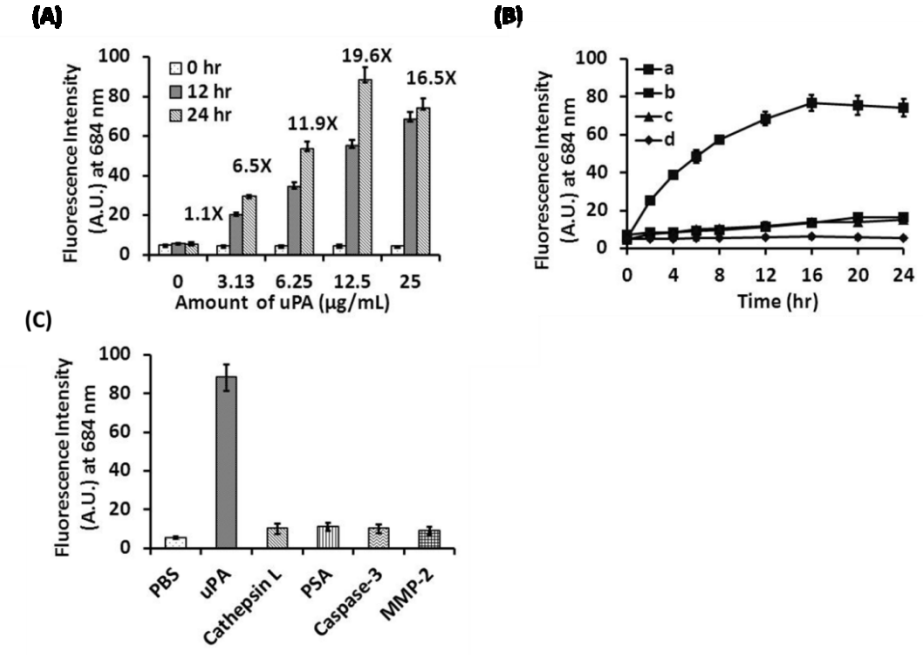

Fig. 10. Fluorescence activation of NIR-NFP. (A) NIR-NFP (100 nm, 2 μM) was incubated with different amounts of uPA (μg/mL). Fluorescence intensities were recorded at different time points (hr). (B) Fluorescence intensity versus time scale (hr). NIR-NFP was incubated with (a) uPA only, (b) uPA plus amiloride inhibitor (1 mM), (c) the same amount of uPA, added to the control NIR-NFP, and (d) a PBS buffer only (10 mM, pH 7.4). (C) Comparison of NIR-NFP activations with different tumor-associated proteases. The NIR-NFP was incubated in either PBS alone or with proteases including uPA (12.5 μg/mL), cathepsin L (12.5 μg/mL), prostate specific antigen (12.5 μg/mL), caspase-3 (0.3 μg/mL), and MMP-2 (12.5 μg/mL). Fluorescence intensities were recorded at 24 hr after incubations.

Previously, we demonstrated that our employed substrate sequence "SGRSANA" for NIR-NFP is specific to uPA [223]. Here, we incubated the NIR-NFP with other tumor-associated proteases including MMP-2, cathepsin L, prostate specific antigen (PSA), and caspase-3. As expected, these proteases did not activate the NIR-NFP (Fig. 10C), suggesting the employed substrate for NIR-NFP is specific to uPA.

We next compared the fluorescence activation of NIR-NFP among various lengths (30, 100 and 400 nm). Surprisingly, all NIR-NFPs showed similar fluorescence activation kinetics (Fig. 11). This may be explained by the fact that all NIR-NFPs had the same surface-area-to-volume ratios, since they were structurally arranged in 2-dimension, thus uPA could assess to the substrate sites on the surfaces regardless of the length of the nanofibers.

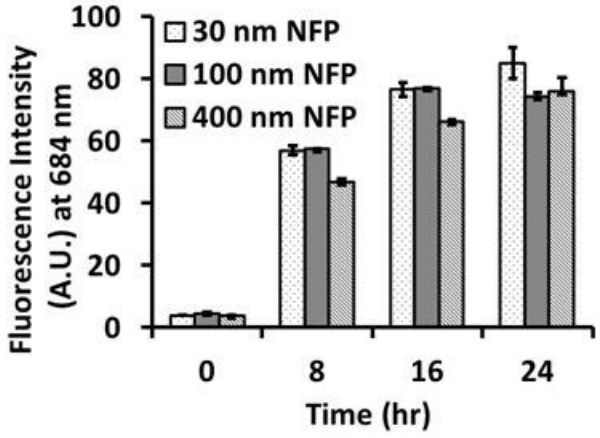

Fig. 11. Comparison of NIR-NFP of various lengths. Activation of NIR-NFP (2 μM). Fluorescence emissions (at 684 nm) were recorded at different time points (hr) after uPA (25 μg/mL) addition in a PBS buffer (10 mM, pH 7.4). (Excitation wavelength = 665 nm)

2.4.4. Structural modification

To investigate the structural modification, 100 nm NIR-NFPs were subjected to TEM analysis. Previous studies of NFP demonstrated that the formation of inter-fibril networks upon protease activation was a stepwise process, involving the formation of intermediates such as elongates and laminates [214].

Here, the NIR-NFP was stable and showed no structural changes after 24 hr (Fig. 12). In contrast, the NIR-NFP transformed into inter-fibril networks after enzyme activation. The control NIR-NFP showed no structural changes with uPA. Our results were comparable to fluorescence activation studies.

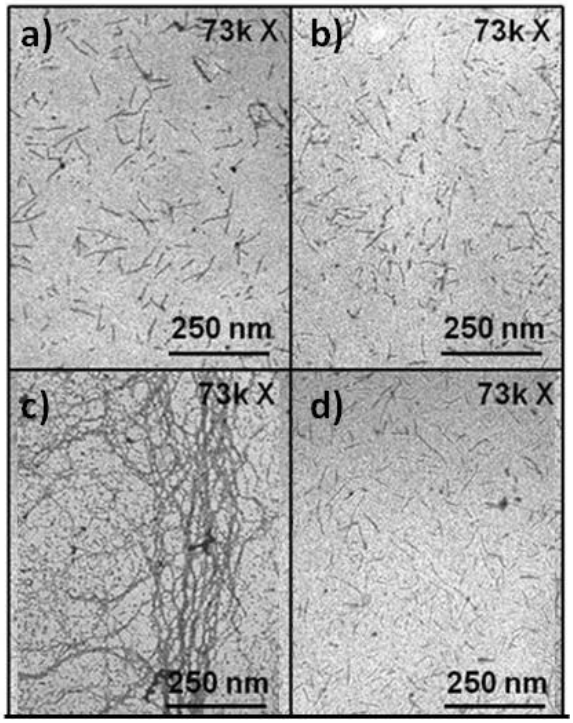

Fig. 12. Structural modification of NIR-NFP (100 nm, 2 μM) upon enzyme activation. TEM images of NIR-NFP. The images of NIR-NFP at (a) t = 0 hr and (b) t = 24 hr in PBS buffer (10 mM, pH 7.4). uPA (25 μg/mL) was incubated with (c) NIR-NFP and (d) control NIR-NFP for 24 hr.

2.4.5. Ex vivo activation of NIR-NFP

To investigate whether NIR-NFP can be used to detect cell-secreted uPA activity, we first collected the culture media from various cancer cell lines (SKBr-3, PANC-1, MCF-7, SKOV-3, MDA-MB-231, PC-3, and HT-1080). We then incubated the NIR-NFP in the media and monitored the fluorescence changes after 24 hr. We found significant increase in fluorescence signal recorded in cell lines expressing high levels of uPA such as HT-1080 and PC-3. On the contrary, no appreciable fluorescence changes in media of SKBR-3 (Fig. 13A) and some non-

cancerous cells. The fluorescence changes were correlated with the protein expressions, as determined by western blot analysis. When control NIR-NFP was added to the HT-1080 media, there was no fluorescence change suggesting that the detection of uPA is specific. The amount of enzyme activities secreted from individual cell lines could be further quantified by interpolating the data from a standard curve (Fig.13B and Table 4). uPA activity can be counterbalanced by its natural inhibitor (uPAI) [224]. To confirm our results, we further employed a commercial activity assay kit. Unlike NIR-NFP, this assay determines uPA activities by using specific substrates that can be monitored by an increase in absorbance at 405 nm.

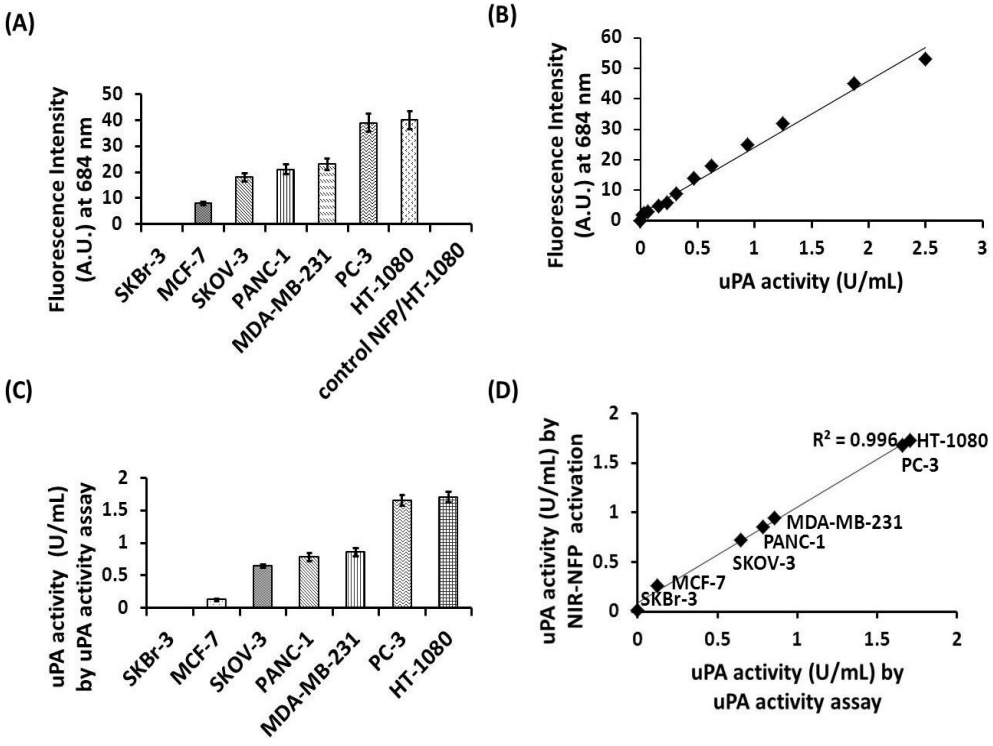

Fig. 13. Ex vivo activation of NIR-NFP. (A) The uPA activities in various cancer cell lines were determined by NIR-NFPs (100 nm, 0.5 μM) in conditioned culture media (100 μL). Control NIR-NFP was incubated in the HT-1080 media. All samples were recorded for fluorescence changes at 24 hr after incubation. (B) A standard curve showing a plot of known amount of uPA activities (0.015-2.5 U in 100 μL, where 1 U = 2 μg of uPA) versus fluorescence activations by NIR-NFPs. (C) The activities of uPA in the culture media (100 μL) were confirmed by AssaySense Human uPA Chromogenic Activity Assay. (D) A linear plot showing NIR-NFP is comparable with the commercial activity assay for determine uPA activities in various cancer cell lines.

Table 4. Comparison between the NIR-NFPs and the uPA activity assay for determining uPA activities from different cancer cell lines.

Cell Line	uPA Activity (U/mL) determined by NIR-NFP	uPA Activity (U/mL) determined by activity assay
SKBr-3	0	0
MCF-7	0.26 ± 0.03	0.12 ± 0.01
SKOV-3	0.71 ± 0.06	0.64 ± 0.02
PANC-1	0.85 ± 0.08	0.78 ± 0.05
MDA-MB-231	0.94 ± 0.09	0.85 ± 0.05
PC-3	1.68 ± 0.14	1.65 ± 0.08
HT-1080	1.72 ± 0.14	1.70± 0.08

As expected, the uPA activities determined by NIR-NFPs were correlated with the activities determined by the commercial assay. There was no significant difference in uPA activities when NIR-NFP was incubated with non-cancerous cell-lines (Fig. 14). Overall, our data suggests that NIR-NFP is specific to uPA and can be used to quantify exogenous enzyme activity in ex vivo.

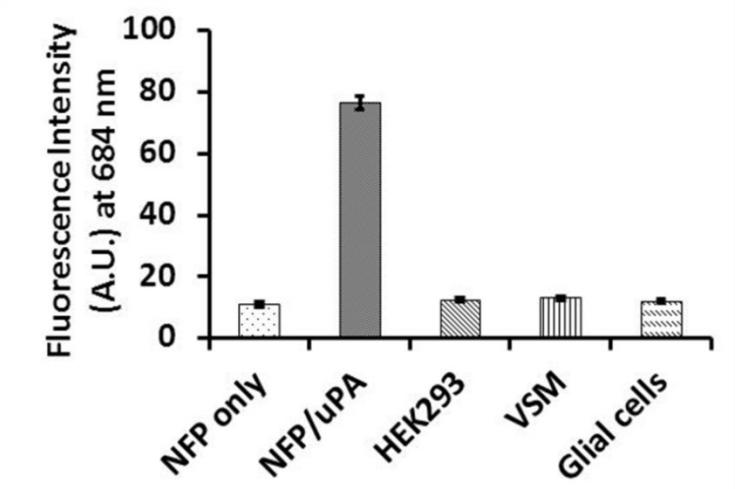

Fig. 14. Fluorescence intensity of NIR-NFP in culture media of non-cancerous cells. NIR-NFP (100 nm, 2 μM) was incubated with culture media obtained from, HEK293, primary vascular smooth muscle cells from rat (VSM), and primary glial cells from rat. Fluorescence intensities were recorded after 24 hr. There was no fluorescence increase in culture media obtained from non-cancerous cells.

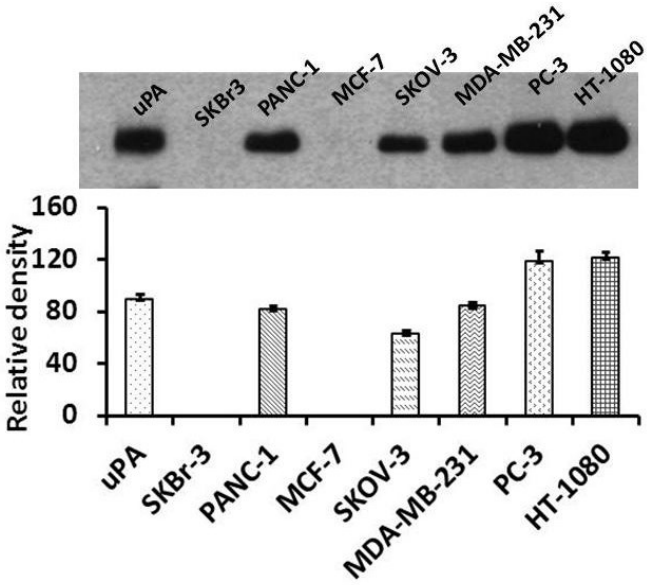

Fig. 15. The expressions of uPA in supernatants of various cancer cell lines. The levels of uPA in SKBr-3, PANC-1, MCF-7, SKOV-3, MDA-MB-231, PC-3, and HT-1080 were determined by western blot. Lane 1 shows the human uPA as the positive control. The underlying bar graph shows the results of densitometric analysis of relative uPA levels from the western blot. The values indicated in the graph are means of three independent experiments.

2.5. Conclusion

Various fluorescent sensors such as polylysine copolymer [131], liposome [225], self-assembly peptides matrices [12, 13], and polymeric nanoparticles [226] have been used for detecting tumor-associated proteases [127]. In the present study, we demonstrate an alternative approach, based on an NIR nanofiber precursor (NIR-NFP) system, for detecting uPA activity. Our optimized formulation (100 nm in size) was able to detect uPA in vitro with a 19.6-fold increase in NIR fluorescence signal; thus, it may be useful for in vivo imaging. The uniqueness of NIR-NFP is that it can transform into a micrometer-sized inter-fibril networking upon enzyme activation. We reasoned that upon uPA digestion, the activated NFP would no longer sustain its normal integrity, due to the loss of PEG-conjugated peptide fragments (PEG_{54}-B-K(*NIR664*)SGR-COOH). The resulting morphologies were similar to the self-assembly peptides

used for tissue engineering and drug delivery [206, 207, 227-229]. We also demonstrated that NFP was able to detect cell-secreted uPA in various cancer cell lines.

A clinical cut-off value of uPA is usually between 3 to 10 ng per mg of protein, depending on the methods of analysis [230]. Our NIR-NFP was able to detect uPA within this range (as low as 3 ng) in 100 μL of sample. Experiments that involve testing the NIR-NFP for imaging uPA activity in xenograft model are currently underway.

In conclusion, we have designed and characterized a peptide-based near infrared reporter for uPA. Our ultimate goal is to develop a patient-specific strategy for the diagnosis and treatment of cancer, based on the differential expression of tumor-associated proteolysis [231]. Overall, this approach may also apply to detecting other proteases.

CHAPTER 3. DESIGN AND SYNTHESIS OF A PEPTIDE-BASED NANOFIBER AS MULTIVALENT PLATFORM FOR INCREASING THE THERAPEUTIC EFFICACY OF HERCEPTIN

3.1. Abstract

A multivalent system is often employed to enhance the effectiveness of a targeted therapy. Here, we investigated the peptide nanofiber (NFP) as a multivalent platform to target the human epidermal growth factor receptor (HER-2), a receptor that is overexpressed in about 20% of breast cancer patients. The nanofiber (HER-NFP) was 100 x 4 nm in size and was assembled from multiple peptide units (mPEG-BK(*FITC*)SGASNRA-kldlkldlkldl-$CONH_2$). HER-NFP was also attached with approximately ten Herceptin antibodies at the surface. Because of an increase in the multivalency, HER-NFP was able to truncate more cell surface HER-2 and thus showed an enhanced cytotoxicity towards HER-2 positive SKBr-3 human breast cancer when compared to the free Herceptin. Western blot and fluorescence microscopy studies confirmed that there was a significant down-regulation of the HER-2 level and also inhibition of the cell survival cell signaling pathways such as the phosphatidylinositol 3-kinase (PI3K) and the mitogen activated protein kinase (MAPK) pathway. Our data suggested that NFP can be a multivalent platform for immunotherapy, especially in combining with other chemotherapeutic agents in the future.

3.2. Introduction

3.2.1. Monoclonal antibody therapy

Monoclonal antibody (mAbs)-based therapy has enormous potential for treating numerous human malignancies including cancer, heart disease, infection, and immune disorders [232-234]. Examples of FDA approved monoclonal antibodies used for the treatment of cancer are summarized in Table 5.

Table 5. List of monoclonal antibodies approved by FDA for different types of cancer.

Product	Generic name	Target	Type	Approval	Indications
Rituxan®/Mabthera®	Rituximab	CD20	Chimeric IgG1	1997	B-cell lymphoma
Herceptin®	Trastuzumab	HER2/neu	Humanized IgG1	1998	Breast cancer
MabCampath®	Alemtuzumab	CD52	Humanized IgG1	2001	Chronic lymphatic leukemia
Zevalin®	90Y-Ibritumomab	CD20	Murine IgG1-radionuclide-conjugate	2002	B-cell lymphoma
Bexxar®	131I-Tositumomab	CD20	Murine IgG1-radionuclide-conjugate	2003	B-cell lymphoma
Avastin®	Bevacizumab	VEGF	Humanized IgG1	2004	Colorectal cancer
Erbitux®	Cetuximab	EGFR	Chimeric IgG1	2004	Colorectal cancer
Vectibix®	Panitumumab	EGFR	Entirely human IgG2	2006	Colorectal cancer
Arzerra®	Ofatumumab	CD20	Entirely human IgG1	2009	Chronic lymphatic leukemia
Yervoy®	Ipilimumab	CTLA-4	Entirely human IgG1	2011	Melanoma
Adcetris®	Brentuximab vedotin	CD30	Chimeric IgG1	2011	Non-hodgkin lymphoma

The main advantage of mAbs is their specificity and low toxicity as compared to small molecule chemotherapeutic drugs. More than 25 mAbs have been approved by the US Food and Drug Administration (FDA), while there are 150 in different phases of clinical trials [235]. For the treatment of cancer, mAbs are most widely studied targeting ligands for diagnosis and therapy [236]. As carrier molecules, they have the ability to selectively localize in tumor tissue upon intravenous injection [237, 238]. Humanized and chimeric mAbs such as trastazumab,

bevacizumab, cetuximab, and panitumumab have been used in the treatment of breast, colorectal, lung, and gynecological cancers [239]. Despite these clear merits, the use of mAbs for monotherapy tends to be variable and non-curative due to their low potency [240, 241].

Various strategies adopted to enhance the potency of antibodies, such as combination with chemotherapy [242], radiation therapy [243], thermal therapy [244], hormone therapy [245], and tyrosine kinase inhibitors [246]. The combination of antibodies with chemotherapy is one of the most common and widely accepted strategies for treatment of cancer, and provides advantage of simultaneous targeting of multiple cellular pathways occurs resulting in prevention of cancer spread [247, 248]. For example, adjuvant treatment of Herceptin with paclitaxel leads to significant improvement in overall survival rate of patients with HER-2 positive cancer [249]. Herceptin has also been used in combination with other chemotherapeutic drugs such as docetaxel [250], gemcitabine [251], capecitabine and CMF (cyclophosphamide, methotrexate, and fluorouracil) [252].

Another strategy is to combine immunotherapy with hormone therapy [245, 253]. Level of hormonal receptors such as estrogen receptor and progesterone receptor are validated for administration of hormonal therapy [254-256]. Combination of Herceptin with hormonal therapy with drugs such as tamoxifen [253], and aromatase inhibitors [257] has been shown to improve outcome in patients with HER-2 overexpression.

Antibodies have also been used in combination with radiotherapy [243]. Radiotherapy has been employed for several years in combination with chemotherapy after surgery and is widely accepted procedure for cancer treatment [258]. It mainly exerts its cytotoxic effect on cells by inducing DNA damage [259]. Herceptin when used along with radiotherapy in clinical trials demonstrated improved clinical benefit with no significant cardiotoxicity [260, 261] .

3.2.2. Strategies to increase therapeutic efficacy of monoclonal antibodies

3.2.2.1. Multivalency

Simultaneous interaction of multiple ligands to multiple receptors has been shown to lead to an increase in avidity in biological systems [262]. Naturally occurring antibodies are classified as IgM, IgG, IgE, IgD and IgA. The majority of mammalian IgG antibodies consist of two antigen binding sites (Fab) and one constant region (Fc). Binding to two antigens simultaneously contributes to enhanced functional avidity of IgG's and longer residence time on cell surfaces [263]. Some antibodies may form higher valency complexes such as a dimer (IgA) or pentamer (IgM). Progress in genetic engineering has enabled easy manipulation of antibody structure to convert recombinant antibodies or their fragments into a multivalent format with the aims of improving the specific properties of antibodies [264]. The structure of the antibody can be modified, either *via* chemically [265] or recombinant technology [266] into a multivalent and/or a multispecific format to improve the stability [267], functional affinity [44], effector function [268], cytotoxicity [269], biodistribution, and pharmacokinetic profile [45].

For example, administration of tetravalent IgG was shown to significantly reduce the tumor growth rate upon homodimers as compared to the parental IgG [270]. The use of trivalent single-chain antibody fragment $F(ab)_3$ complexes resulted in increased tumor uptake as compared to divalent $F(ab)_2$ [271, 272]. Multimerization through engineering has also been applied for therapeutic antibodies, such as Herceptin. It was demonstrated that when anti-HER2 741F8 (scFv) was constructed in a divalent format, there was a 3.5 to 4-fold increase in tumor accumulation as compared to monovalent scFv [273]. In another study, multimerization of anti-HER-2 4D5 into di- and tetravalent minibodies led to significant improvement in functional affinity [45, 274].

3.2.2.2. Cell-mediated immunity

Immune cells such as natural killer cells (NK), monocytes, and macrophages have the ability to serve as a natural defense mechanism against cancerous cells, through certain mediating processes such as antibody-dependent cellular cytotoxicity or complement-mediated lysis [275]. The reaction is triggered when the Fc region of the antibody binds the tumor cell, and the tumor cell is recognized by the Fcγ receptors on immune effector cells and results in phagocytosis and the release of granzymes leading to cell lysis [276]. Rituximab, monoclonal antibody used in the treatment of non-Hodgkin's lymphoma acts by interacting with the Fc receptor of natural killer (NK) cells [277, 278]. Glycosylation or the incorporation of specific sugar residues on the antibody's Fc region affects its binding with the immune cells. Degree of glycosylation can be controlled through protein engineering and may be employed for improving antibody's stability, activity, pharmacokinetic profile and immunogenicity [279, 280]. In some cases, "defucylation" or the removal of core fucose residue has been performed [281]. For example, more than 50 fold improvement in antibody-dependent cellular cytotoxicity (ADCC) response was achieved through improved IgG binding to Fcγ receptor IIIa (FcγIIIa) [281-283]

3.2.2.3. Attaching drug molecules to antibodies

Antibody-drug conjugates (ADCs) are an emerging class of biotherapeutics with the potential to deliver highly potent drug specifically to the target cells [284-286]. ADCs combine the specificity of an antibody with the potency of small molecule anticancer drugs (Fig. 16). The resultant construct can efficiently localize in tumor cells and deliver its payload. Although the concept has been around for a long time, early ADCs had limited success in clinical trials due to limited selectivity, insufficient potency, and potential to cause immunogenicity [287, 288].

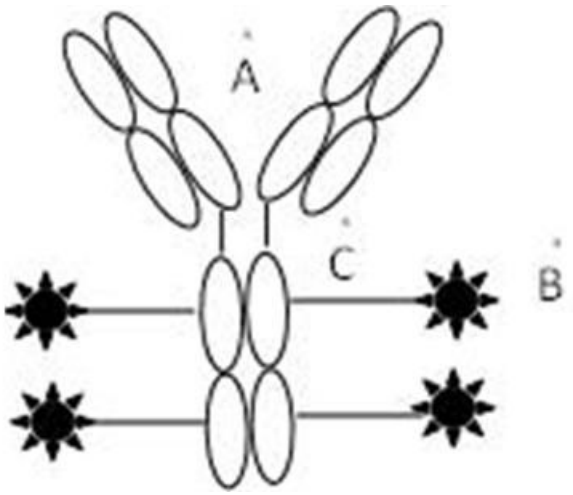

Fig. 16. Diagrammatic representation of an antibody-drug conjugate. Antibody (A) is attached to drug molecules (B) with a covalent linker (C).

The approval of Mylotarg (gemtuzumab ozogamicin) for patients with acute myeloid leukemia (AML) in 2000, there has been a renewed interest in ADCs, particularly in cancer therapy. In 2011, another ADC, Adcetris (Brentuximab vedotin), was approved by US-FDA for treating lymphoma. Several companies have ADC products in various stages of clinical development.

ADCs typically have three components: an antibody, small molecule drug, and a linker. Antibodies function as the targeting element in the construct and help in localizing the ADC into the tumor cells. Extensive research that has been done to improve the specificity of antibodies towards certain surface antigens and these advances can be leveraged in the rational design of the ADCs [289, 290]. Previously ADCs were mostly constructed from murine or chimeric antibodies which results in low binding affinity, faster clearance, and immunogenicity [291]. These concerns have been addressed lately by use of humanized or human antibodies with high target specificity and affinity. Small molecule drugs that have been used in ADCs are cytotoxic agents that target either tubulin or cellular DNA [292]. Examples of therapeutic agents conjugated to antibodies are summarized in Table 6.

Table 6. List of antibody-drug conjugates approved by FDA.

Antibody-drug conjugate (ADC)	Antigen	Conjugated Drug	Cancer	Reference
mAb-DM1	CD56	Maytansine	Lung	[293]
Mylotarg	CD33	Ozogamicin	Leukemia	[294]
BR96-doxorubicin	LeY	Doxorubicin	Breast	[295]
mAb-MMAF	CD70	Auristatin	Renal	[296]
mAb-MMAE	CD30	Auristatin	Hodgkin	[297]

These molecules are generally very potent but lack selectivity towards target cells. Therefore, when administered systemically, they exhibit toxicity towards normal tissues even at very low doses which severely limits their application as anticancer agents [298, 299]. Conjugation with a targeting element such as an antibody drastically reduces the dose required and can provide efficient tumor targeting.The attachment of antibody require a linker that conjugate the drug with the monoclonal antibody covalently without affecting their individual function [300, 301]. Linkers are a key component to a successful ADC as they must be designed to be stable during systemic circulation but degrade in the cellular environment to release the cytotoxic agent [302-305]. Therefore, routing of drug into the desired component in the cell can be adjusted by choosing the appropriate linker. The most commonly used linkers include hydrazone linkers that degrade in the acidic microenvironment of the lysosomes and disulfide-based linkers that are cleaved in the reductive environment of the cytosol [306-308].

For example, hydrazone linkers are designed so that they can be to be pH-sensitive and release drug in slightly acidic compartments of the cell, such as lysosomes [309]. Lysosomal drug release can also be achieved by using peptide linkers that can be cleaved by lysosomal proteases such as cathepsins [310]. Peptide linkers such as the valine-citruline linker are also commonly used, especially for auristatin drugs [311]. Recently polyethylene-based linkers (PEG)

have been explored to improve solubility and extend circulation half-life of the conjugate [312, 313]. They have been attached not only to antibodies but also several nanoparticles.

3.2.3. HER-2 receptor signaling

The EGFR family of transmembrane receptor comprises of HER-1, HER-2, HER-3 and HER-4 [314, 315]. They are 185 kDa and comprise of three specific regions extracellular domain (ECD), membrane spanning region, and cytoplasmic tyrosine kinase domain. These receptors are crucial for normal growth and functioning of cells, and can be activated upon the binding to various EGFR proteins and growth factors [316-318]. Activation of the receptor can lead to either cross-linking of same receptor to the form homodimer or heterodimer between two EGFR receptors, which in turn results in phosphorylation of tyrosine residues in the intracellular domains of the receptor and triggering activation of pathways such as phosphoinositol (PI3K), mitogen activated protein kinase (MAPK) and phospholipase (PLC) [319, 320]. Upon phosphorylation, the downstream signaling events lead to the promotion of cell growth and inhibition of apoptosis. Among the HER family, HER-2 has emerged as an attractive therapeutic target for breast cancer. Under normal conditions, HER-2 levels are low on surface of epithelial cells; however, gene amplification up to 20-30% is observed in breast cancer [46-48]. Overexpression of HER-2 has also been noted in many other human cancers such as, ovarian [321], lung [322], and gastric cancer [323]. In addition, clinical data has shown that enhanced HER-2 levels are associated with metastasis potential and overall poor patient prognosis [72].

3.2.4. Herceptin

Herceptin is a humanized monoclonal antibody directed against the ECD of HER-2 and was the first monoclonal antibody approved by FDA in 1998 for the treatment of patients with metastatic breast cancer (MBC) [324]. Clinical trials of Herceptin have been conducted in both

mono-therapy and in combination with chemotherapy [325-330]. Initial approval of Herceptin was based on randomized phase III studies combining Herceptin with chemotherapeutic agents such as paclitaxel and anthracycline in previously untreated patients and showed significant improvement in overall survival rate, progression free survival, and objective response rate over treatment with chemotherapy alone. As single therapy agent in MBC, Herceptin resulted in overall response rate of 19-26% [327]. Subsequent clinical trials have shown that Herceptin could be combined with other therapeutic agents such as docetaxel [328], gemcitabine [329] and vinorelbine [330]. Herceptin has also been used to improve targeting and reduce systemic toxicity by conjugating to a variety of drugs or drug loaded nanocarrier systems such as quantum dots, liposomes, nanoparticles, and iron oxide nanoparticles [331-333].

3.2.5. Herceptin: Mechanisms of action

3.2.5.1. Disruption of downstream MAPK and PI3K/Akt signaling pathways

The two main pathways downstream of HER-2, phosphoinositol-3 kinase (PI3K) and mitogen activated protein kinase (MAPK) pathways are crucial for cell growth, proliferation, and inhibition of apoptosis [334, 335]. Interference in the i.e. MAPK and PI3K is most widely accepted mechanism that is crucial for the inhibitory action of Herceptin [336]. It is believed that the binding of Herceptin to the HER2 receptor prevents the dimerization of HER-2 and subsequent phosphorylation of downstream signaling substrates such as Akt [337] (Fig. 17). In a preclinical study, the binding of Hereptin to HER-2 overexpressing breast cancer cells lead to upregulation of tumor suppressor PTEN (phosphatase and tensin homolog) and downregulation of PI3K activity [338]. There is also evidence to suggest that the binding of Herceptin to HER-2 can result in inhibition of tyrosine kinase Src and, thus, increase PTEN level, which is a tumor suppressor [338].

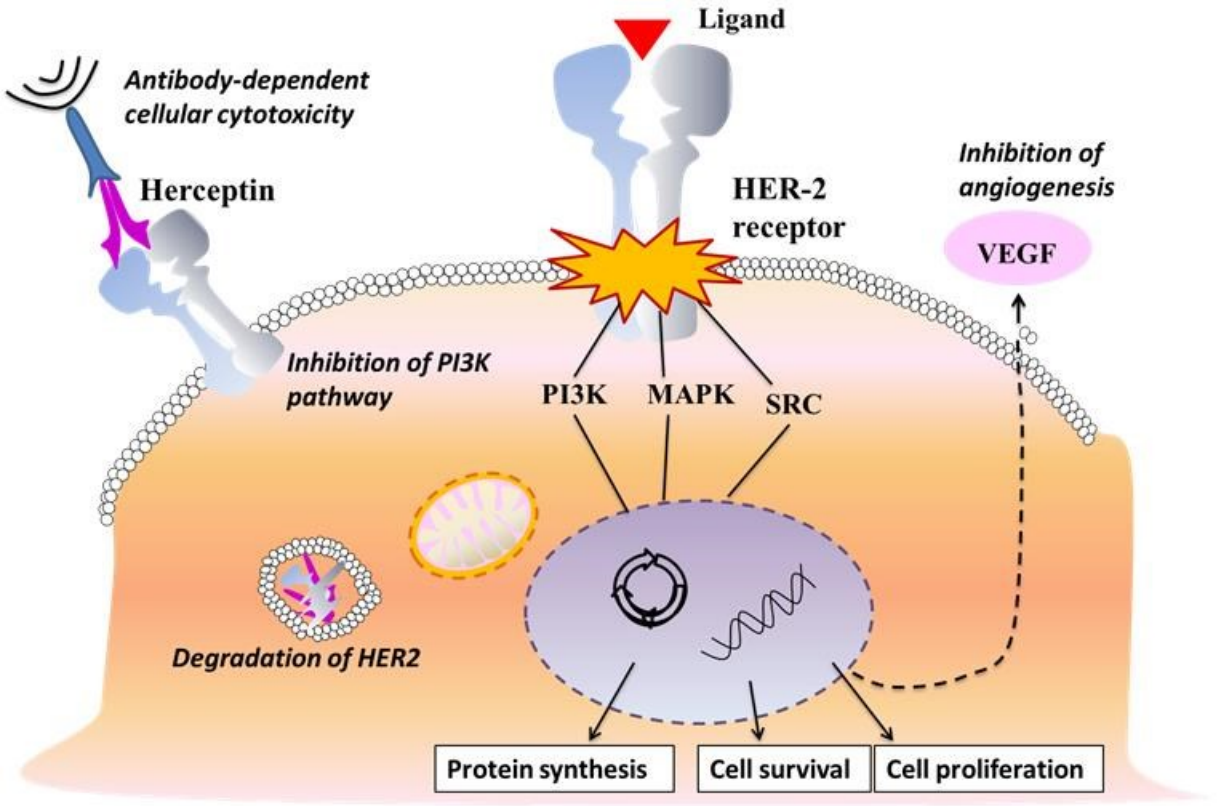

Fig. 17. Schematic scheme showing the various mechanism of action of Herceptin.

3.2.5.2. Inhibition of angiogenesis

In cancer, there is often high vascularization in tumors since they require constant supply of nutrients for their growths and proliferations [339, 340]. It is reported that HER-2 positive tumors overexpress vascular epidermal growth factor receptor (VEGF). In a preclinical study involving HER-2 overxpressing cells, Herceptin treatment was shown to suppress angiogenesis and vascularization due to downregulation of VEGF [341]. Similar observation was observed in mice when Herceptin treatment led to normalization of blood vessels [342]. When Herceptin treatment was combined with Paclitaxel, synergistic results were obtained [343]. This was believed to be due to the fact that paclitaxel is more efficient in delivery to tumor due to normalization of tumor vasculature [343].

3.2.5.3. Induction of antibody-dependent cell cytotoxicity

Antibody-dependent cellular cytotoxicity (ADCC) is one of the major mechanisms of action of Herceptin. Immune effector cells, such as natural killer cells have Fcγ receptor which can be detected by Fc portion of Herceptin [344]. Binding of Herceptin to HER-2 receptor attracts immune cells to tumor sites and results in lysis of HER-2 positive target cells (Fig. 17). This was evidenced by study in which antitumor activity of Herceptin was markedly reduced in mice bearing defective Fcγ receptors [345].

3.2.5.4. HER-2 degradation

Inhibitory action of Herceptin may be due to internalization and degradation of HER-2 receptor. Herceptin first binds to the HER-2 receptor, and the antibody bound receptor undergoes sorting in degradation compartments in the cell, a process known as "ubiquitination" through the activation of enzyme ubiquitin ligase cCbl [346]. A study previously demonstrated that Herceptin can enhance the activity of ubiquitin ligase c-Cbl, which further promotes HER-2 degradation [347].

3.2.5.5. Inhibition of ErbB2 extracellular domain proteolysis

Studies have shown that 185 kDa HER-2 receptor can undergo proteolytic cleavage to form a 115 kDa HER-2 fragment. Interestingly, patients with high level of 115 kDa p95HER2 fragments in their serum are associated with more aggressive tumors [348]. When treated with Herceptin, these patients exhibited dose-dependent decrease in HER-2 ECD level in serum and improved tumor response rates and PFS [348]. Previous study indicated that Herceptin prevents proteolytic cleavage through steric hindrance, which could be possible mode of action for Herceptin [349].

3.2.6. Limitations associated with Herceptin therapy

Herceptin has been a remarkable example for successful monoclonal antibody therapy; however, despite the success of Herceptin, there are limitations due to potential development of side-effects [350]. It is found that about 4% of the patients treated with Herceptin developed congestive heart disease (CHF) [351, 352]. Moreover, the incidence of cardiotoxicity increased upto 28% when patients were co-administered chemotherapeutic agents such as anthracyclines [353].

Another cause of modest duration of response is development of primary or secondary resistance. It has been observed that about 70% of patients who initially responded to therapy experienced metastatic progression of the disease within one year [354]. Very little information on development of primary and secondary resistance, however multiple potential mechanisms of resistance to Herceptin were proposed [355, 356]. Understanding the mechanisms behind Herceptin resistance is crucial for development of novel anti-HER-2 strategies for breast cancer.

3.2.7. Strategies to encounter Herceptin resistance

There are various strategies that are used to overcome resistance of Herceptin towards HER-2 positive cells (Table 7). Herceptin has been administered along with other antibodies, such as Pertuzumab. Pertuzumab acts by preventing heterodimerization of HER-2 with other members of HER receptor family [357]. Phase III clinical trials are being performed to evaluate the outcome of co-administering Herceptin and Pertuzumab in patients with HER-2 overexpressing metastatic breast cancer [358]. Herceptin has also been combined with agents targeting other pathway such as inhibitors of mTOR signaling and PI3K-AKT pathway such as RAD001 (Novartis, NY) [359] and CCI-779 (Wyeth-Ayerst; Madison, NJ) [360]. In another strategy, Herceptin has been fused with toxins, such as DM1 [361].

Table 7. Examples of various drug combinations to overcome resistance of Herceptin.

Drug/antibody	Pharmaceutical company	Phase of study	Combination with Herceptin	Reference
mTOR inhibitors				
Everolimus (RAD001)	Novartis	Phase II	Yes	[359]
PI3K inhibitors				
BKM120	Novartis			
Angiogenesis inhibitors				
Bevacizumab	Genentech	Phase II	Yes	[362]
Dimerisation inhibitor				
Pertuzumab	GlaxoSmithKline			[358]
Pazopanib	GlaxoSmithKline	Phase III	No	[363]
Tyrosine Kinase Inhibitors				
Neratinib (HK-272)	Pfizer	Phase II	Yes	[364]
Afatinib (BIBW-2992)	Boehringer Ingelheim			[365]
Antibody-Drug Conjugate				
Herceptin-DM1	Genentech	Phase II	----	[361]

Lapatinib belongs to the family of inhibitors of tyrosine kinase activity of receptors such as EGFR and HER-2 and has proven to be successful in inhibiting the downstream signaling through these receptors in preclinical studies [366]. The synergistic effect of Herceptin and lapatinib has been evaluated in advanced stage of breast cancer [367].

3.2.8. Nanomaterial as tumoral delivery cargos

Over the last several decades, numerous nanoparticles have been developed for both imaging and therapeutic application [368-370]. Designing material at nanometer scale provides the flexibility of modifying some of their important fundamental properties for enhancing drug

deliver, such as solubility, biodistribution, pharmacokinetic properties, which can be translated into enormous advantages in clinical situations by causing reduction in dosage, better pharmaceutical effects, minimization of side-effects, and enhanced drug stability. In the field of imaging, nano-scaling of materials has been exploited to achieve enhanced optical, magnetic and radioactive signals [371].

Nanocarriers have been investigated for a broad range of diagnostic and therapeutic applications. Owing to their size, nanocarriers provide unique advantages when compared to larger systems, such as improved biodistribution, pharmacokinetics, and reduction of side-effects. [372-375]. Nanocarriers have been of particular interest in tumor targeting because they are flexible in meeting the needs of pathological conditions of cancer. Traditionally, two strategies that have been employed for delivering nanocarriers to the tumors, passive and active targeting [376]. Passive targeting utilizes an important characteristic of tumor anatomy. Growing tumors have leaky vasculature with pores in the range of 100-400 nm that allow extravasation of particles smaller than 100 nm. The ability of particles < 100 nm to pass through leaky vasculature of tumor presents an excellent opportunity for passive targeting of drugs [377, 378]. Upon reaching the tumor tissue, nanocarriers release the drug. Clearance of nanocarriers from the tumor is slow due to impaired lymphatic drainage. This phenomenon, known as enhanced permeability and retention (EPR), results in preferential accumulation of nanocarriers in the tumor tissue [379]. However, a majority of nanoparticles tend to undergo non-specific uptake by reticuloenothelial system (RES) such as monocytes and macrophages and therefore have less circulation time. Therefore, nanocarriers have been to have longer circulation time and escape recognition by reticuloendothelial system (RES). Polyethylene glycol is routinely used for this application as it can reduce protein interaction on the surface due to its hydrophilicity [380].

Although passive targeting is attractive, it does have some limitations such as dependence on tumor pore size and elevated interstitial pressure which make this approach inefficient in certain cases [381, 382]. Active targeting involves conjugation of a drug, biologics, or a diagnostic agent on the surface of a nanocarrier [236, 376, 383]. Moieties that can be delivered through conjugation include peptides [384], proteins [385], polysaccharides [386], DNA [387], and siRNA [388]. Nanocarriers provide large surface area to volume ratios which facilitate greater binding efficiency and penetrability compared to larger systems. Active targeting as generally been more successful compared to passive targeting since the assembly is internalized quickly inside the cells after interaction with surface proteins [389]. Antibodies have been used most commonly as a targeting agent. Conjugation of nanoparticles with antibodies offers the unique advantage of combining specificity of antibodies with the size advantage of nanoparticles. A number of studies have explored targeting efficiency of nanoparticles conjugated with antibodies [390-393]. Results suggest that active targeting may not necessarily be superior to passive targeting in terms of tumor localization but would lead to more efficient cellular internalization [376]. Whereas in case of passive targeting, the assembly may not be internalized quickly leading to eventual clearance from the tissue. Active targeting is also more susceptible to clearance by the RES system since the targeting molecule is exposed on the surface [394]. To further enhance the capability of entrapment, efforts are directed towards creating functionalizing nanoparticles surfaces with targeting molecules, such as antibodies, peptides, small molecules and oligonucleotides. The combination of small size of nanoparticle and the specific recognition properties of the targeting moiety allows excellent discrimination between hypervasculature and established blood vessels and accumulation at desired locations [395, 396].

3.2.9. Self-assembly peptide based material

Materials derived from self-assembly peptides are generating interest in a variety of biomedical applications such as tissue engineering, drug delivery and diagnostic imaging [397-399]. The first self-assembly peptide nanofiber sequence EAK16, "zuotin" was discovered from yeast. It was a 16 amino acid residue and contained DNA binding properties. After its initial discovery, there have been numerous reports on use of peptide nanofibers in a variety of biological and biomedical applications Their main advantage is biocompatibility, flexibility of design and structure, and low immunogenicity [400, 401]. The design principle of most peptide nanofibers is the placement of alternating hydrophobic and electrostatic amino acids. Individual beta sheet peptide in nanofiber is about 8-16 amino acids long. Under aqueous conditions, there is formation of stable beta sheets which is mediated by electrostatic interaction, hydrophobic interaction, and Van der Waals interaction [402, 403]. The formation of these peptide assemblies may be enhanced upon exposure to physiological salt and different pH environments [404, 405]. Once formed, beta sheet peptides are stable across wide range of temperature, pH, and presence of denaturating agents such as urea and guanidine hydrochloride [207]. Depending on the nature of self-assembly, the fibers may be of varying diameters (7-20 nm), but are usually composed of 99% water. Another interesting property of peptide nanofibers is that they mimic extracellular matrix, and therefore have been used to improve cell adhesiveness, induce differentiation and proliferation in three-dimensional tissue engineering and regenerative medicine.

3.2.10. Nanofibers as a carrier for drugs

Recently, there are increasing recognitions of using peptide-based nanofiber (PF) in tissue engineering [207], diagnostic imaging [11, 13], and drug delivery [208, 222]. The main advantage of using peptide nanofiber is that they are composed from biocompatible amino acids.

The uniqueness of PF is its flexibility to subject to modification. Since nanofibers are composed of amino acids, the side groups of the amino acids can be used to conjugate functional moities, such as small molecules, proteins and, fluorescent dyes. For example, functional motifs such as collagen derivatives and platelet derived growth factor receptor (PDGF) have been integrated into PFs to retain the degree of cellular entrapment or recruitment in tissue engineering [406, 407], or peptide substrates have been inserted into PF for imaging tumor-associated protease activity [11, 13, 214]. Furthermore, various therapeutic agents including small drug molecules [408-410], peptide [411, 412], proteins [413, 414] have also been incorporated into the PFs to enhance the delivery to the target sites. The exploration of peptide nanofiber as template for multivalent presentation of molecules is especially attractive for the following reasons: (1) peptide nanofibers present certain functional groups such as $–NH_2$ and –COOH for conjugation of optical fluorophores or protein molecules (2) High loading capacity, which is not in the case of high molecular weight, which is not possible in the case of polymers [415]. (3) Flexibility of design and structure and scope for multifunctional platform and imaging application, and (4) Ease of synthesis and biocompatibility. Multiple antibodies can be covalently attached to the surface of a nanomaterial such as gold nanoparticles [416], quantum dots [417], magnetic nanoparticles [418], liposomes [419], polymeric nanoparticles [420] and dendrimers [421]. For example, antibodies against intercellular adhesion molecule 1 (anti-ICAM1) have been attached to a polymeric nanoparticle to improve the pulmonary targeting [420, 422].

In other study, antibodies against epidermal growth factor receptor (anti-EGFR) were conjugated to a gold nanoparticle to enhance its tumor accumulation [423]. Examples of self-assembly peptide based nanofibers used in drug delivery application have been listed in Table 8.

Table 8. Self-assembly peptide-based material used in drug delivery applications.

Peptide	Drug/Protein	Application	Reference
Heparin-binding peptide amphiphile	VEGF/FGF-2	Islet transplantatio	[424]
AcN-RARADADARARADADA-CNH_2	PDGF-BB	Myocardial protection	[425]
Ac-(R-A-D-A)$_4$-$CONH_2$	Insulin	Diabetes	[426]
RADA16-II	IGF-1	Myocardial infarction	[427]
Ac-FEFQFNFK-NH_2	Ellipticine	Cancer	[428]
RADA-16	Paclitaxel	Cancer	[429]
Palmitoyl-$A_4G_3E_3$	Camptothecin	Cancer	[430]
Dex-peptide amphiphile	Dexamethasone	Inflammation	[431]
GTAGLIGQRGDS	Cisplatin	Cancer	[216]
Taxol-SA-GSSG	Taxol	Solid Tumors	[432]
Peptide amphiphile	BMP-2	Tissue engineering scaffold	[433]
RADA16-I	--	Wound dressing	[434]
RADA16-I	EGF	Wound healing	[435]

3.2.11. Unique features of peptide nanofibers for drug delivery applications

The size of NFP is small enough to permeate through small capillaries of tumor. A large portion of the NFP consists of hydrophilic polyethylene glycol (PEG). Several PEG protein conjugates have been approved by FDA such as PEG-Asys®, PEG-intron™, Oscaspar®, Neulasta™ as demonstrated in previous studies [436]. Similar to previous studies, we expect that PEG conjugation to HER-NFP will reduce its immunogenicity, improve its stability, and prolong its half-life by preventing renal elimination and avoidance of receptor-mediated protein uptake

by reticuloendothelial system (RES) [437]. 3) A large fraction of the peptide is constructed with D-amino acids. For clinical applications, constructing nanomaterial with D-peptides is advantageous as they are highly resistant to proteolytic degradation and relatively immunologically inert in comparison to their natural counterparts [438]. Upon reaching the target, the slow degradation of D-peptides could be used for controlled drug delivery applications.

3.3. Material and methods

3.3.1. Materials

All solvents were purchased from Fisher Scientific (Fair Lawn, NJ). The amino acids were purchased from Novabiochem (San Diego, CA). Methoxyl polyethyleneglycol N-hydroxysuccinimide ester (mPEG NHS ester, average MW of 2 kDa) was purchased from Jenkem Technology USA Inc. (Allen, TX). Anisole, ethandithiol, fluorescein isothiocyanate (FITC), sodium borohydride, sodium periodate, thioanisole were obtained from Sigma (St. Louis, MO). Herceptin was purchased from Genentech (South San Francisco, CA). Cy5.5 hydroxysuccinimide ester was purchased from GE Healthcare (Piscataway, NJ). And finally, the antibody-conjugated gold nanoparticles were purchased from Rockland Immunochemicals Inc, (Gilbertsville, PA).

3.3.2. Synthesis and characterization of NFP

The NFP peptide construct ($mPEG_{2000}$-BK(*FITC*)SGASNRA-kldlkldlkldl-$CONH_2$) was synthesized on an automatic peptide synthesizer using the traditional Fmoc methodology as previously described [13, 214]. The NFP was assembled by dissolving the peptide constructs (10 mg) in 50% (v/v) acetonitrile in water (5 mL) and was further stirred overnight to evaporate the organic solvent. The resulting NFP was then homogenized by a mini-extruder (Avanti polar

lipids Ltd., Alabaster, AL) using the polycarbonate membrane (Whatman, Florham Park, NJ) of 0.1 μm pore size, which was then purified by size exclusion chromatography using Sephadex G-75 (Sigma, St. Louis, MO) in PBS buffer. The concentration of NFP was determined according to the extinction coefficient of FITC in 95% (v/v) methanol (65,000 $M^{-1}cm^{-1}$ at 500 nm), unless otherwise stated.

3.3.3. TNBSA assay

A commercial spectrophotometric 2,4,6-trinitrobenzenesulfonic acid (TNBSA) assay kit (Pierce, Rockford, IL) was employed to determine the loading efficiency of NFP. Briefly, a known concentration of NFP (30 μM, 250 μL), in Na_2CO_3 solution (10 mM, 250 μL), was mixed with TNBSA reagent (250 μL) and 10% (w/v) sodium dodecyl sulfate solution (SDS) in water (250 μL). This solution mixture was then transferred to 96-well polystyrene plate and further allowed to incubate for 3 hr at 37°C. Following incubation, the absorbance of the TNBSA-NFP adduct was read at 335 nm. Under the same conditions, a standard curve was generated based on known concentrations of L-cysteine solution (0, 15, 30, 60, and 120 μM) to calculate the percentage of free $-NH_2$ groups.

3.3.4. Conjugation of Cy5.5 to the NFP

The NFP solution (30 μM), in PBS buffer (10 mM, pH 7.4, 250 μL) was reacted with Cy5.5 NHS ester (250 ng), and allowed to incubate at room temperature in the dark for 2 hr. Following incubation, the unreacted fluorophores were removed by size exclusion chromatography using Sephadex G-75 column (GE Healthcare Biosciences, Piscataway, NJ). The fluorophore concentration was determined by absorbance according to molar extinction coefficient of Cy5.5 (250,000 $M^{-1}cm^{-1}$ at 675 nm) in PBS buffer. The total NFP peptide concentration was calculated according to molar extinction coefficient of FITC (65,000 M^{-1} cm^{-1}

at 500 nm) in 95% (v/v) methanol. To calculate the percentage of -NH_2 groups reacted with Cy5.5 *N*-hydroxysuccinimide, the total concentration of Cy5.5 was divided by the concentration of NFP peptide multiplied by 3 (the number of -NH_2 groups per peptide) and then times 100 %.

3.3.5. Synthesis of Herceptin conjugated nanofiber (HER-NFP)

A series of HER-NFP conjugates (100 nm) of different loading density of Herceptin (2, 4, 10 and 20 Herceptin per NFP) were prepared. Briefly, sodium periodate (180 mM, 50 μL) was added to varying concentrations of Herceptin (1 mg/mL, 2 mg/mL, 10 mg/mL and 20 mg/mL) in a fixed volume (50 μL) of sodium acetate buffer (10 mM, pH 4) to obtain Herceptin-to-NFP ratio of 2:1, 4:1, 10:1 and 20:1 respectively. The mixtures were then kept at room temperature for 1 hr and further dialyzed against $NaHCO_3$ solution (0.1 N) employing a membrane with 14 kDa molecular weight cut-off (MWCO) (Spectrum Laboratories Inc., Rancho Dominguez, CA) for 3 hr. NFP (20 μM, 250 μL) were then added to the solution mixture and incubated overnight. The resulting conjugates were reduced by adding sodium borohydride (1 mg) to the reaction mixture. The unconjugated antibody was then removed by dialysis using membrane with a 300 kDa MWCO in PBS buffer (10 mM, pH 7.4). The purified conjugates (HER-NFP) were homogenized and further purified by gel filtration.

3.3.6. Determination of molar ratio of Herceptin and NFP in HER-NFP

The number of peptides in each HER-NFP could be calculated from thickness of each beta-sheet strand (~0.47 nm) [439]. At the same time, the concentration of Herceptin in each HER-NFP was determined by BCA assay (Pierce, Rockford, IL). To calculate number of Herceptin conjugated to nanofiber, the concentration of Herceptin was divided by the concentration of NFP in the stock solution.

3.3.7. Confirmation of the covalent attachment of Herceptin to NFP by electrophoresis

Herceptin (300 nM), HER-NFP (300/30 nM), and a mixture of Herceptin (300 nM) and NFP (30 nM) were loaded in sodium dodecyl sulfate-polyacrylamide (SDS-PAGE) gel. The concentrations indicated were normalized for Herceptin. As negative control, NFP alone (6 μM) was also used for analysis. Electrophoreses was performed for 2 hr at 80V on a Mini-Protean 3 cell (Bio-Rad Laboratories, Hercules, CA). Following electrophoresis, the samples were stained using Coommassie Blue staining solution (Bio-Rad Laboratories, Hercules, CA). Images of the gel were taken with FluorChem 5500 imaging system (Alpha Innotech, Santa Clara, CA).

3.3.8. Transmission electron microscopy staining

HER-NFP (2 μM) suspended in PBS buffer (10 μL) was incubated with secondary anti-human IgG-conjugated gold nanoparticles (10 μL) for 1 min at room temperature. HER-NFP was incubated with anti-mouse IgG-conjugated gold nanoparticles as the control sample. The samples were then added to 200 mesh form var-coated copper grids and further stained negatively with uranyl formate solution in water (2% w/v). Excess solution was removed by adsorbing on filter paper, followed by three washes, and air dried. The grids were then examined under the TEM (JEOL 100CX, Peabody, MA).

3.3.9. Cell culture

Human breast cancer cell lines SKBr-3, MCF-7, and MDA-MB-231 cells expressing high, moderate, and low level of HER-2, respectively, were purchased from ATCC (Manassas, VA). SKBr-3 cells were cultured in McCoy's medium. MCF-7 cells were cultured in Eagle's Minimum Essential Medium (EMEM) media supplemented with insulin (10 μg/mL), also purchased from ATCC (Manassas, VA). MDA-MB-231 cells were grown in Dulbecco's Modified Eagle's medium (DMEM). All culture media were supplemented with 10% v/v fetal

bovine serum (FBS) (Mediatech Inc., Manassas, VA). All culture media was supplemented with antibiotics such as penicillin G (100 U/mL) and streptomycin (100 μg/mL), which were obtained from ATCC (Manassas, VA). All cells were cultured in incubators at 37^{o}C with 5% CO_2 under humidified conditions.

3.3.10. Cellular uptake of HER-NFP with varying density of Herceptin

HER-NFP (100 nm) preparations with varying density of Herceptin-to-NFP (H/N) ratio (2:1, 4:1, 10:1 and 20:1) were normalized to fixed concentration of Herceptin (200 nM). The HER-NFP's were then conjugated to the same amount of Cy5.5 NHS ester (250 ng) according to manufacturer's recommendation (GE Healthcare, Piscataway, NJ). The Cy5.5-conjugated HER-NFP (Cy5.5-HER-NFP) preparations were incubated with SkBr-3 cells for 12 hr. After incubation, cells were lysed in cell lysis buffer (110 μL) (Cell Signaling Technology, Danvers, MA), centrifuged at 12,000 rmp and fluorescence intensity in supernatants (100 μL) was recorded in a sub-microcuvette (StarnaCells, Atascadero, CA, USA) by a fluorescence spectrometer (Cary Eclipse, Varian, Palo Alto, CA, USA). At the same time, a standard curve of known concentration of Cy5.5-Herceptin (0, 10, 20, 40, 80, 160 and 450 nM) was plotted. Amount of Herceptin internalized was interpolated from standard curve. All samples were excited at 665 nm, and their emissions were recorded at 684 nm. To investigate kinetics of internalization, either Cy5.5-HER-NFP (H/N 10:1) or Cy5.5-Herceptin were incubated with SKBr-3 cells for 12 hr. The concentration of Herceptin was same (300 nM) in both these samples. The amount of Herceptin internalized at various time points (2, 4, 8, 12 and 24 hr) was determined using standard curve of Cy5.5-Herceptin, as described above. To investigate size-dependency on cellular uptake, Cy5.5-HER-NFP (200/20 nM) was passed through mini-extruder (Avanti polar lipids Ltd., Alabaster, AL) fitted with polycarbonate membranes (Whatman,

Florham Park, NJ) of different pore size (50 nm, 100 nm and 400 nm). Uncut Cy5.5-HER-NFP, Cy5.5-Herceptin and Cy5.5-IgG-NFP (100 nm) were treated as controls. After 12 hr of incubation, the amount of Herceptin/IgG internalized in cells for all samples was analyzed as mentioned above.

3.3.11. Cellular imaging

SkBr-3 cells (10,000 cells/ well) were seeded in a 4-chamber slide (Thermo Fisher Scientific, Rochester, NY) in McCoy's culture media and allowed to attach for 24 hr. Cy5.5-HER-NFP, at a different density of H/N ratio (4:1, 10:1 and 20:1), in PBS buffer (10 mM, 100 μL) were then added to the chambers. All HER-NFP preparations were normalized to same concentration of Herceptin (200 nM). After 12 hr of incubation, the cells were imaged under a fluorescent microscope (Olympus IX-81, Melville, NY). The cell nucleus was also counterstained with DAPI staining (1 μg/mL) (Invitrogen, Carlsbad, CA).

3.3.12. Determination of cytotoxicity of HER-NFP

MTS assay was performed according to the manufacturer's recommendation (Promega, Madison, WI). All cancer cells (3,000 cells/well) were seeded on a 96-well plate and allowed to attach for 24 hr. Herceptin (67 nM), HER-NFP (H/N: 67/6.7 nM), IgG-NFP (H/N: 67/6.7 nM), or NFP (6.7 nM) in McCoy's culture media (200 μL) supplemented with FBS (5% v/v) were then added to the cells. At different time points, a solution of 3-(4,5-dimethylthiazol-2-yl)-5-(3-carboxymethoxyphenyl)-2-(4-sulfophenyl)-2H-tetrazolium, inner salt (MTS reagent) was added (20 μL) to the wells. The absorbance was then monitored at 490 nm in a microplate reader. The cell viability was calculated as a percentage of cell samples incubated with the corresponding culture media only.

3.3.13. Lysosomal staining

SKBr-3 cells were seeded on in 4-chamber slide (Thermo Fisher Scientific, Rochester, NY) in the McCoy's culture media and allowed to attach for 24 hr as described in previous section. Either Cy5.5-Herceptin (67 nM) or Cy5.5-HER-NFP (67/6.7 nM) in McCoy's culture media (200 µL) supplemented with FBS (5% v/v) were then added to the cells. After 12 hr of incubation, old media was discarded and the cells were washed twice with PBS buffer (10 mM, pH 7.4). Cells were incubated with Lyso Tracker® dye (1 µg/mL), in McCoy's culture media (200 µL) (Invitrogen, Carlsbad, CA) at 37^{o}C for 30 min. The cells were then imaged under fluorescence microscope as described above.

3.3.14. Western blot

To perform the western blot analysis, SKBr-3 cells (1.5 x 10^{6}) were seeded in a 6-well plate. Herceptin (H/N: 67 nM), HER-NFP (H/N: 67/6.7 nM), IgG-NFP (H/N: 67/6.7 nM), and NFP (6.7 nM) in McCoy's culture media (2.5 mL) supplemented with FBS (5% v/v) were incubated along with the cells. After 12 hr of incubation, the old media was discarded and the cells were washed twice with PBS. For cell lysis, denaturation buffer (Cell Signaling Technology, Danvers, MA) was added (200 µL) to the cells, and the cell debris was removed by centrifugation (1000 rpm). The total protein concentrations in the supernatants were determined by a micro-BCA assay kit (Bio-Rad, Richmond, USA). The samples (20 µg, 10 µL) were then resolved by electrophoresis using a SDS-PAGE gel. The proteins were then transferred to a Hybond™-P membrane (Amersham, Piscataway, NJ). The membrane was then probed with primary antibodies against HER-2, total AKT, phosphorylated AKT at serine 473 (p-AKT), and phosphorylated ERK1/2 at threonine 202/tyrosine 204 (p-ERK1/2) (Cell Signaling Technology, Danvers, MA). The proteins were then detected by horseradish peroxidase conjugated anti-

mouse or anti-rabbit secondary antibody (Cell Signaling Technology, Danvers, MA) for 1.5 hr. The membranes were washed again with Tween 20-TBS (0.1% v/v) and the various protein bands were detected with ECL™ Western Blot Detection Reagents (Amersham, GE Healthcare Bio-Sciences, Piscataway, NJ) on Blue Ultra Autorad Film (BioExpress®, Kaysville, UT).

3.4. Results and discussion

3.4.1. Synthesis of NFP platform

The peptide constructs (mPEG-B-K(*FITC*)-SGASNRA-[kldl]$_3$) were synthesized in solid phase peptide synthesis, assembled into 2-dimensional nanofibers, and further homogenized into the desired lengths as previously described [13, 214]. The number of peptides in NFP could be calculated based on the distance (0.47 nm) between two peptide strands in a typical β-sheet structure [439].

3.4.2. Determination of number of amino functional groups available for bioconjugation

NFP consisted of multiple -NH_2 and -COOH groups contributed by the side chains of the lysine and aspartic acid residues, respectively. Theoretically, NFP could provide a maximum of 639 reactive sites for each of the two functional groups. To determine the number of -NH_2 groups available for bioconjugation, a 2,4,6-trinitrobenozene sulfonic acid (TNBSA) assay was performed (Fig. 18). TNBSA reacted with the -NH_2 groups to form TNBSA-NFP adduct that could be monitored by an increase in the absorbance at 335 nm [440]. Using the TNBSA assay, we calculated there was only 60% of the -NH_2 groups reacted to the TNBSA. On the other hand, a maximum of 35% -NH_2 groups were available for reacting with Cy5.5 *N*-hydroxysuccinimide ester (Fig. 19). Overall, our results suggested that some of the -NH_2 groups could be hindered by the bulky mPEG presented in the NFP and that the degree of couplings might depend on the molecular size of the reactant.

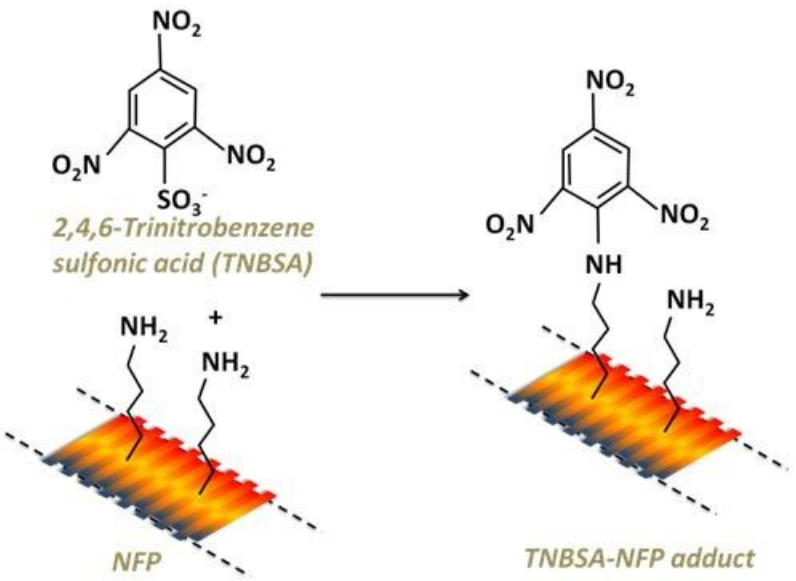

Fig. 18. Synthetic scheme of conjugation of 2,4,6-trinitrobenzenesulfonic acid (TNBSA) to nanofiber precursor (NFP).

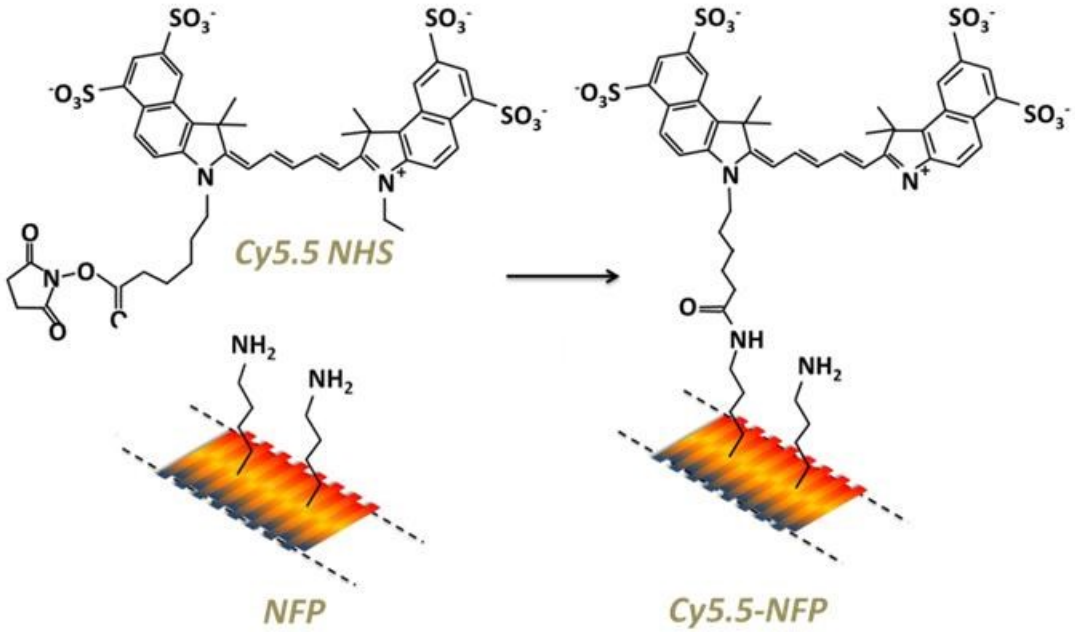

Fig. 19. Synthetic scheme of conjugation of Cy5.5 NHS ester with nanofiber precursor (NFP).

3.4.3. Synthesis and characterization of Herceptin-NFP conjugate (HER-NFP)

Next, we attached Herceptin, an antibody against HER-2 overexpressing metastatic breast cancer, to the NFP (Fig. 20). A previously described sodium periodate oxidation was employed as the bioconjugation chemistry [441]. This method gave the advantage to conserve the binding affinity of antibody after reaction [442, 443].

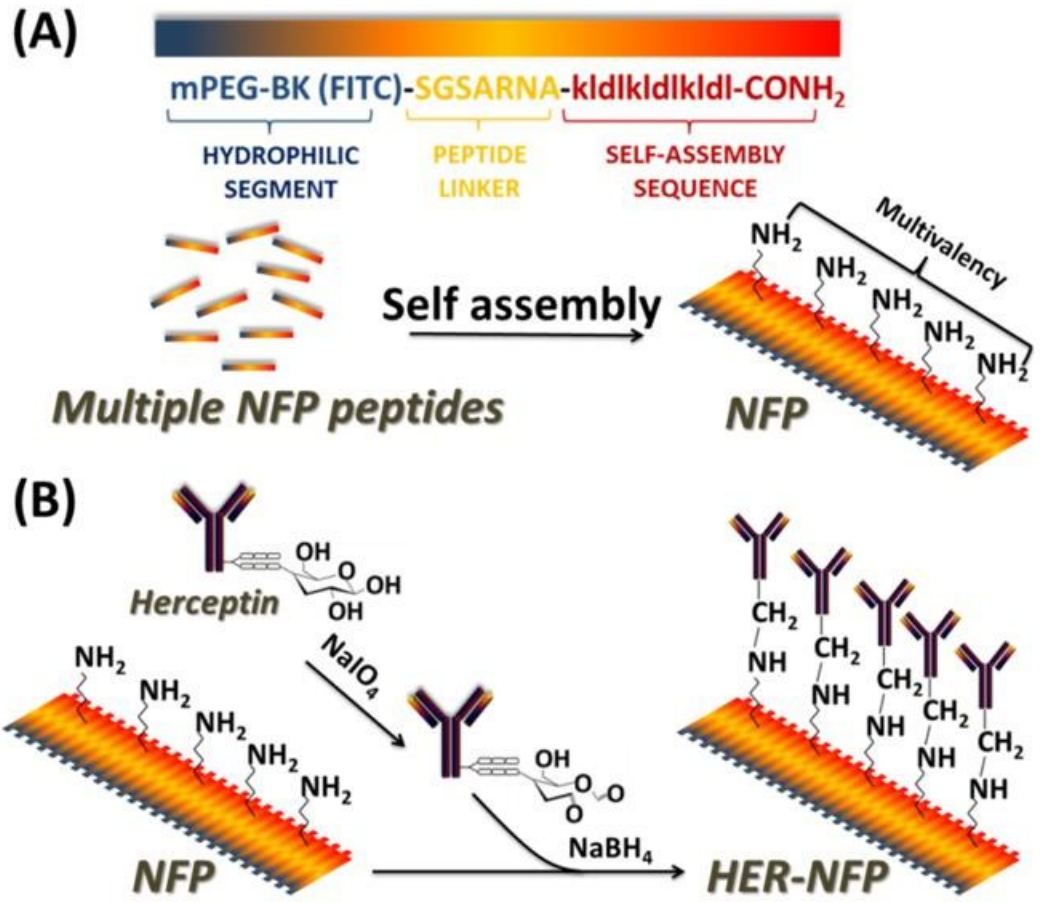

Fig. 20. Design and synthesis of HER-NFP. (A) The peptide construct of HER-NFP was composed of a self-assembly peptide sequence (kldlkldlkldl), a linker peptide sequence (SGASNRA), methoxypolyethylene glycol (mPEG), and a fluorescence label (FITC). The nanofiber (NFP) was assembled from multiple NFP peptides (mPEG-BK(*FITC*)SGASNRA-$[kldl]_3$-NH_2) and had multiple –NH_2 groups originated from lysine residues for bioconjugation**.** (B) A synthetic scheme of HER-NFP.

The resulting conjugate (HER-NFP) was purified by dialysis. The total number of NFP in the stock solution was determined by absorbance (Fig. 21), according to the extinction coefficient of fluorescein isothiocyanate in 95% methanol (65,000 $M^{-1}cm^{-1}$ at 500 nm). The amount of Herceptin was quantified with micro-bicinchoninic acid (BCA) protein assay (Fig. 21B) [444].

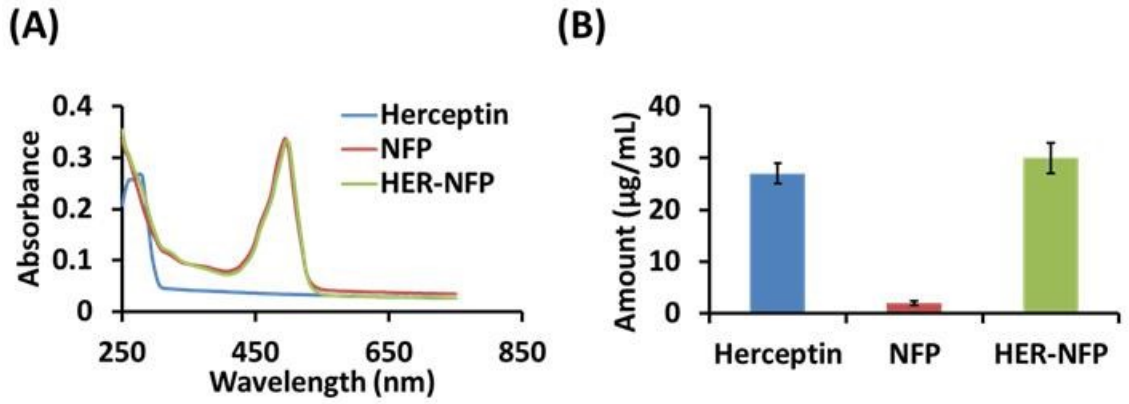

Fig. 21. Determination of molar ratio of NFP peptide to Herceptin. (A) Absorbance spectra of Herceptin (250 nM), NFP (5 µM) and HER-NFP (250 nM). The concentrations of indicated samples were based on Herceptin. (B) The amount of antibody was determined by Micro-BCA assay.

Electrophoresis was then performed to confirm that Herceptin was covalently attached to the nanofiber. After electrophoresis, HER-NFP appeared as a single band showing a significantly higher molecular weight than Herceptin. HER-NFP was pure, as no unconjugated Herceptin was found (Fig. 22A and 23). The fact that HER-NFP band was not found in a physical mixture of Herceptin and NFP further suggesting that Herceptin was covalently conjugated to the surface of the HER-NFP.

To confirm HER-NFP displayed in a multivalent format, immuno-gold staining was performed using secondary anti-human IgG-conjugated gold nanoparticles (Fig. 22B). The transmission electron microscopy images of immuno-stained HER-NFP revealed that multiple antibodies were attached on the nanofiber (Fig. 22C). On the contrary, there was no staining

observed when control anti-mouse IgG-conjugated gold nanoparticles were used (Fig. 22C). The valency of the HER-NFP could be adjusted either by attaching more Herceptin to the nanofiber (data not shown) or using the nanofiber with a longer length (Fig. 22C).

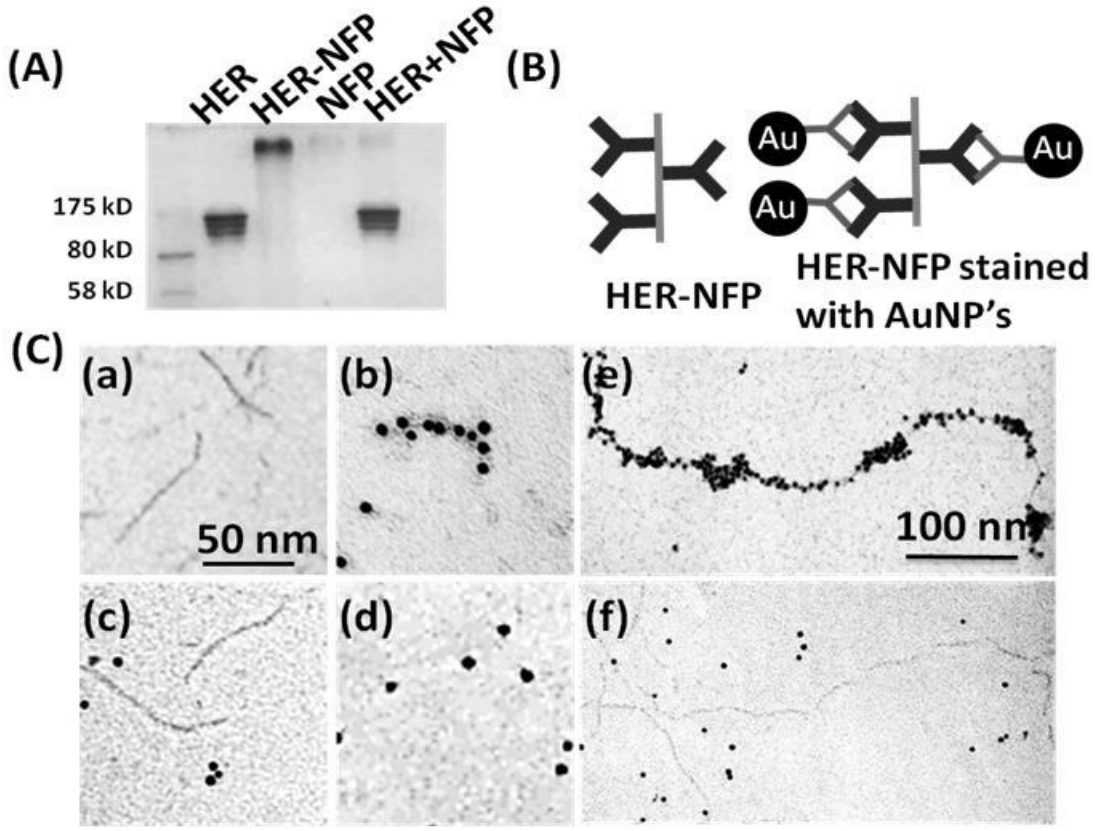

Fig. 22. Characterization of HER-NFP. (A) A comparison of the molecular weights of Herceptin (300 nM), NFP (6 μM), HER-NFP (H/N ratio: 300/30 nM), and a physical mixture of Herceptin (300 nM) and NFP (30 nM) by electrophoresis. The gel was stained with Coommassie Blue solution prior to imaging. (B) A schematic diagram showing the immuno-gold staining of HER-NFP. (C) The TEM images of (a) HER-NFP only (100 nm), (b) HER-NFP stained with secondary anti-human IgG-conjugated gold nanoparticles, and (c) HER-NFP stained with secondary anti-mouse IgG-conjugated gold nanoparticles. (d) A control TEM image showing a suspension of secondary anti-human IgG-conjugated gold nanoparticles. (e) A TEM image of HER-NFP (1-2 μm) stained with secondary anti-human IgG-conjugated gold nanoparticles and (f) HER-NFP stained with secondary anti-mouse IgG-conjugated gold nanoparticles. The nanofibers were negatively stained with uranyl formate in water (2% w/v).

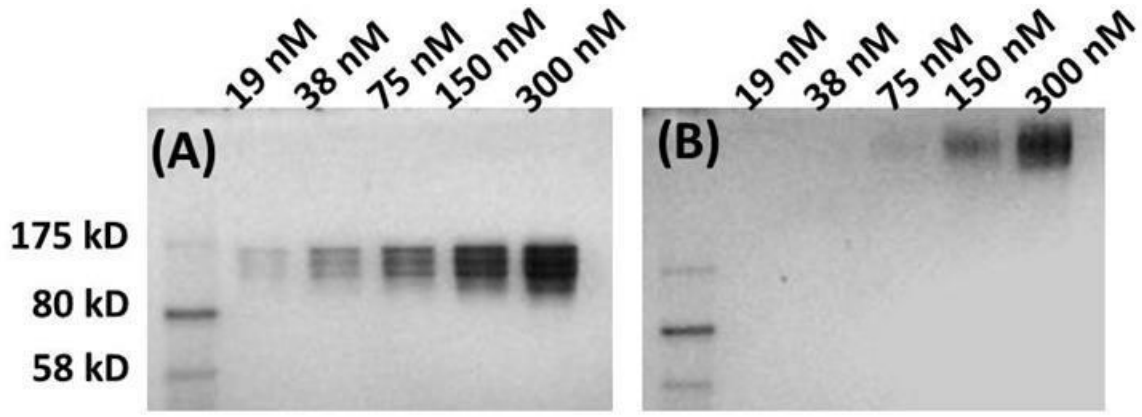

Fig. 23. Herceptin was covalently attached to HER-NFP. Optical images of SDS-PAGE gels loaded with different concentrations (nM) of (A) Herceptin and (B) HER-NFP.

3.4.4. Investigation of the Herceptin density on cellular uptake

Studies have shown that the density of antibody appeared on a nanoparticle surface could affect the rate as well as the degree of cellular internalization [445-447]. To investigate the effect of the density antibody on cellular uptake, HER-NFPs composing of different Herceptin-to-nanofiber (H/N) ratio (2:1 to 20:1) were synthesized. All the nanofibers were also labeled with the same amount of Cy5.5 for quantifications. As expected from the multivalent effect, increasing the number of Herceptin antibodies (from 2 to 10) attached to the nanofibers would enhance the cellular uptake and, thus, the amount of antibody (Fig. 24A). An optimum cellular uptake of Herceptin (4.5 pg /cell) was observed in the preparation with an H/N ratio of 10:1. However, further increasing the H/N ratio to >10 did not enhance the cellular uptake, possibly because of steric hindrance (Fig. 24A).

Next, we investigated the intracellular distribution of the Cy5.5-labeled HER-NFP by fluorescence microscopy (Fig. 24B). There was no significant difference in terms of the localization among all the nanofibers, which indicated that they were taken up by SKBr-3 cells through the same mechanism [448]. The nanofibers appeared as discrete fluorescence spots in the cytoplasm, which were co-localized with the lysosome staining (Fig. 24B).

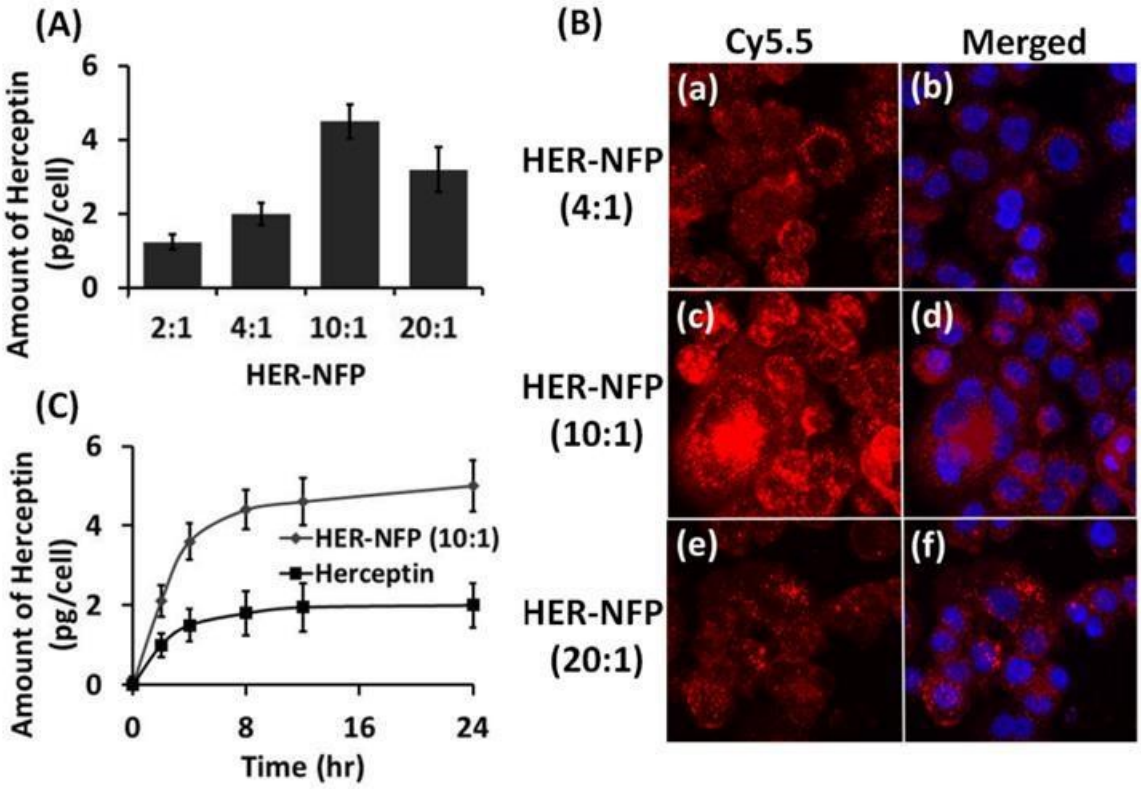

Fig. 24. A comparison of internalization of HER-NFP loaded with different density of Herceptin in SKBr-3 cells. (A) Amount of Herceptin internalized (pg/mL) in cells incubated with HER-NFP of different loading (2, 4, 10 and 20 Herceptin per nanofiber) at 12 hr. (B) Cellular distribution and localization of different of loading of HER-NFP at H/N ratio 4:1, 10:1 and 20:1. (C) Amount of Herceptin internalized in cells incubated with H/N ratio10:1 HER-NFP at various time points (2, 4, 8, 12 and 24 hr.).

These above results suggested that the HER-NFP's were possibly internalized into the cells via receptor-mediated endocytosis. Interestingly, both the Cy5.5-labeled HER-NFPs and Herceptin shared similar kinetics of cellular uptake (Fig. 24C), but the amount of antibodies inside the cells was significantly higher (>2-fold) in the case of Cy5.5-labeled HER-NFP.

3.4.5. The effect of the length of nanofiber on cellular uptake

The endocytosis of an antibody-conjugated nanoparticle is dependent on its ability to cross-link the cell-surface receptors and, subsequently, to create an in-folding of the cell membrane [449]. This process can be influenced by the size, shape, and surface characteristics of

a particle [450-452]. Here, we investigated whether the internalization of HER-NFP could be affected by its length. Experiments were performed for determining the cellular uptake, by adding various Cy5.5-labeled HER-NFP of the same H/N ratio (10:1), but with different lengths (50 nm, 100 nm, 400 nm, and uncut), to the SKBr-3 cell lines (Fig. 25).

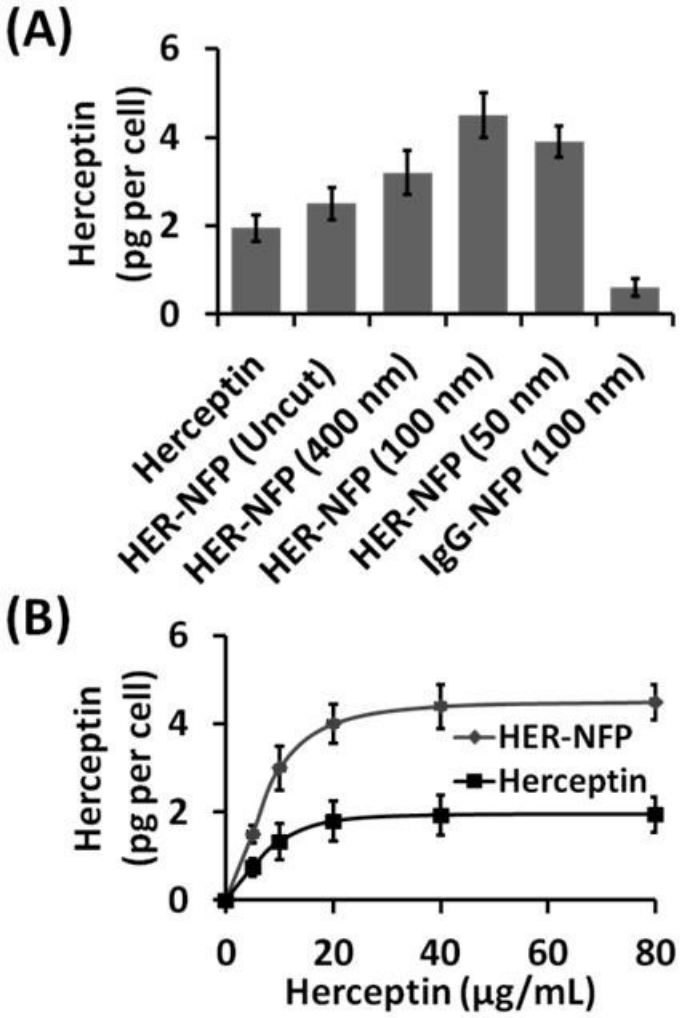

Fig. 25. A comparison of internalization of different size HER-NFP in SkBr-3 cells. (A) Amount of Herceptin internalized (pg/mL) in cells incubated with 50 nm, 100 nm, 400 nm and uncut HER-NFP. (B) Dependence of internalization of HER-NFP on its concentration. Amount of Herceptin internalized (pg/mL) in cells incubated at 0, 5, 10, 20, 40 and 80 µg/mL HER-NFP (H/N: 10:1) for 12 hr.

Our results demonstrated that all NFP conjugates regardless of the size efficiently delivered more antibodies inside the cells as compared to the Herceptin alone (Fig. 25A). The optimal length of nanofiber was 100 nm, since it revealed the maximum cellular uptake. As expected, increasing the amount of Cy5.5-labeled HER-NFP during incubation would enhance the cellular internalization of Herceptin (Fig. 25B). However, there was no further enhancement at a higher concentration, possibly because of the cell-surface HER2 were saturated from the bindings. Overall, our data suggested that a NFP conjugated with ten antibodies and of 100 nm in length was the optimized preparation and, thus, was employed for the rest of our studies.

3.4.6. The enhanced cytotoxic effect of HER-NFP

Next, MTS assay was performed to compare the cytotoxicity of HER-NFP and Herceptin in SKBr-3, MCF-7, and MDA-MB-231 breast cancer cell lines. These cell lines expressed various levels of HER2 (Fig. 26A). NFP was confirmed to be intrinsically nontoxic (Fig. 26B). On the other hand, HER-NFP was more effective than Herceptin in inhibiting cell growth of HER2-positive SKBr-3 cells. At 72 hr after incubation, 80% of the cells treated with Herceptin were viable while it was only 40% in the case HER-NFP. The enhanced cytotoxic effect of HER-NFP was specific, as it did not induce toxicity towards the HER-2 negative MCF-7 and MDA-MB-231 cell lines (Fig. 26C and D). Furthermore, the control IgG-NFP was unable to inhibit any cell growth. Our results indicated that the cytotoxicity of Herceptin could be enhanced by converting the antibody into a multivalent format using NFP [372, 419].

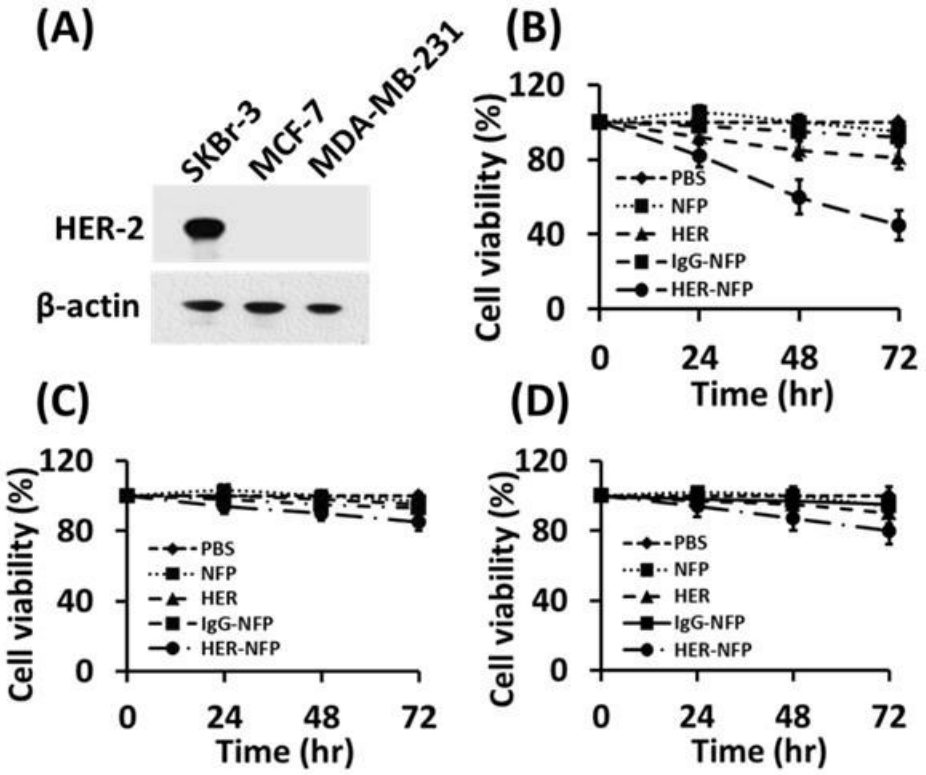

Fig. 26. The cytotoxicity of HER-NFP was specific. (A) A western blot showing the HER-2 expressions of SKBr-3, MCF-7 and MDA-MB-231 cell lines. MTS assays were performed to determine the percentage of cell viability of (B) SKBr-3, (C) MCF-7, and (D) MDA-MB-231 at different time points (hr) after treatment with Herceptin (67 nM), HER-NFP (H/N ratio 67/6.7 nM), IgG-NFP (H/N ratio 67/6.7 nM), or NFP (6.7 nM) in McCoy's culture media (200 μL). All the data was presented as an average of three independent experiments.

3.4.7. Modulation of cell signaling pathway by HER-NFP

The underlying mechanism(s) of Herceptin is not completely clear. It was proposed that Herceptin could exhibit its anti-tumor activity indirectly through the induction of various immunological responses including antibody-dependent cytotoxicity and complement-dependent cytotoxicity [453] and/or directly by modulating the downstream cell signaling pathways that involving in cell proliferation, invasion, and survival [454-456]. Recent studies have shown that a multivalent format of the Herceptin could promote the cytotoxic effect by further blocking some of the essential cell survival pathways, including the phosphatidylinositol 3-kinase (PI3K) and the mitogen activated protein kinase (MAPK) pathways, through clustering more of the

antigen/antibody complex [419]. As expected, when SKBr-3 was treated with Herceptin, both the phosphorylation of AKT (at Serine 473) and the phosphorylation of ERK1/2 (at Threonine 202/Tyrosine 204) decreased with time (Fig. 27A and B) but with the effect was more profound in HER-NFP, which indicated that the enhanced cytotoxic effect of HER-NFP could be attributed to further downregulation of both the PI3K and MAPK pathways [372, 419].

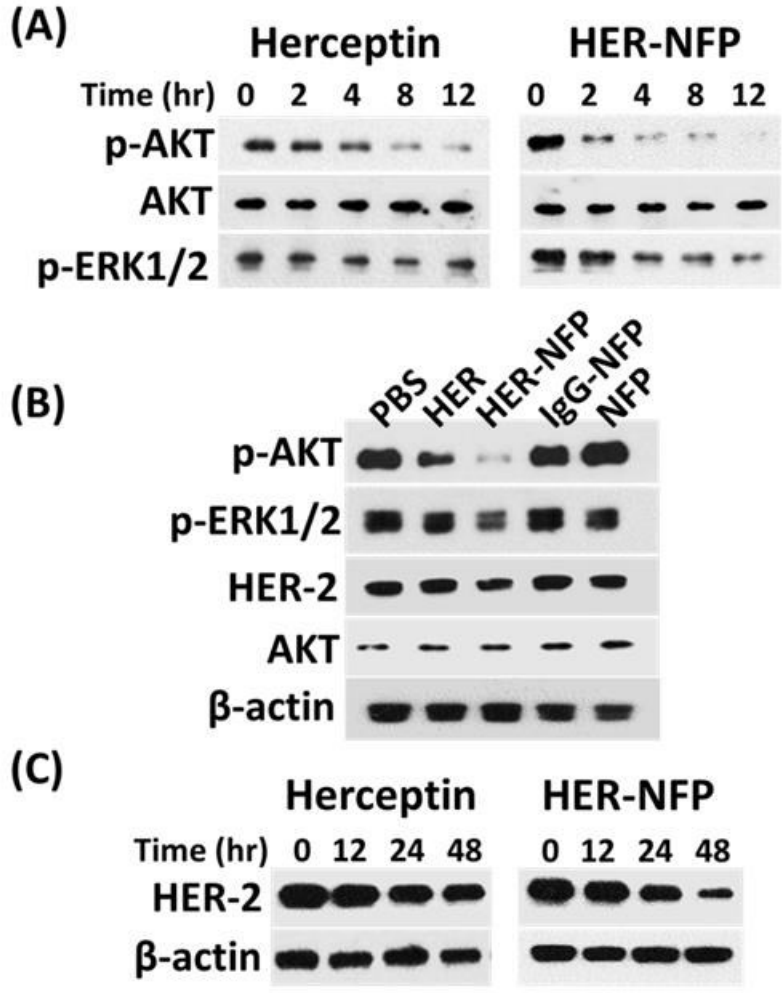

Fig. 27. HER-NFP downregulated certain cell survival signaling pathways. (A) Western blots showing the total AKT, p-AKT, and p-MAPK expressions in SKBr-3 cell lines at different time points (hr) after treatment with Herceptin (67 nM) or HER-NFP (H/N ratio 67/6.7 nM). (B) A comparison of the protein expressions in SKBr-3 cell at 6 hr after treatments with PBS, Herceptin (67 nM), HER-NFP (H/N ratio 67/6.7 nM), IgG-NFP (H/N ratio 67/6.7 nM), or NFP (6.7 nM). (C) Western blots showing the HER-2 expressions in SKBr-3 cell lines at 12 hr after treatment with Herceptin (67 nM) or HER-NFP (67/6.7 nM).

3.4.8. Downregulation of HER-2 expression by HER-NFP

Here, we compared the HER-2 levels in the SKBr-3 cell lines after treatment with Herceptin and HER-NFP. At 48 hr, we observed a marginal decrease of the HER-2 in the cells treated with Herceptin. In contrast, there was a significant reduction of the HER-2 level in the cells treated with HER-NFP.

Our cellular imaging data demonstrated that there was more cellular uptake of HER-NFP than the Herceptin, and that HER-NFP were predominantly localized at the lysosomes rather than distributed evenly throughout the cytoplasm after cellular internalization (Fig. 28). Therefore, it is possible that the enhanced cytotoxic effect of HER-NFP was caused by a downregulation of HER-2 *via* an increase in the endocytosis and degradation of the antigen/antibody complex [457] which ultimately prevented the recycling of HER-2 to the cell surface.

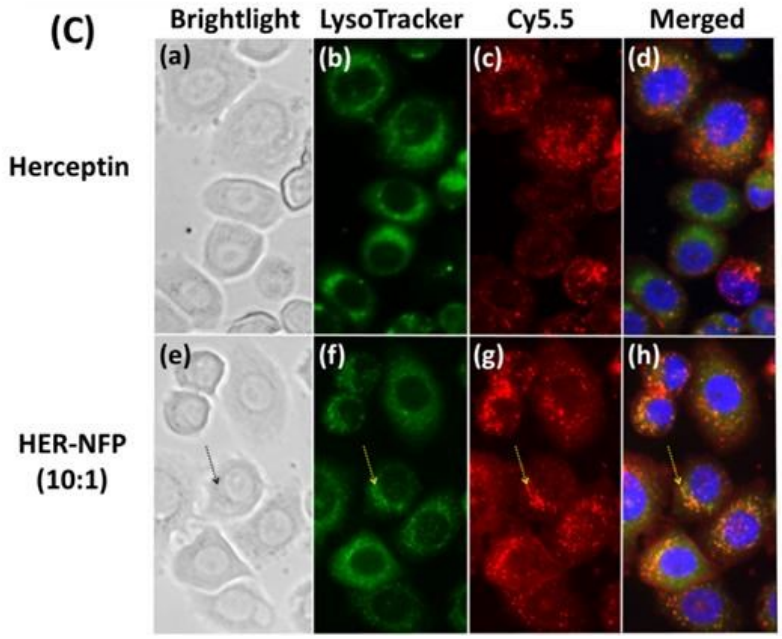

Fig. 28. The cellular distribution of HER-NFP. SKBr-3 cells were treated with either Herceptin (200 nM) or HER-NFP (H/N ratio 200/20 nM) that labeled with Cy5.5 for 6 hr at 37^{o}C and followed by addition of Lyso-Tracker® (green). The nuclei were counterstained with DAPI staining solution (blue).

3.5. Conclusion

Various strategies have been proposed to increase the effectiveness of a monoclonal antibody [458-460]. In the present study, we successfully employed a new type of peptide nanofiber (NFP) as a multivalent platform. All the components of NFP are non-toxic and hemocompatible since the employed PEG is known to be non-toxic and non-immunogenic and the self-assembly peptide sequence (kldlkldlkldl) has been used for tissue engineering [461]. Furthermore, NFP consists of multiple amino functional groups on the surfaces, which allowed further attachment of various ligands for targeted delivery. Here, we covalently conjugated approximately ten Herceptin antibodies to one nanofiber and demonstrated that the resulting HER-NFP was more effective in inhibiting SKBr-3 cell growth than the free Herceptin. This enhanced cytotoxic effect could be explained by the multivalency which promoted direct inhibitions of the downstream cell survival PI3K and MAPK pathways *via* an increase in the clustering of the antigen/antibody complex or indirectly downregulated the cell surface HER-2 *via* an increase in the internalization and degradation, rather than the recycling, of the receptor. It is noteworthy that peptide-based nanofibers have been used as carriers for chemotherapeutic agents [216, 408-410]. The co-delivery of tumor-targeted antibody would provide an additional benefit to optimize therapeutic efficacy in cancer treatments in the future.

CHAPTER 4. UPREGULATION OF UROKINASE PLASMINOGEN ACTIVATOR IN PROSTATE CANCER CELLS OVEREXPRESSING 15-LIPOXYGENASE-1

4.1. Abstract

Proteases, such as urokinase plasminogen activator (uPA) are often involved in cancer growth and invasion due to their ability to degrade the extracellular matrix. Several studies have indicated that lipid-peroxidizing enzymes, such as lipoxygenases may act an upstream molecule in the activation of variety of signaling pathways that may be involved in the progression of cancer. Of all studies documented, the investigation of 15-lipoxygenase-1 (15-LOX-1) is particularly interesting because this enzyme acts as a tumor suppressor in most cancers, however behaves very differently in prostate cancer (demonstrating a strong pro-carcinogenic role). In the present study, we provide evidence for the first time that indicates the role of 15-LOX-1 in the upregulation of urokinase plasminogen activator (uPA), a cancer related protease. For proof of concept, we selected prostate cancer PC-3 cells which were transfected with 15-LOX-1 as a model for our studies. Our data demonstrated that there was upto five-fold increase in mRNA as well as protein expression of uPA in 15-LOX-1 transfected cells (15-LOX-1/PC-3) as compared to parental PC-3 cells. The mechanism of upregulation of uPA was explained through the activation of various subfamilies of the MAPK pathway, especially the stress-activated JNK1/2 pathway. In summary, our data supports previous studies that 15-LOX-1 has a pro-carcinogenic role in prostate cancer. Furthermore, we believe that the information about the link between of lipoxygenase family of enzymes and cancer-related uPA enzyme would help us to identify new strategies to target prostate cancer more effectively.

4.2. Introduction

4.2.1. PUFAs and prostate cancer

Prostate cancer is the most common malignancy and the second leading cause of cancer death among men in the United States [462]. Ecological and epidemiological studies have revealed there are large differences in rates development of prostate cancer between different ethnic regions [463]. Dietary fat consumption had been positively linked to prostate cancer development [464, 465]. African-Americans are at higher risk of developing prostate cancer than non-Hispanic whites [466]. Interestingly, omega-3 (n-3) polyunsaturated fatty acids have been associated with decreased risk of developing prostate cancer whereas positive association between alpha-linolenic acid and advanced and fatal prostate cancer [467].

4.2.2. Polyunsaturated fatty acids (PUFAs)

Polyunsaturated fatty acids or "PUFA" belong to the class of simple lipids. They are termed "polysaturated" because these fatty acids contain multiple carbon-carbon double bonds. The classification of PUFAs is further based on the position of the first carbon-carbon double bond with respect to the methyl group termini. Omega-3 PUFA has double bond between third and fourth carbons, whereas omega-6 PUFA have double bond between sixth and seventh carbon.

In mammals, two types of PUFA, Linoleic acid (n-6) (LA) and alpha-linolenic acid (n-3) (LNA) cannot be synthesized by humans and therefore are acquired through diet [468]. Since these fatty acids have important biochemical roles, they are usually referred as essential fatty acids (EFA) [469, 470]. Fatty acids may interconvert to other fatty acids, for example linoleic acid converts into arachidonic acid (AA), which acts as a precursor for different eicosanoids [471].

Omega-3 fatty acids, includes alpha linolenic acid which is abundant in fish oil and green leafy vegetables, such as spinach, flax seed oil, walnuts [468, 472]. Examples of other omega-3 fatty acids are eicosapentaenoic acid (EPA), docosahexanoic acid (DHA) and eicosatetranoic acids (ETA). On the other hand, omega-6 fatty acids includes linoleic acid (LA), one of the most important fatty acid of this group and is main component of safflower oil, corn oil, sunflower oil and soybean oil. Ratio of omega-3 and omega-6 fatty acids is important for maintaining normal physiological conditions [473]. Other omega-6 fatty acids are gamma-linolenic acid (GLA), arachidonic acid (AA) and dihomo-gama-linolenic acid (DLGA).

4.2.3. Relationship between polyunsaturated fatty acids and cancer

Polyunsaturated fatty acids (PUFAs) are important components of the cells. They are important component of diet and play an important role in maintaining cell membrane structure, cell signaling and regulation of gene expression [474]. Evidence suggests that individual PUFA's may play a role in cancer progression, especially in the development of breast [475], prostate [476, 477] and colon cancer [478, 479]. Therefore, PUFA's have been proposed to be useful as chemotherapeutic agents or as adjuvant to radio- or chemotherapy for cancer treatment. Alternately, some PUFA's have been known have a protective role in cancer development [480]. Although there are many studies which implicate the role of PUFA in cancer development, there is still no epidemiological evidence to confirm this.

4.2.4. Type of PUFA and cancer development

Type of PUFA may be crucial developing risk for cancer development. Monosaturated and n-3 PUFA may have a protected role in cancer development [481]. On the other hand, n-6 PUFAs are thought to be positively correlated with cancer development [467]. In general, the most selective cytotoxic effects have been obtained with the three eicosanoid precursors, GLA,

AA and EPA, intermediate effects were observed with LA and ALA, and least effects were observed with DHA [482-486]. Cytotoxic effect may be dependent on the number of double bonds. Studies indicated that PUFA containing 3, 4 and 5 double bonds are more effective than PUFAs with 2 and 6 double bonds [483]. Animal model fed with strict controlled diets have been utilized to understand relationship PUFAs and cancer development [487], however, there are difficulties in transference of outcome when rodent system is compared to human system. Till now, it is generally accepted that factors such as increase in oxidative stress, ability to metabolize fatty acids and cause changes in membrane integrity may influence cell signaling pathways that may result in cancer growth or apoptosis [488].

4.2.5. Lipoxygenases

Lipoxygenases (LOXs) are a family of enzymes that oxidize polyunsaturated fatty acids to form biologically active metabolites [489]. The metabolism of polyunsaturated fatty acids is strongly regulated by two classes of lipid peroxidation enzymes, the lipoxygenases and cyclooxygenases [490, 491]. Depending on the position of inserting oxygen in substrate, these enzymes generate different products. The cyclooxygenase (COXs) are actively involved in the conversion of arachidonic acid to prostaglandins (PGs) [492], whereas the lipoxygenases are involved in the conversion of arachidonic acid and linoleic acid into hydroxyoctadecadienoic acid (HODE), and hydroperoxyeicosatetraenoic acid (HETE) metabolites respectively [60]. There are a total of eight lipoxygenases (5-, 8-, 9-, 10-, 11-, 12-, 13- and 15-) identified, depending on the position of peroxidation of polyunsaturated fatty acids [493]. In animals, there are four lipoxygenases 5-, 8-, 12-, and 15-LOX. Lipoxygenases catalyse the insertion of oxygen at carbon 5, 8, 12 and 15 position of arachidonic acid resulting in formation of products 5S-, 12S-, or 15S-hydroperoxyeicosatetraenoic acid (5-, 8-, 12-, or 15-HPETE), which are reduced

further to their hydroxyl forms (5-, 8-, 12-, 15-HETE) by glutathione peroxidase enzyme [59, 494]. These enzymes mainly catalyze pathways from membrane lipids to signaling molecules. Phospholipase cleaves the membrane lipid to form polysaturated fatty acids (Fig. 29).

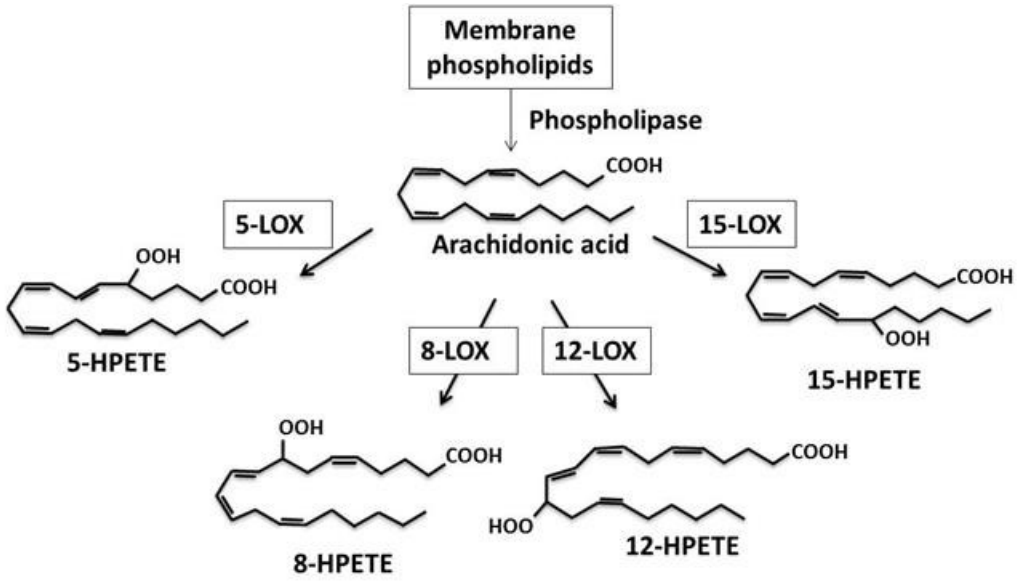

Fig. 29. Synthetic scheme showing metabolism of arachidonic acid by lipoxygenases. The lipoxygenases5-LOX, 8-LOX, 12-LOX and 15-LOX resulting in the formation of metabolites 5-HPETE, 8-HPETE, 12-HPETE and 15-HPETE, respectively.

Arachidonic acid, linoleic acid, and linolenic acid are some of the important LOX enxymes. The 5-LOX pathway leads to the formation of 5 (S)-HETE and leukotrienes, whereas the 12- and 15-LOXs can form 12- and 15-HETE, respectively. The lipoxygenases and their metabolites have been strongly implicated for their role in inflammation, immunity, and also in other pathological conditions such as cancer, atherosclerosis, asthma, and ulcerative colitis [495].

4.2.6. Role of lipoxygenases in cancer

The expression of LOXs has found to be upregulated in some types of cancer, and has been associated with stimulation of cell growth, induction of mutations, inhibition of apoptosis, and cell invasion [496]. For example, metabolites of 5-LOXs in the arachidonic acid pathway can enhance cancer cell growth. 5(S)-HETE, a major metabolite of 5-LOX is involved in

stimulating proliferation of pancreatic cancer cells through the activation of mitogen activated protein kinases (MAPK) pathway [497]. The formation of reactive oxygen species (ROS) through the degradation of lipid in membranes can also trigger downstream signaling events that lead to the transcription of genes such as NF-kappa B and peroxisome proliferator-activated receptors (PPAR). The LOX signaling can also capable of causing mutations in target genes. 5-LOX product LT4 forms adducts with DNA bases, suggesting that it may serve as modulator of transcription [498].

4.2.7. 15-Lipoxygenase-1 (15-LOX-1)

15-Lipoxygenase-1 (15-LOX-1) is one of the two isoforms of 15-LOX that differ in tissue distribution and substrate preference [59] and is expressed in reticulocytes [499], eosinophils [500], macrophages [501], mast cells [502], and bronchial epithelial cells [503]. On the other hand, 15-LOX-2 can be found in tissues such as prostate gland [504], cornea [505], skin, and keratinocytes [506]. 15-LOX-1 functions to converting the substrate, linoleic acid, into its metabolite, 13-(S)-hydroxyoctadecadienoic acid (13-HODE) [507]. Fig. 30 shows the synthetic scheme of 15-LOX-1 mediated conversion of arachinonic acid and linoleic acid into 15-HPETE and 13-HPODE, respectively. Studies have shown that 15-LOX-1 and 13-HODE were involved in certain diseases including cancer [60-62], inflammatory disorders [500, 508-510], atherosclerosis [511], and angiogenesis [512]. For example, 15-LOX-1 was shown to increase metastasis of cancer cells to lymph nodes in mammary carcinoma xenograft [513]. It was also found overexpressing in Hodgkin lymphoma derived L-1236 cells [514]. On the other hand, 13-HODE can induce mitogenic response in human breast cancer BT-20 cells [515].

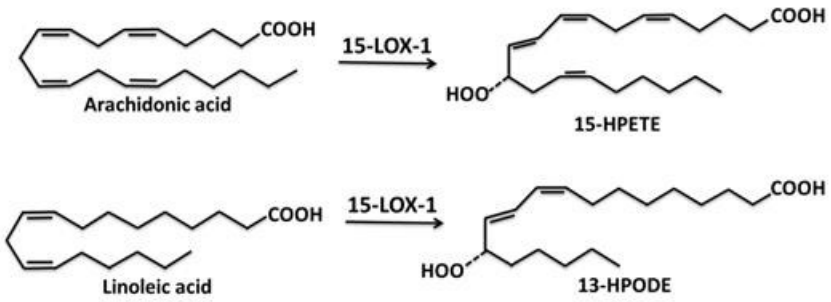

Fig. 30. Synthetic scheme showing the 15-LOX-1 mediated conversion of PUFA's. Arachidonic acid and linoleic acid were conversted into 15-HPETE and 13-HPODE respectively.

4.2.7.1. Role of 15-LOX-1 in prostate cancer

In prostate cancer, there is a strong evidence to suggest that 15-LOX-1 is pro-tumorigenic. Studies have shown that the expression of 15-LOX-1 in prostate cancer tissue was much higher as compared to normal prostate tissue and the level was correlated with the Gleason score [516]. *In vitro* studies demonstrated that 13-HODE increased cell growth in PC-3 cells, and the addition of specific inhibitor of 15-LOX-1, PD146176 reversed this effect in a dose-dependent manner [61]. *In vivo* studies demonstrated that PC-3 cells overexpressed with 15-LOX-1 resulted in a greater number of tumors and larger volume as compared to parental PC-3 cells [61]. Taken together, this data suggested a contributory role of 15-LOX-1 in cell growth and proliferation in prostate cancer.

4.2.7.2. Role of 15-LOX-1 in colon cancer

The role of 15-LOX-1 in cancer development has been controversial, as there are a number of studies that also demonstrate its anti-tumorigenic effect, particularly in colon cancer [517-520]. 15-LOX-1 expression was down-regulated in colorectal adenomas [521], and the restoration of 15-LOX-1 in colon cancer xenografts cell lines induces formation of apoptotic proteins [522]. The anti-tumorigenic effect of 15-LOX-1 has also been observed in other forms

of cancer such as esophageal cancer [523], gastric cancer [524], bladder cancer [525], pancreatic cancer [526], breast cancer [527] and glioma [528].

4.2.8. Urokinase plasminogen activator

uPA is a 54 kDa serine protease which consists of three conserved domains, a growth factor domain, a kringle domain and a serine protease domain. It is secreted as a zymogen (pro-uPA), which gets activated upon binding to its receptor uPAR [529]. The active uPA converts plasminogen to plasmin, which can act on broad range of substrates and leads to the activation of growth factors [530, 531]. Plasmin acts on degrades fibrin, fibronectin, vitronectin, and laminin [532, 533]. The binding of uPA to uPAR also facilitates signaling events involving integrins, growth factors, receptors associated with cell growth and proliferation, angiogenesis and cell adhesion [534]. The turnover rate of uPA is tightly controlled by PA1 and PA2, which are endogeneous inhibitors of uPA [63, 535]. Both PA1 and PA2 can counterbalance the activity of uPA by forming stable 1:1 complexes. PA1 is thought to be the primary inhibitor of uPA, and its levels are also upregulated in cancer [63, 536].

4.2.9. MAPK pathway

The MAPK Pathway is one of the most important pathways which is actively involved in the transduction of signals from cell membrane to the nucleus [537, 538]. These consist of protein serine/threonine kinases and can be divided into three well defined groups: the extracellular signal regulated kinases (ERK 2 c-Jun) N-Terminal kinases (JNK 1, JNK 2, JNK 3) and p38 MAPK [539]. All subfamilies of MAPK pathway are involved in the regulation, growth, and survival of normal cell proliferation [540]. For example, the ERK pathway is activated by MEK, which in turn is activated by RAS. RAS is MAP3K protein kinases, which is downstream of growth receptors such as tyrosine kinases and epidermal growth factor [541]. Various growth

factors bind to these receptors and induce their dimerization and activation [542]. In mammalian systems, three subfamilies of MAPK signaling units have been identified, the extracellular signal-regulated kinases (ERKs) [543], the c-Jun amino-terminal kinases (JNKs; also referred to as stress-activated protein kinases (SAPKs) [544] and the p38 MAPKs (p38s) [545, 546]. The MAPK pathway has emerged as an important target in cancer therapeutics [541]. Individual members of MAPK family require specific stimuli to become activated and the activated form of the proteins further act on their substrates. Intracellular cascade to cell proliferation, survival, angiogenesis and migration [547].

4.2.10. The role of MAPK pathway in the upregulation of uPA

Numerous studies have indicated that tumor cells produce large amounts of oxygen species as compared to normal cells [548, 549]. In some studies it is indicated that reactive oxygen species contribute to invasive ability of cells by regulating the levels of tumor associated proteases such as uPA [550, 551]. This process involves activation of multiple signaling pathways including the phosphorylation cascade of MAPK family. The hepatocyte growth factor (HGF) is a multipotent growth factor which is normally secreted by mesenchymal cells [552]. A recent study indicated that HGF activated in human hepatoma cells lines HEPG2 and HEPG3 lead to production of ROS, which resulted in activation of MAPK pathway [553]. The activation of MAPK pathway further led to upregulation of uPA in these cells [553]. Thus, there may be some role of MAPK pathway in the upregulation of uPA.

4.3. Material and methods

4.3.1. Materials

The 15-LOX-1 inhibitors PD146176 and nordihydroguaiaretic acid (NDGA) were purchased from Cayman Chemicals (Ann Arbor, MI). Stock solutions of inhibitors (10 mM)

were made in dimethylsulfoxide (DMSO) and stored at -20°C until use. ERK 1/2 inhibitor (U1026) was obtained from Cell Signaling Technology (Danvers, MA). p38 MAPK inhibitor (SB203580) and SAPK/JNK inhibitor (SP600125) were obtained from Cayman chemicals (Ann Arbor, MI). Primary antibodies specific to ERK1/2 phosphorylated at Thr^{202}/Tyr^{204} (pERK 1/2), p38 MAPK phosphorylated at Thr^{180}/Tyr^{182} (p38MAPK), and SAPK/JNK phosphorylated at Thr^{183}/Tyr^{185} (p-SAPK/JNK) were purchased from Cell Signaling Technology (Danvers, MA). Secondary antibody conjugated to horseradish peroxidase (HRP) was also purchased from Cell Signaling Technology (Danvers, MA). Monoclonal antibodies specific to uPA and 15-LOX-1 were purchased from Abcam (Cambridge, MA).

4.3.2. Cell culture

Human prostate cancer cells PC-3 were purchased from ATCC (Manassas, VA). PC-3 cells transfected with 15-LOX-1 (15-LOX-1/PC-3 cells) were provided as a generous gift from Dr. Steven Qian (North Dakota State University, North Dakota). Both PC-3 and 15-LOX-1/PC-3 cells were grown in RPMI-1640 growth medium supplemented with fetal bovine serum (FBS) (10% v/v). The RPMI-1640 growth medium was purchased from Hyclone Laboratories (Logan, UT) and FBS was purchased from Mediatech Inc. (Manassas, VA). All culture media were supplemented with antibiotics such as penicillin G (100 U/mL) and streptomycin (0.1 mg/mL), purchased from ATCC (Manassas, VA). In some experiments, we used serum-free and phenol-red free media which was obtained from Hyclone Laboratories (Logan, UT). All cells were cultured in incubators at 37°C with 5% CO_2 under humidified conditions. Culture media of 15-LOX-1/PC-3 cells was supplemented with Zeocin (50 μg/mL), purchased from Invitrogen (Carlsbad, CA).

4.3.3. Migration assay

The migration assay was performed using transwell invasion chambers (BD Biosciences, San Jose, CA) of 24-well plate with an 8 μm pore size polycarbonate filter. PC-3 cells, 15-LOX-1/PC-3 cells alone, or in combination with NDGA was analyzed for their migratory potential. All cells were trypsinized, washed, and suspended in serum-free media. Aliquots of cells (1 x 10^4/well), in serum-free media (200 μL) were transferred to the inner side of invasion chamber and allowed to attach overnight in incubator at 37^{o}C. The outer side of the chamber was incubated with culture media (300 μL) containing FBS (10% v/v). After 12 hr of incubation, the supernatant in the inner side of the chamber was discarded and cells were treated with NDGA (5 μM) in serum-free media (200 μL). Cells treated with dimethylsulfoxide (DMSO) (0.01% v/v) diluted in media (200 μL) were treated as controls. The plate was then transferred to the incubator and incubated for additional 24 hr. at 37^{o}C. After incubation, non-migrated cells in the inner side of the transwell membrane were removed using cotton swabs. Cells that had migrated through the membrane were fixed by incubating the filter in paraformaldehyde solution (3.7% w/v) in PBS buffer at room temperature for 30 min. The cells were washed twice with PBS buffer and visualized by staining with crystal violet (0.005% w/v) in PBS buffer. Under 4X magnification, 4 randomly selected fields were examined using optical microscope (Am Scope Microscopes, Irvine, CA) and the number of migrated cells were calculated by staining with crystal violet (0.005% w/v) in PBS buffer.

4.3.4. Wound healing assay

PC-3 and PC-3-LOX cells were seeded in 6-well plate and incubated until they were 80-90 % confluent. Some cells were treated and NDGA (5 μM) in serum free media (5 mL). A scratch was carefully made in the monolayer of cells with a sterile pipette tip (100 μL size). The

cells were washed once with PBS (10 mM, pH 7.4) to remove debris and incubated in culture media (2.5 mL) containing FBS (10% v/v). The cells were immediately photographed under the microscope (Olympus IX-81, Melville, NY) and the distances between wound edges were measured with a ruler. The plate was transferred to the incubator and incubations were performed for 4, 8, 12 and 24 hr. at 37^{o}C. At each time point, number of cells that migrated per mm^{2} area from the wound edges into the cell free zone was counted.

4.3.5. siRNA transfection

Small interfering RNA's (siRNA's) for 15-LOX was purchased from Dharmacon (Lafayette, CO). The siRNA for 15-LOX consisted of a pooled mixture of four SMART-selected siRNA duplexes. For siRNA transfection, PC-3 cells were seeded (1 x 10^{5} cells per well) in 6-well plate in culture media containing FBS (1% v/v). We used antibiotic free media throughout our siRNA transfection studies. PC-3 cells were then transfected with 15-LOX siRNA using Lipofectamine 2000 (Invitrogen, Carlsbad, CA). Briefly, siRNA (100 nM, 5 μL) and Lipofectamine 2000 (5 μL) were separately diluted in culture medium (250 μL) containing FBS (1% v/v), and allowed to incubate at room temperature for 15 min. The solutions were mixed, incubated for additional 20 min. The mixture (500 μL) was diluted with an equal volume of culture media (500 μL) and incubated with the cells in incubator at 37^{o}C. The cells were further allowed to incubate with siRNA's for additional 24 hr and harvested for analysis.

4.3.6. RT-PCR

The mRNA expression of uPA was determined by real-time reverse transcriptase polymerase chain reaction (RT-PCR) using Stratagene Mx 3000 Real-Time PCR System (Agilent Technologies, Santa Clara, CA). RNA was extracted using PureLink^{TM} RNA Mini Kit (Invitrogen, San Francisco, CA) and the samples were kept in ice. The concentration of total

RNA was quantitated by measuring the absorbance at 260 nm using the extinction coefficient (25 $\mu L/\mu g/cm^{-1}$) in distilled water. RNA (50 ng, 20 μL) was transcribed into cDNA using AMV reverse transcriptase (Promega, Madison, WI) for 15 min at 60°C in Accublock Digital Dry Bath (Labnet International, Inc., Woodbridge, NJ). The resulting cDNA was amplified in the presence of SuperScript®VILO™ (Invitrogen, Carlsbad, CA) and primers for either uPA or beta actin. Primers for both genes were purchased from Integrated DNA technologies (Coralville, IA). The sequences of primers for uPA were 5′-GTGGGCTGTGAGTGTAAGTGTGA-3′ (forward) and 5′-GACTTAACAATCAGACACCAGCTCTT-3′ (reverse). The primers for beta actin were 5′-CATGTACGTTGCTATCCAGGC-3′ (forward) and 5′-CTCCTTAATGTCACGCACGAT-3′ (reverse). There were a total of 40 thermal cycling steps in the reaction. The mRNA levels among the test cells were analyzed by relative quantification $2^{-\Delta\Delta Ct}$ method [341]. PCR reaction was performed in triplicate.

4.3.7. Western blot

PC-3 and PC-3/15-LOX-1 cells were seeded (1.5×10^6) in 6-well plate in RPMI-1640 culture medium containing FBS (10% v/v). After 12 hr. of incubation, the cells were treated as per requirement. The old media was discarded and cells were washed with PBS (10 mM, pH 7.4) and lysed in lysis buffer (Cell Signaling Technology, Danvers, MA). Lysates of cells were then cleared at 10, 000 rpm for 5 min, and the protein concentrations with determined using Micro-Bincinconinic acid (BCA) assay (Pierce, Rockford, IL). Proteins (20 μg, 10 μL) were then separated by a polyacrylamide gel electrophoresis on a sodium dodecyl sulfate-polyacrylamide gel (12% w/v) and transferred to a polyvinylidene difluoride (PVDF) Hybond™-P membrane (Amersham, Piscataway, NJ). The membrane was blocked with nonfat dry milk (5% w/v) in Tween 20-TBS buffer (0.1% v/v), followed by incubation with mouse-anti-human primary

antibodies specific for 15-LOX-1 and uPA. Primary antibodies were used to detect pERK1/2, p38 MAPK, pJNK1/2, and beta actin. The incubations were performed overnight at 4^{o}C. The membranes were then washed three times with Tween 20-TBS buffer (0.1% v/v) followed by incubation with horseradish peroxidase (HRP)-conjugated secondary antibodies for 1 hr. The membranes were washed again and the bound antibody was detected using the Enhanced Chemiluminescence System (ECL). The protein bands were detected using Western Blot Detection Reagents (Amersham, GE Healthcare Bio-Sciences, Piscataway, NJ) on Blue Ultra Autorad Film (BioExpress® Kaysville, UT). All experiments were performed in triplicate.

4.3.8. uPA activity assay

To perform the uPA activity assay, we employed the AssaySense Human uPA Chromogenic Activity Assay Kit (Assaypro, St. Charles, MO). PC-3 and 15-LOX-1/PC-3 cells were seeded at a density of 1x10^{6} cells in tissue culture dishes. The cells were allowed to attach for 12 hr and then treated with either NDGA or ALOX siRNA for additional 24 hr. Cells in media only were treated as controls. Conditioned media from PC-3 and 15-LOX-1/PC-3 cells, either alone or treated was collected, centrifuged at 1500 rpm, and concentrated with an Amicon Ultra-4 10k filter (Millipore, Billerica, MA). The concentrated media (30 µL) were incubated with assay buffer (50 µL) and uPA substrate solution (20 µL). The assay buffer and uPA substrate were provided in the assay kit. The solutions were then transferred to flat-bottom 96-well plates and incubated in the incubator at 37^{o}C. After 6 hr, the enzyme activities were monitored by absorbance at 405 nm. While performing the assay, we plotted a standard curve of known activities of uPA (between 0 and 6.25 U/mL). The activities of the supernatants were then interpolated from the standard curve. The experiment was performed in triplicate.

4.4. Results and discussion

4.4.1. Overexpression of 15-LOX-1 in PC-3 cells upregulates uPA

Secretion of proteases, such as urokinase plasminogen activator (uPA), is a key requirement for cancer cells to invade surrounding tissues [554]. We examined the possible role of 15-lipoxygenase-1 (15-LOX-1) in the upregulation of uPA in PC-3 cells, a prostate cancer cell line which has high expression of uPA [555]. Levels of 15-LOX-1 in parental and transfected PC-3 cells (15-LOX-1/PC-3) selected for this study were confirmed using western blot (Fig. 31A). 15-LOX-1/PC-3 cells showed up to a four-fold increase in mRNA expression of uPA as compared to parental PC-3 cells (Fig 31C). The increase in expression of uPA was further confirmed by western blot analysis and uPA activity assay (Fig 31A). Incubation with NDGA, an inhibitor of 15-LOX-1 [556], decreased the expression of uPA in 15-LOX-1/PC-3 cells, suggesting that 15-LOX-1 is involved in the upregulation of uPA (Fig. 31D).

To confirm our results, we examined the effect of siRNA gene silencing in reducing the level of 15-LOX-1 in 15-LOX-1/PC-3 cells and parental PC-3 cells. A significant reduction in 15-LOX-1 by siRNA was achieved in both cell lines, as determined by western blot (Fig. 31C). 15-LOX-1/PC-3 cells had a significant reduction in uPA upon incubation with the siRNA (Fig. 31D). However, reduction of 15-LOX-1 in PC-3 cells did not appreciably affect the expression of uPA (Fig. 31D). The fact that gene silencing with siRNA could not result in reduction of uPA in PC-3 cells may indicate that basal level of uPA in normal PC-3 cells is not sufficient to activate downstream signaling pathways that upregulate uPA expression.

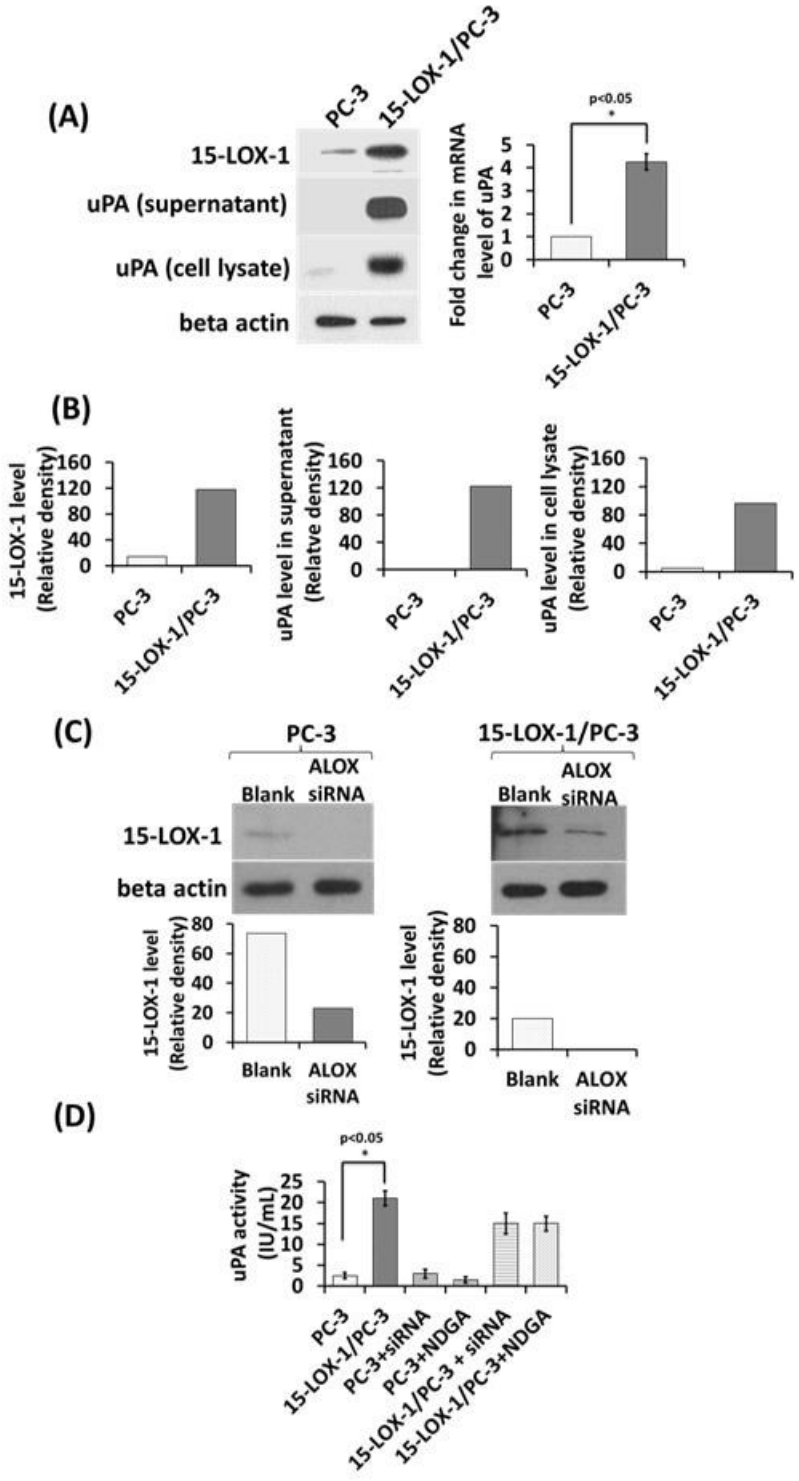

Fig. 31. The level of uPA is upregulated in 15-LOX-1/PC-3 cells. (A) Comparison of expression of uPA in PC-3 cells versus 15-LOX-1/PC-3 cells. (B) The effect of ALOX siRNA on the expression of uPA in PC-3 cells and 15-LOX-1/PC-3 cells (C) The fold change in the mRNA level of uPA in PC-3 cells versus 15-LOX-1/PC-3 cells.

4.4.2. Activation of MAPK pathway in LOX-overexpressing PC-3 cells

Studies have shown that lipoxygenases (LOXs) may act as secondary messengers and participate in the activation of cancer related signaling pathways, including mitogen activated protein kinases pathway (MAPK) [557]. There are three subfamilies of mammalian MAPKs which includes the extracellular signal regulated kinases (ERKs), Jun NH_2-terminal kinases (JNK), and the p38 MAPK kinases. ERK (also known as p42/44 MAPK) is crucial for regulating cancer growth and differentiation, the JNK pathway plays important role in the regulation of stress responses and apoptosis, and the p38 MAPK is also involved in the regulation of signaling pathways controlling cellular responses to stress and cytokines [546]. We were particularly interested in investigating the total versus phosphorylated status of different MAPK subfamilies because it would provide us crucial information regarding further downstream signals that may potentially be activated. To identify whether MAPK pathway was activated in 15-LOX-1/PC-3 cells, the level of different phosphorylated proteins of the MAPK family such as phospho-ERK1/2 (p-ERK1/2), phospho-JNK (p-JNK), phospho-p38 MAPK (p-p38 MAPK) was compared in 15-LOX-1/PC-3 cells and PC-3 cells. In agreement with previous studies [558], it was found that there was overexpression of phosphorylated forms of ERK1/2 in 15-LOX-1/PC-3 cell line as compared to PC-3 cells (Fig. 32A).The other two members, p38 MAPK and JNK1/2, were also activated as indicated by higher levels of p-p38MAPK and p-JNK1/2 proteins in PC-3-LOX cells as compared to PC-3 cells. Therefore, these results indicated that overexpression of 15-LOX-1 in PC-3 prostate cancer may indeed contribute to activation of mitogenic pathways which are implicated in cancer development.

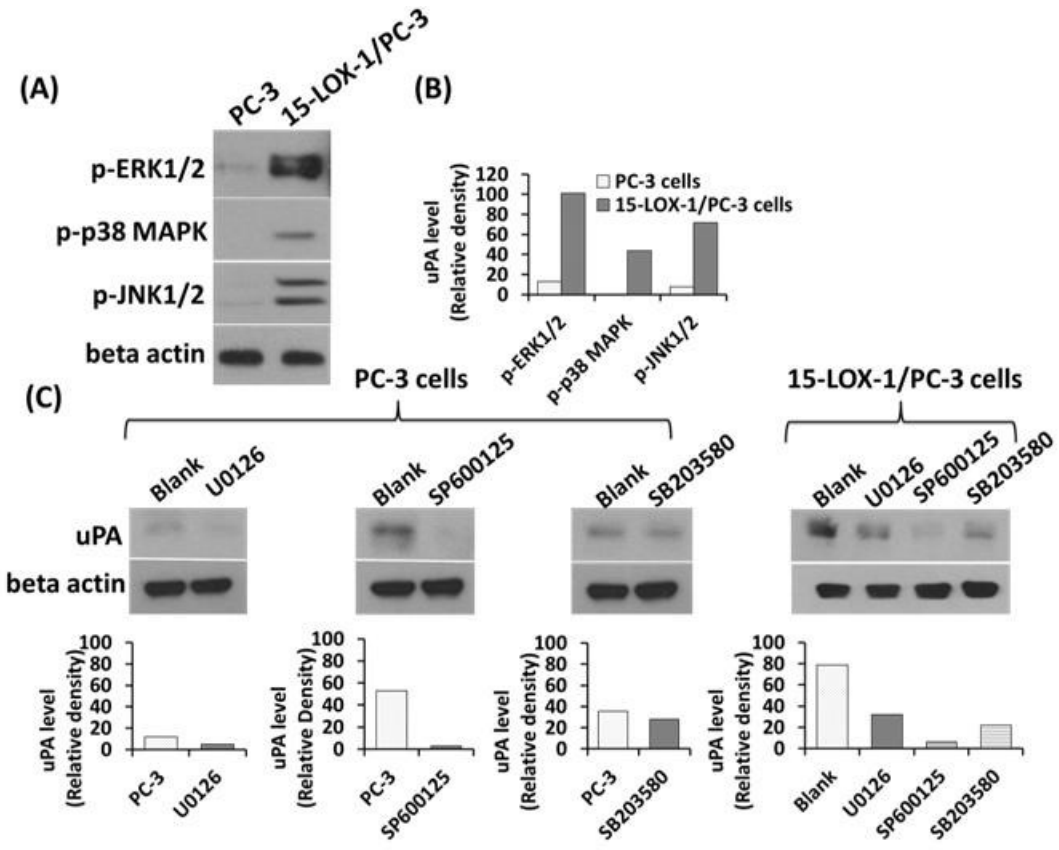

Fig. 32. Role of MAPK pathway in the regulation of uPA. (A) Activation of MAPK pathway in 15-LOX-1/PC-3 cells. Effect of MAPK inhibitors on the expression of uPA on (B) PC-3 and (C) 15-LOX-1/PC-3 cell.

4.4.3. Involvement of MAPK pathway in the upregulation of uPA in 15-LOX-1/PC-3 cells

Studies have shown that MAPK activation, mediated by various signaling cascades such as generation of reactive oxygen species may lead to upregulation of uPA [559, 560]. To investigate whether the overexpression of 15-LOX-1 in PC-3 cells was associated with upregulation of uPA, we incubated the cells with specific inhibitors of the MAPK family such as ERK1/2 inhibitor U0126 (10 μM), p-38MAPK inhibitor SB203580 (10 μM), and JNK1/2 inhibitor SP600125 (10 μM) with either PC-3 cells or PC-3-LOX cells. The cells were subjected to western blot analysis to assess the effect of the MAPK pathway inhibitors (Fig. 32C). We observed that treatment with all MAPK inhibitors significantly reduced the level of uPA in PC-3-

LOX cell lines, with maximum inhibition observed in case of JNK1/2 inhibitor (SP600125). Studies have shown that the JNK pathway and p-38 MAPK pathway can be activated by oxidative stress. Since lipoxygenases are good candidates for generating reactive oxygen species [561], they may be involved in the activation of members of the MAPK family, especially the JNK1/2 pathway since it involved activated by stress [562]. It is worthy to note that involvement of JNK1/2 pathway has already been implicated in the upregulation of uPA in PC-3 cells [563]. In agreement with this study, we found that upon incubation of PC-3 cells with JNK1/2 inhibitor, there was complete suppression of uPA production. On the other hand, there was either a slight changes in uPA level observed in PC-3 cells when they were incubated with ERK1/2 inhibitor and p-p38 MAPK inhibitor respectively. Our results indicated that JNK1/2 pathway is the major pathway that may be at least partially involved in the upregulation of uPA in 15-LOX-1 overexpressing PC-3 cells.

4.4.4. Migration assay

The level of uPA in cancer cells can influence its cell migration ability. Certain forms of lipoxygenases may alter cancer cell motility [513, 564], however; there are no studies so far which suggest that lipoxygenases may play role in uPA production. In previous section, it was found that transfection of 15-LOX-1 in PC-3 cells enhances the mRNA and protein levels of uPA. To study whether 15-LOX-1 transfection in PC-3 cells can enhance their migration ability, the migration of PC-3 cells and 15-LOX-1/PC-3 cells was compared. Fetal bovine serum (10% v/v) was used as a chemotactant in the study. As expected, we found that 15-LOX-1/PC-3 cells had greater migratory potential as compared to parental PC-3 cells ($p<0.05$) (Fig. 33). Our results suggest that overexpression of 15-LOX-1 in PC-3 cells may contribute to migratory potential in these cells.

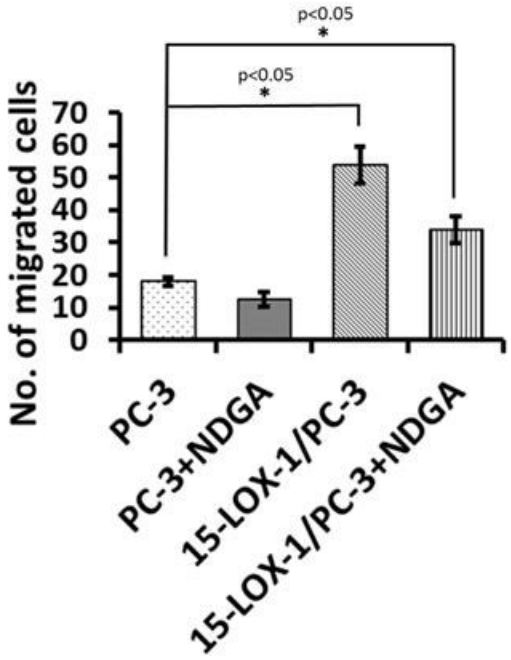

Fig. 33. Migration assay. Comparison of migratory potential of PC-3 cells versus 15-LOX-1/PC-3 cells. 15-LOX-1/PC-3 cells demonstrated significantly greater migration as compared to PC-3 cells ($p<0.05$). Upon incubation of 15-LOX-1.PC-3 cells with NDGA inhibitor, there was significant reduction in migration observed ($p<0.05$).

4.4.5. Wound healing assay

To compare the wound healing ability, monolayers of PC-3 cells and 15-LOX-1/PC-3 cells were scratched with a 100 µL pipette tip. After 24 hr of wounding, a large amount of both the cell lines had already migrated into the wound space; however, 15-LOX-1/PC-3 cells demonstrated significantly greater wound healing ability (Fig. 34). Both PC-3 cells as well as 15-LOX-1/PC-3 cells demonstrated typical features of migration, indicated by elongated morphology of few cells as well as their placement of longitudinal axis towards the center of the wound. To investigate whether the wound healing ability was contributed by 15-LOX-1 in cells, we incubated lipoxygenase inhibitors such as NDGA [565] as well as PD146176 [566]. It was found that both PC-3 cells and 15-LOX-1/PC-3 cells incubated with the inhibitors demonstrated decrease in wound healing ability as compared to their respective controls. These data suggested that 15-LOX-1 might contribute to the wound healing ability of PC-3 cells.

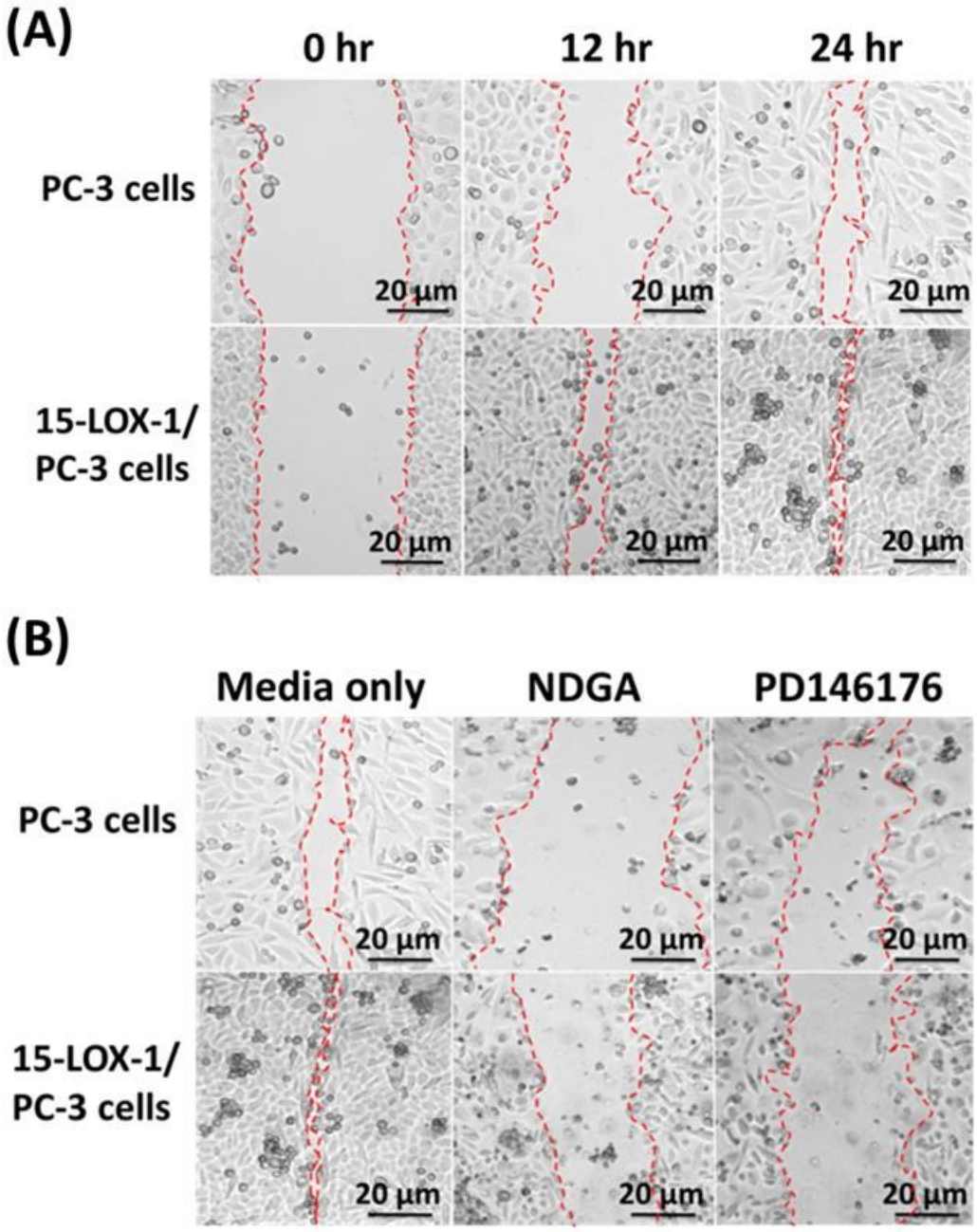

Fig. 34. Wound healing assay. (A) Kinetics (0, 12, 24 hr) of wound healing in PC-3 and 15-LOX-1/PC-3 cells. (B) Comparison of wound healing ability in PC-3 cells and 15-LOX-1/PC-3 cells.

4.5. Conclusion

A variety of studies have shown that lipoxygenases are involved in diseases including cancer, inflammatory disorders, atherosclerosis and angiogenesis. 15-Lipoxygenase-1 (15-LOX-1) is one of the two isoforms of 15-LOX that has been implicated to have a pro-tumorigenic role in prostate cancer. In the present study, we examined the relationship between the expression of 15-LOX-1 and urokinase plasminogen activator (uPA), a serine protease which is overexpressed in cancer. By performing a variety of in vitro and biofunctional assays, we demonstrated that the overexpression of 15-LOX-1 in PC-3 cells increased the mRNA as well as protein level of uPA upto 5-fold and contributed to their migratory ability. The incubation of lipoxygenase inhibitor (NDGA) reversed this effect, and therefore decreased the migratory ability of parental as well as 15-LOX-overexpressing PC-3 cells. In summary, our results are in agreement with the previous studies which suggested that 15-LOX-1 has a protumorigenic role in prostate cancer. We believe that investigation of 15-LOX-1 as an upstream of uPA would help in designing new strategies for treating prostate cancer.

CHAPTER 5. GENERAL CONCLUSION

The research conducted in this thesis discusses nanotechnology-based approaches for diagnosis and treatment of cancer. The first two chapters in this thesis focus on conjugation of peptide nanofibers recombinant antibodies and near infrared dyes, whereas the third chapter focuses on a novel pathway involved in the tumor promoting role of 15-LOX-1 prostate cancer. The important conclusions drawn from research in chapter I have been listed as follows:

- A near infrared nanofiber (NIR-NFP) for imaging urokinase plasminogen activator (uPA) was successfully synthesized and characterized. The NIR-NFP was (100 x 4) nm in dimension and contained an uPA cleavable substrate and multiple near infrared dye molecules. The fluorescence of nanofiber was quenched due to close proximity of near infrared dye molecules. Incubation with recombinant uPA *in vitro* resulted in about 20-fold increase in uPA.
- NIR-NFP was able to detect uPA secreted from different cancer cells. The levels of uPA detected by NIR-NFP correlated with very well with the actual uPA level of the cells (as confirmed by a commercial uPA activity assay kit).

Our data in chapter I suggest that NIR-NFP can be used as a potential near infrared imaging agent for recombinant as well as cell-secreted uPA activity. Overall, we believe that this strategy has potential for designing personalized, protease-based inhibitors and prodrug targeted therapies in future.

In chapter II, we demonstrate the synthesis of multivalent Herceptin conjugated nanofibers for increasing the therapeutic efficacy of Herceptin. Our results are:

- A peptide nanofiber conjugated with multivalent display of antibodies was synthesized. Each HER-NFP contained approximately 10 Herceptin antibodies. Significant

improvement in therapeutic efficacy was achieved when Herceptin was displayed in multivalent format. HER-NFP was approximately 2.5 fold more effective in inhibiting cell growth as compared to unconjugated Herceptin.

- Optimized HER-NFP preparation was able to induce HER-2 membrane receptor mediated internalization to downregulate its expression level to a greater extent as compared to Herceptin alone.
- Along with the alteration in downstream signaling and cellular responses, the HER-NFP internalized to a greater extent as compared to Herceptin alone.

Overall, our findings in chapter II provide strong evidence that this approach may be useful for increasing the therapeutic efficacy of monoclonal antibodies.

The third chapter of thesis is focused on the role of 15-LOX-1 in the upregulation of uPA in PC-3 prostate cancer cells. In this chapter, our findings are:

- For the first time, we demonstrate that 15-LOX-1 overexpression can lead to upregulation uPA. Western blot analysis showed higher levels and activity of uPA in 15-LOX-1/PC-3 cells as compared to parental PC-3 cells.
- In vitro migration assay and wound healing assay revealed that in PC-3 cells revealed that 15-LOX-1/PC-3 cells had greater migratory potential than PC-3 cells.
- Upregulation of uPA in 15-LOX-1/PC-3 cells may be mediated through the activation of members of mitogenic activated protein kinase pathways.

Overall, conclusions drawn from chapter III suggest that 15-LOX-1 may contribute to metastatic potential mediated by upregulation of uPA in prostate cancer and that targeting 15-LOX-1 pathway may be a useful strategy for treatment and/or prevention of prostate cancer.

CHAPTER 6. FUTURE DIRECTIONS

The research performed in this thesis indicates that nanofiber may serve as a diagnostic and drug delivery platform for the treatment and/or prevention of cancer. Since we obtained promising results in our preliminary in vitro studies, it would be of great interest to explore in vivo applications of nanofiber in xenograft model. Results from these studies so far serve as proof of concept for the application of this technology in future biomedical research.

In first chapter, we demonstrated the design and synthesis of a near infrared peptide nanofiber probe for imaging urokinase activity. This project is ultimately aimed at improving individualized therapy through biomarker-driven approaches by identifying subset of patients that are more likely to undergo metastasis. Some prospective studies that may be included are:

- To investigate the ability of NIR-NFP to detect tumor-secreted uPA tumor in nude mice by in vivo fluorescence imaging technique.
- To compare biodistribution and pharmacokinetic profile of NIR-NFP with free dye and other nanomaterial. Given the unique physicochemical properties and biocompatibility, nanofiber may be explored as an alternate nanomaterial for clinical applications.

In second chapter, we explore the applications of nanofiber for immuno-based treatments for cancer. We demonstrate that nanofiber can serve as a platform for conjugating multiple Herceptin antibodies. The resulting multivalent Herceptin-conjugated nanofiber showed significant improvement in therapeutic activity over Herceptin alone. With improvement in understanding additional mechanisms Herceptin, it would be interesting to perform these additional studies:

- To simultaneously target multiple cellular pathways involved in cancer growth by combinination of HER-NFP with chemotherapy. Potential studies would involve the

investigation of improvement in targeting ability of anti-cancer chemotherapeutic drugs such as doxorubicin, ellipticine and pyrene by co-delivering with HER-NFP.

- Another potential study would be to investigate whether HER-NFP is able to overcome resistance due to Herceptin in HER-2 positive cells.

In third chapter, our studies revealed that 15-LOX-1 may lead to upregulation of uPA in PC-3 prostate cancer cells. Based on our preliminary results, it is suggestive that targeting 15-LOX-1 may be potential strategy in the treatment of prostate cancer. However, further studies need to confirm this concept in vivo. Some potential future studies for chapter III include:

- In vivo work may be performed to confirm if there are any dietary risks factors associated with cancer. To achieve this, nude mice bearing either PC-3 or 15-LOX-1/PC-3 tumors may be utilized to compare cancer metastasis and median survival rate. Roles of LOXs and their metabolites can have important implications to cancer therapy.
- To investigate other members of the lipoxygenase family which are also implicated to play a role in cancer development (eg. such as 5-LOX and 12-LOX) and see if similar relationship exists.
- To gain further insight into association between uPA and 15-LOX-1, levels of uPA and 15-LOX-1 in tumors obtained from prostate cancer patients would be a potential study to perform.

REFERENCES

1. Siegel, R., Naishadham, D., and Jemal, A. Cancer statistics, 2012. CA Cancer J Clin *62*, 10-29.
2. Sajja, H.K., East, M.P., Mao, H., Wang, Y.A., Nie, S., and Yang, L. (2009). Development of multifunctional nanoparticles for targeted drug delivery and noninvasive imaging of therapeutic effect. Curr Drug Discov Technol *6*, 43-51.
3. Nie, S., Xing, Y., Kim, G.J., and Simons, J.W. (2007). Nanotechnology applications in cancer. Annu Rev Biomed Eng *9*, 257-288.
4. Zhong, W. (2009). Nanomaterials in fluorescence-based biosensing. Anal Bioanal Chem *394*, 47-59.
5. Pansare, V., Hejazi, S., Faenza, W., and Prud'homme, R.K. Review of Long-Wavelength Optical and NIR Imaging Materials: Contrast Agents, Fluorophores and Multifunctional Nano Carriers. Chem Mater *24*, 812-827.
6. Gunasekera, U.A., Pankhurst, Q.A., and Douek, M. (2009). Imaging applications of nanotechnology in cancer. Target Oncol *4*, 169-181.
7. Siddiqui, I.A., Adhami, V.M., Chamcheu, J.C., and Mukhtar, H. Impact of nanotechnology in cancer: emphasis on nanochemoprevention. Int J Nanomedicine *7*, 591-605.
8. Colson, Y.L., and Grinstaff, M.W. Biologically responsive polymeric nanoparticles for drug delivery. Adv Mater *24*, 3878-3886.
9. Rakowska, P.D., and Ryadnov, M.G. Nano-enabled biomarker discovery and detection. Biomark Med *5*, 387-396.
10. Dasilva, N., Diez, P., Matarraz, S., Gonzalez-Gonzalez, M., Paradinas, S., Orfao, A., and Fuentes, M. Biomarker discovery by novel sensors based on nanoproteomics approaches. Sensors (Basel) *12*, 2284-2308.
11. Malik, R., Qian, S., and Law, B. Design and synthesis of a near-infrared fluorescent nanofiber precursor for detecting cell-secreted urokinase activity. Anal Biochem *412*, 26-33.
12. Law, B., Curino, A., Bugge, T.H., Weissleder, R., and Tung, C.H. (2004). Design, synthesis, and characterization of urokinase plasminogen-activator-sensitive near-infrared reporter. Chem Biol *11*, 99-106.
13. Law, B., Weissleder, R., and Tung, C.H. (2007). Protease-sensitive fluorescent nanofibers. Bioconjug Chem *18*, 1701-1704.
14. Duffy, M.J., Maguire, T.M., McDermott, E.W., and O'Higgins, N. (1999). Urokinase plasminogen activator: a prognostic marker in multiple types of cancer. J Surg Oncol *71*, 130-135.
15. Duffy, M.J., Duggan, C., Mulcahy, H.E., McDermott, E.W., and O'Higgins, N.J. (1998). Urokinase plasminogen activator: a prognostic marker in breast cancer including patients with axillary node-negative disease. Clin Chem *44*, 1177-1183.
16. Shariat, S.F., Roehrborn, C.G., McConnell, J.D., Park, S., Alam, N., Wheeler, T.M., and Slawin, K.M. (2007). Association of the circulating levels of the urokinase system of plasminogen activation with the presence of prostate cancer and invasion, progression, and metastasis. J Clin Oncol *25*, 349-355.

17. Swiercz, R., Wolfe, J.D., Zaher, A., and Jankun, J. (1998). Expression of the plasminogen activation system in kidney cancer correlates with its aggressive phenotype. Clin Cancer Res *4*, 869-877.
18. Kuhn, W., Schmalfeldt, B., Reuning, U., Pache, L., Berger, U., Ulm, K., Harbeck, N., Spathe, K., Dettmar, P., Hofler, H., Janicke, F., Schmitt, M., and Graeff, H. (1999). Prognostic significance of urokinase (uPA) and its inhibitor PAI-1 for survival in advanced ovarian carcinoma stage FIGO IIIc. Br J Cancer *79*, 1746-1751.
19. Kobayashi, H., Fujishiro, S., and Terao, T. (1994). Impact of urokinase-type plasminogen activator and its inhibitor type 1 on prognosis in cervical cancer of the uterus. Cancer Res *54*, 6539-6548.
20. Harvey, S.R., Hurd, T.C., Markus, G., Martinick, M.I., Penetrante, R.M., Tan, D., Venkataraman, P., DeSouza, N., Sait, S.N., Driscoll, D.L., and Gibbs, J.F. (2003). Evaluation of urinary plasminogen activator, its receptor, matrix metalloproteinase-9, and von Willebrand factor in pancreatic cancer. Clin Cancer Res *9*, 4935-4943.
21. Hsu, D.W., Efird, J.T., and Hedley-Whyte, E.T. (1995). Prognostic role of urokinase-type plasminogen activator in human gliomas. Am J Pathol *147*, 114-123.
22. Skelly, M.M., Troy, A., Duffy, M.J., Mulcahy, H.E., Duggan, C., Connell, T.G., O'Donoghue, D.P., and Sheahan, K. (1997). Urokinase-type plasminogen activator in colorectal cancer: relationship with clinicopathological features and patient outcome. Clin Cancer Res *3*, 1837-1840.
23. Nekarda, H., Schmitt, M., Ulm, K., Wenninger, A., Vogelsang, H., Becker, K., Roder, J.D., Fink, U., and Siewert, J.R. (1994). Prognostic impact of urokinase-type plasminogen activator and its inhibitor PAI-1 in completely resected gastric cancer. Cancer Res *54*, 2900-2907.
24. Janicke, F., Prechtl, A., Thomssen, C., Harbeck, N., Meisner, C., Untch, M., Sweep, C.G., Selbmann, H.K., Graeff, H., and Schmitt, M. (2001). Randomized adjuvant chemotherapy trial in high-risk, lymph node-negative breast cancer patients identified by urokinase-type plasminogen activator and plasminogen activator inhibitor type 1. J Natl Cancer Inst *93*, 913-920.
25. Harbeck, N., Kates, R.E., Look, M.P., Meijer-Van Gelder, M.E., Klijn, J.G., Kruger, A., Kiechle, M., Janicke, F., Schmitt, M., and Foekens, J.A. (2002). Enhanced benefit from adjuvant chemotherapy in breast cancer patients classified high-risk according to urokinase-type plasminogen activator (uPA) and plasminogen activator inhibitor type 1 (n = 3424). Cancer Res *62*, 4617-4622.
26. Piironen, T., Laursen, B., Pass, J., List, K., Gardsvoll, H., Ploug, M., Dano, K., and Hoyer-Hansen, G. (2004). Specific immunoassays for detection of intact and cleaved forms of the urokinase receptor. Clin Chem *50*, 2059-2068.
27. Schmitt, M., Sturmheit, A.S., Welk, A., Schnelldorfer, C., and Harbeck, N. (2006). Procedures for the quantitative protein determination of urokinase and its inhibitor, PAI-1, in human breast cancer tissue extracts by ELISA. Methods Mol Med *120*, 245-265.
28. Benraad, T.J., Geurts-Moespot, J., Grondahl-Hansen, J., Schmitt, M., Heuvel, J.J., de Witte, J.H., Foekens, J.A., Leake, R.E., Brunner, N., and Sweep, C.G. (1996). Immunoassays (ELISA) of urokinase-type plasminogen activator (uPA): report of an EORTC/BIOMED-1 workshop. Eur J Cancer *32A*, 1371-1381.
29. Dublin, E., Hanby, A., Patel, N.K., Liebman, R., and Barnes, D. (2000). Immunohistochemical expression of uPA, uPAR, and PAI-1 in breast carcinoma.

Fibroblastic expression has strong associations with tumor pathology. Am J Pathol *157*, 1219-1227.
30. Sinsheimer, J.E., Jagodic, V., and Burckhalter, J.H. (1974). Fluorescein isothiocyanates: improved synthesis and purity. Spectral studies. Anal Biochem *57*, 227-231.
31. Adams, K.E., Ke, S., Kwon, S., Liang, F., Fan, Z., Lu, Y., Hirschi, K., Mawad, M.E., Barry, M.A., and Sevick-Muraca, E.M. (2007). Comparison of visible and near-infrared wavelength-excitable fluorescent dyes for molecular imaging of cancer. J Biomed Opt *12*, 024017.
32. Yuan, L., Lin, W., Zhao, S., Gao, W., Chen, B., He, L., and Zhu, S. A unique approach to development of near-infrared fluorescent sensors for in vivo imaging. J Am Chem Soc *134*, 13510-13523.
33. Luo, S., Zhang, E., Su, Y., Cheng, T., and Shi, C. A review of NIR dyes in cancer targeting and imaging. Biomaterials *32*, 7127-7138.
34. Dahabreh, I.J., Linardou, H., Siannis, F., Fountzilas, G., and Murray, S. (2008). Trastuzumab in the adjuvant treatment of early-stage breast cancer: a systematic review and meta-analysis of randomized controlled trials. Oncologist *13*, 620-630.
35. Nelson, A.L., Dhimolea, E., and Reichert, J.M. Development trends for human monoclonal antibody therapeutics. Nat Rev Drug Discov *9*, 767-774.
36. Paintaud, G., Divine, M., and Lechat, P. Monoclonal Antibodies for Therapeutic Use: Specific Characteristics of Clinical Development, Evaluation by the Agencies, and Long-term Monitoring of Safety. Therapie *67*, 329-337.
37. Modjtahedi, H., Ali, S., and Essapen, S. Therapeutic application of monoclonal antibodies in cancer: advances and challenges. Br Med Bull.
38. Chames, P., Van Regenmortel, M., Weiss, E., and Baty, D. (2009). Therapeutic antibodies: successes, limitations and hopes for the future. Br J Pharmacol *157*, 220-233.
39. Wong, A.L., and Lee, S.C. Mechanisms of Resistance to Trastuzumab and Novel Therapeutic Strategies in HER2-Positive Breast Cancer. Int J Breast Cancer *2012*, 415170.
40. Villamor, N., Montserrat, E., and Colomer, D. (2003). Mechanism of action and resistance to monoclonal antibody therapy. Semin Oncol *30*, 424-433.
41. Isaacs, J.D. (2001). From bench to bedside: discovering rules for antibody design, and improving serotherapy with monoclonal antibodies. Rheumatology (Oxford) *40*, 724-738.
42. Deyev, S.M., and Lebedenko, E.N. (2008). Multivalency: the hallmark of antibodies used for optimization of tumor targeting by design. Bioessays *30*, 904-918.
43. Pluckthun, A., and Pack, P. (1997). New protein engineering approaches to multivalent and bispecific antibody fragments. Immunotechnology *3*, 83-105.
44. Barat, B., Sirk, S.J., McCabe, K.E., Li, J., Lepin, E.J., Remenyi, R., Koh, A.L., Olafsen, T., Gambhir, S.S., Weiss, S., and Wu, A.M. (2009). Cys-diabody quantum dot conjugates (immunoQdots) for cancer marker detection. Bioconjug Chem *20*, 1474-1481.
45. Kubetzko, S., Balic, E., Waibel, R., Zangemeister-Wittke, U., and Pluckthun, A. (2006). PEGylation and multimerization of the anti-p185HER-2 single chain Fv fragment 4D5: effects on tumor targeting. J Biol Chem *281*, 35186-35201.
46. Moliterni, A., Menard, S., Valagussa, P., Biganzoli, E., Boracchi, P., Balsari, A., Casalini, P., Tomasic, G., Marubini, E., Pilotti, S., and Bonadonna, G. (2003). HER2 overexpression and doxorubicin in adjuvant chemotherapy for resectable breast cancer. J Clin Oncol *21*, 458-462.

47. Guarneri, V., Bengala, C., Orlandini, C., Gennari, A., Donati, S., Campani, D., Collecchi, P., Maur, M., and Conte, P.F. (2004). HER2 overexpression as a prognostic factor in metastatic breast cancer patients treated with high-dose chemotherapy and autologous stem cell support. Bone Marrow Transplant *34*, 413-417.
48. Orphanos, G., and Kountourakis, P. Targeting the HER2 Receptor in Metastatic Breast Cancer. Hematol Oncol Stem Cell Ther *5*, 127-137.
49. Loo, Y., Zhang, S., and Hauser, C.A. From short peptides to nanofibers to macromolecular assemblies in biomedicine. Biotechnol Adv *30*, 593-603.
50. Zhao, Y., Tanaka, M., Kinoshita, T., Higuchi, M., and Tan, T. Nanofibrous scaffold from self-assembly of beta-sheet peptides containing phenylalanine for controlled release. J Control Release *142*, 354-360.
51. Nakane, P.K., and Kawaoi, A. (1974). Peroxidase-labeled antibody. A new method of conjugation. J Histochem Cytochem *22*, 1084-1091.
52. Dasgupta, S., Srinidhi, S., and Vishwanatha, J.K. Oncogenic activation in prostate cancer progression and metastasis: Molecular insights and future challenges. J Carcinog *11*, 4.
53. Alberti, C. (2006). Prostate cancer progression and surrounding microenvironment. Int J Biol Markers *21*, 88-95.
54. Bairati, I., Meyer, F., Fradet, Y., and Moore, L. (1998). Dietary fat and advanced prostate cancer. J Urol *159*, 1271-1275.
55. Narita, S., Tsuchiya, N., Saito, M., Inoue, T., Kumazawa, T., Yuasa, T., Nakamura, A., and Habuchi, T. (2008). Candidate genes involved in enhanced growth of human prostate cancer under high fat feeding identified by microarray analysis. Prostate *68*, 321-335.
56. Berquin, I.M., Edwards, I.J., Kridel, S.J., and Chen, Y.Q. Polyunsaturated fatty acid metabolism in prostate cancer. Cancer Metastasis Rev *30*, 295-309.
57. Lophatananon, A., Archer, J., Easton, D., Pocock, R., Dearnaley, D., Guy, M., Kote-Jarai, Z., O'Brien, L., Wilkinson, R.A., Hall, A.L., Sawyer, E., Page, E., Liu, J.F., Barratt, S., Rahman, A.A., Eeles, R., and Muir, K. Dietary fat and early-onset prostate cancer risk. Br J Nutr *103*, 1375-1380.
58. Aronson, W.J., Barnard, R.J., Freedland, S.J., Henning, S., Elashoff, D., Jardack, P.M., Cohen, P., Heber, D., and Kobayashi, N. Growth inhibitory effect of low fat diet on prostate cancer cells: results of a prospective, randomized dietary intervention trial in men with prostate cancer. J Urol *183*, 345-350.
59. Kuhn, H., Walther, M., and Kuban, R.J. (2002). Mammalian arachidonate 15-lipoxygenases structure, function, and biological implications. Prostaglandins Other Lipid Mediat *68-69*, 263-290.
60. Pidgeon, G.P., Lysaght, J., Krishnamoorthy, S., Reynolds, J.V., O'Byrne, K., Nie, D., and Honn, K.V. (2007). Lipoxygenase metabolism: roles in tumor progression and survival. Cancer Metastasis Rev *26*, 503-524.
61. Kelavkar, U.P., Nixon, J.B., Cohen, C., Dillehay, D., Eling, T.E., and Badr, K.F. (2001). Overexpression of 15-lipoxygenase-1 in PC-3 human prostate cancer cells increases tumorigenesis. Carcinogenesis *22*, 1765-1773.
62. Menna, C., Olivieri, F., Catalano, A., and Procopio, A. Lipoxygenase inhibitors for cancer prevention: promises and risks. Curr Pharm Des *16*, 725-733.
63. Duffy, M.J. (2004). The urokinase plasminogen activator system: role in malignancy. Curr Pharm Des *10*, 39-49.

64. Harbeck, N., Kates, R.E., Schmitt, M., Gauger, K., Kiechle, M., Janicke, F., Thomassen, C., Look, M.P., and Foekens, J.A. (2004). Urokinase-type plasminogen activator and its inhibitor type 1 predict disease outcome and therapy response in primary breast cancer. Clin Breast Cancer *5*, 348-352.
65. Tracy, M. Latest advances in biomarker discovery and development. Drugs Today (Barc) *48*, 735-739.
66. Sun, X., and Jia, Z. A brief review of biomarkers for preventing and treating cardiovascular diseases. J Cardiovasc Dis Res *3*, 251-254.
67. Kumar, S., Mohan, A., and Guleria, R. (2006). Biomarkers in cancer screening, research and detection: present and future: a review. Biomarkers *11*, 385-405.
68. Jungic, S., Tubic, B., and Skrepnik, T. The role of biomarkers in the development of novel cancer therapies. Drug Metabol Drug Interact *27*, 89-99.
69. Duffy, M.J., O'Donovan, N., and Crown, J. Use of molecular markers for predicting therapy response in cancer patients. Cancer Treat Rev *37*, 151-159.
70. Soresi, M., Magliarisi, C., Campagna, P., Leto, G., Bonfissuto, G., Riili, A., Carroccio, A., Sesti, R., Tripi, S., and Montalto, G. (2003). Usefulness of alpha-fetoprotein in the diagnosis of hepatocellular carcinoma. Anticancer Res *23*, 1747-1753.
71. Kawakami, K., Brabender, J., Lord, R.V., Groshen, S., Greenwald, B.D., Krasna, M.J., Yin, J., Fleisher, A.S., Abraham, J.M., Beer, D.G., Sidransky, D., Huss, H.T., Demeester, T.R., Eads, C., Laird, P.W., Ilson, D.H., Kelsen, D.P., Harpole, D., Moore, M.B., Danenberg, K.D., Danenberg, P.V., and Meltzer, S.J. (2000). Hypermethylated APC DNA in plasma and prognosis of patients with esophageal adenocarcinoma. J Natl Cancer Inst *92*, 1805-1811.
72. Ross, J.S., and Fletcher, J.A. (1998). The HER-2/neu Oncogene in Breast Cancer: Prognostic Factor, Predictive Factor, and Target for Therapy. Oncologist *3*, 237-252.
73. Ulmert, D., Cronin, A.M., Bjork, T., O'Brien, M.F., Scardino, P.T., Eastham, J.A., Becker, C., Berglund, G., Vickers, A.J., and Lilja, H. (2008). Prostate-specific antigen at or before age 50 as a predictor of advanced prostate cancer diagnosed up to 25 years later: a case-control study. BMC Med *6*, 6.
74. Kruijff, S., Bastiaannet, E., Kobold, A.C., van Ginkel, R.J., Suurmeijer, A.J., and Hoekstra, H.J. (2009). S-100B concentrations predict disease-free survival in stage III melanoma patients. Ann Surg Oncol *16*, 3455-3462.
75. Fures, R., Bukovic, D., Hodek, B., Klaric, B., Herman, R., and Grubisic, G. (1999). Preoperative tumor marker CA125 levels in relation to epithelial ovarian cancer stage. Coll Antropol *23*, 189-194.
76. Cornford, P.A., Dodson, A.R., Parsons, K.F., Desmond, A.D., Woolfenden, A., Fordham, M., Neoptolemos, J.P., Ke, Y., and Foster, C.S. (2000). Heat shock protein expression independently predicts clinical outcome in prostate cancer. Cancer Res *60*, 7099-7105.
77. Lenhard, M., Tsvilina, A., Schumacher, L., Kupka, M., Ditsch, N., Mayr, D., Friese, K., and Jeschke, U. Human chorionic gonadotropin and its relation to grade, stage and patient survival in ovarian cancer. BMC Cancer *12*, 2.
78. Pedraza, V., Gomez-Capilla, J.A., Escaramis, G., Gomez, C., Torne, P., Rivera, J.M., Gil, A., Araque, P., Olea, N., Estivill, X., and Farez-Vidal, M.E. Gene expression signatures in breast cancer distinguish phenotype characteristics, histologic subtypes, and tumor invasiveness. Cancer *116*, 486-496.

79. Duffy, M.J. (2002). Urokinase plasminogen activator and its inhibitor, PAI-1, as prognostic markers in breast cancer: from pilot to level 1 evidence studies. Clin Chem *48*, 1194-1197.
80. Collette, L., de Reijke, T.M., and Schroder, F.H. (2003). Prostate specific antigen: a prognostic marker of survival in good prognosis metastatic prostate cancer? (EORTC 30892). Eur Urol *44*, 182-189; discussion 189.
81. Vineis, P., and Perera, F. (2007). Molecular epidemiology and biomarkers in etiologic cancer research: the new in light of the old. Cancer Epidemiol Biomarkers Prev *16*, 1954-1965.
82. Bonassi, S., and Au, W.W. (2002). Biomarkers in molecular epidemiology studies for health risk prediction. Mutat Res *511*, 73-86.
83. Reis-Filho, J.S., and Pusztai, L. Gene expression profiling in breast cancer: classification, prognostication, and prediction. Lancet *378*, 1812-1823.
84. Liao, C.C., Mehta, A., Ward, N.J., Marsh, S., Arulampalam, T., and Norton, J.D. Analysis of post-operative changes in serum protein expression profiles from colorectal cancer patients by MALDI-TOF mass spectrometry: a pilot methodological study. World J Surg Oncol *8*, 33.
85. Nott, S.L., Huang, Y., Li, X., Fluharty, B.R., Qiu, X., Welshons, W.V., Yeh, S., and Muyan, M. (2009). Genomic responses from the estrogen-responsive element-dependent signaling pathway mediated by estrogen receptor alpha are required to elicit cellular alterations. J Biol Chem *284*, 15277-15288.
86. Chen, W.G., and White, F.M. (2004). Proteomic analysis of cellular signaling. Expert Rev Proteomics *1*, 343-354.
87. Nic An Ultaigh, S., and Ryan, M.F. (2007). Classes and crossreactivity of proteinases in the excretory-secretory products of Caenorhabditis elegans. J Helminthol *81*, 93-99.
88. Solgaard, G., Standal, I.B., and Draget, K.I. (2007). Proteolytic activity and protease classes in the zooplankton species Calanus finmarchicus. Comp Biochem Physiol B Biochem Mol Biol *147*, 475-481.
89. Arastu-Kapur, S., Ponder, E.L., Fonovic, U.P., Yeoh, S., Yuan, F., Fonovic, M., Grainger, M., Phillips, C.I., Powers, J.C., and Bogyo, M. (2008). Identification of proteases that regulate erythrocyte rupture by the malaria parasite Plasmodium falciparum. Nat Chem Biol *4*, 203-213.
90. Edwards, M.G., Gatehouse, J.A., and Gatehouse, A.M. Molecular and biochemical characterisation of a dual proteolytic system in vine weevil larvae (Otiorhynchus sulcatus Coleoptera: Curculionidae). Insect Biochem Mol Biol *40*, 785-791.
91. Powers, J.C., Odake, S., Oleksyszyn, J., Hori, H., Ueda, T., Boduszek, B., and Kam, C. (1993). Proteases--structures, mechanism and inhibitors. Agents Actions Suppl *42*, 3-18.
92. Zamolodchikova, T.S. Serine proteases of small intestine mucosa--localization, functional properties, and physiological role. Biochemistry (Mosc) *77*, 820-829.
93. Tanaka, K.A., Key, N.S., and Levy, J.H. (2009). Blood coagulation: hemostasis and thrombin regulation. Anesth Analg *108*, 1433-1446.
94. Obermajer, N., Repnik, U., Jevnikar, Z., Turk, B., Kreft, M., and Kos, J. (2008). Cysteine protease cathepsin X modulates immune response via activation of beta2 integrins. Immunology *124*, 76-88.

95. Fonovic, M., and Bogyo, M. (2007). Activity based probes for proteases: applications to biomarker discovery, molecular imaging and drug screening. Curr Pharm Des *13*, 253-261.
96. Alaoui-Jamali, M.A., and Xu, Y.J. (2006). Proteomic technology for biomarker profiling in cancer: an update. J Zhejiang Univ Sci B *7*, 411-420.
97. Bjellqvist, B., Ek, K., Righetti, P.G., Gianazza, E., Gorg, A., Westermeier, R., and Postel, W. (1982). Isoelectric focusing in immobilized pH gradients: principle, methodology and some applications. J Biochem Biophys Methods *6*, 317-339.
98. Weiss, W., Weiland, F., and Gorg, A. (2009). Protein detection and quantitation technologies for gel-based proteome analysis. Methods Mol Biol *564*, 59-82.
99. Blomberg, A., Blomberg, L., Norbeck, J., Fey, S.J., Larsen, P.M., Larsen, M., Roepstorff, P., Degand, H., Boutry, M., Posch, A., and et al. (1995). Interlaboratory reproducibility of yeast protein patterns analyzed by immobilized pH gradient two-dimensional gel electrophoresis. Electrophoresis *16*, 1935-1945.
100. Bunai, K., and Yamane, K. (2005). Effectiveness and limitation of two-dimensional gel electrophoresis in bacterial membrane protein proteomics and perspectives. J Chromatogr B Analyt Technol Biomed Life Sci *815*, 227-236.
101. Findeisen, P., and Neumaier, M. (2009). Mass spectrometry based proteomics profiling as diagnostic tool in oncology: current status and future perspective. Clin Chem Lab Med *47*, 666-684.
102. Baggerly, K.A., Morris, J.S., Wang, J., Gold, D., Xiao, L.C., and Coombes, K.R. (2003). A comprehensive approach to the analysis of matrix-assisted laser desorption/ionization-time of flight proteomics spectra from serum samples. Proteomics *3*, 1667-1672.
103. Yates, J.R., Ruse, C.I., and Nakorchevsky, A. (2009). Proteomics by mass spectrometry: approaches, advances, and applications. Annu Rev Biomed Eng *11*, 49-79.
104. deVera, I.E., Katz, J.E., and Agus, D.B. (2006). Clinical proteomics: the promises and challenges of mass spectrometry-based biomarker discovery. Clin Adv Hematol Oncol *4*, 541-549.
105. Burnette, W.N. (2009). Western blotting : remembrance of past things. Methods Mol Biol *536*, 5-8.
106. Jensen, E.C. The basics of western blotting. Anat Rec (Hoboken) *295*, 369-371.
107. MacPhee, D.J. Methodological considerations for improving Western blot analysis. J Pharmacol Toxicol Methods *61*, 171-177.
108. Ramos-Vara, J.A. (2005). Technical aspects of immunohistochemistry. Vet Pathol *42*, 405-426.
109. Mandell, J.W. (2008). Immunohistochemical assessment of protein phosphorylation state: the dream and the reality. Histochem Cell Biol *130*, 465-471.
110. Hwang, C.J., Vaccaro, A.R., Hong, J., Lawrence, J.P., Fischgrund, J.S., Alaoui-Ismaili, M.H., and Falb, D. Immunogenicity of osteogenic protein 1: results from a prospective, randomized, controlled, multicenter pivotal study of uninstrumented lumbar posterolateral fusion. J Neurosurg Spine *13*, 484-493.
111. Ye, G.J., Oshins, R., Rouhani, F., Brantly, M.L., and Chulay, J.D. Development, validation and use of ELISA for antibodies to human alpha-1 antitrypsin. J Immunol Methods.

112. Arendt, J.F., Quadros, E.V., and Nexo, E. Soluble transcobalamin receptor, sCD320, is present in human serum and relates to serum cobalamin - establishment and validation of an ELISA. Clin Chem Lab Med *50*, 515-519.
113. Mizukami, S., Takikawa, R., Sugihara, F., Hori, Y., Tochio, H., Walchli, M., Shirakawa, M., and Kikuchi, K. (2008). Paramagnetic relaxation-based 19f MRI probe to detect protease activity. J Am Chem Soc *130*, 794-795.
114. Bremer, C., Ntziachristos, V., Weitkamp, B., Theilmeier, G., Heindel, W., and Weissleder, R. (2005). Optical imaging of spontaneous breast tumors using protease sensing 'smart' optical probes. Invest Radiol *40*, 321-327.
115. Weissleder, R., and Pittet, M.J. (2008). Imaging in the era of molecular oncology. Nature *452*, 580-589.
116. Gregoire, V., Bol, A., Geets, X., and Lee, J. (2006). Is PET-based treatment planning the new standard in modern radiotherapy? The head and neck paradigm. Semin Radiat Oncol *16*, 232-238.
117. Jaffer, F.A., and Weissleder, R. (2005). Molecular imaging in the clinical arena. Jama *293*, 855-862.
118. Yang, Y., Hong, H., Zhang, Y., and Cai, W. (2009). Molecular Imaging of Proteases in Cancer. Cancer Growth Metastasis *2*, 13-27.
119. Choi, K.Y., Swierczewska, M., Lee, S., and Chen, X. Protease-activated drug development. Theranostics *2*, 156-178.
120. Caliendo, G., Santagada, V., Perissutti, E., Severino, B., Fiorino, F., Frecentese, F., and Juliano, L. Kallikrein protease activated receptor (PAR) axis: an attractive target for drug development. J Med Chem *55*, 6669-6686.
121. Panteleakou, Z., Lembessis, P., Sourla, A., Pissimissis, N., Polyzos, A., Deliveliotis, C., and Koutsilieris, M. (2009). Detection of circulating tumor cells in prostate cancer patients: methodological pitfalls and clinical relevance. Mol Med *15*, 101-114.
122. Sheth, R.A., Upadhyay, R., Stangenberg, L., Sheth, R., Weissleder, R., and Mahmood, U. (2009). Improved detection of ovarian cancer metastases by intraoperative quantitative fluorescence protease imaging in a pre-clinical model. Gynecol Oncol *112*, 616-622.
123. Scherer, R.L., McIntyre, J.O., and Matrisian, L.M. (2008). Imaging matrix metalloproteinases in cancer. Cancer Metastasis Rev *27*, 679-690.
124. Shah, K., and Weissleder, R. (2005). Molecular optical imaging: applications leading to the development of present day therapeutics. NeuroRx *2*, 215-225.
125. Huang, X., Lee, S., and Chen, X. Design of "smart" probes for optical imaging of apoptosis. Am J Nucl Med Mol Imaging *1*, 3-17.
126. Kobayashi, H., and Choyke, P.L. Target-cancer-cell-specific activatable fluorescence imaging probes: rational design and in vivo applications. Acc Chem Res *44*, 83-90.
127. Lee, S., Park, K., Kim, K., Choi, K., and Kwon, I.C. (2008). Activatable imaging probes with amplified fluorescent signals. Chem Commun (Camb), 4250-4260.
128. Nolting, D.D., Nickels, M.L., Guo, N., and Pham, W. Molecular imaging probe development: a chemistry perspective. Am J Nucl Med Mol Imaging *2*, 273-306.
129. Schellenberger, E., Rudloff, F., Warmuth, C., Taupitz, M., Hamm, B., and Schnorr, J. (2008). Protease-specific nanosensors for magnetic resonance imaging. Bioconjug Chem *19*, 2440-2445.

130. Olson, E.S., Aguilera, T.A., Jiang, T., Ellies, L.G., Nguyen, Q.T., Wong, E.H., Gross, L.A., and Tsien, R.Y. (2009). In vivo characterization of activatable cell penetrating peptides for targeting protease activity in cancer. Integr Biol (Camb) *1*, 382-393.
131. Weissleder, R., Tung, C.H., Mahmood, U., and Bogdanov, A., Jr. (1999). In vivo imaging of tumors with protease-activated near-infrared fluorescent probes. Nat Biotechnol *17*, 375-378.
132. Licha, K., Hessenius, C., Becker, A., Henklein, P., Bauer, M., Wisniewski, S., Wiedenmann, B., and Semmler, W. (2001). Synthesis, characterization, and biological properties of cyanine-labeled somatostatin analogues as receptor-targeted fluorescent probes. Bioconjug Chem *12*, 44-50.
133. Calfon, M.A., Rosenthal, A., Mallas, G., Mauskapf, A., Nudelman, R.N., Ntziachristos, V., and Jaffer, F.A. In vivo near infrared fluorescence (NIRF) intravascular molecular imaging of inflammatory plaque, a multimodal approach to imaging of atherosclerosis. J Vis Exp.
134. Zhang, X., Bloch, S., Akers, W., and Achilefu, S. Near-infrared molecular probes for in vivo imaging. Curr Protoc Cytom *Chapter 12*, Unit12 27.
135. He, X., Wang, K., and Cheng, Z. In vivo near-infrared fluorescence imaging of cancer with nanoparticle-based probes. Wiley Interdiscip Rev Nanomed Nanobiotechnol *2*, 349-366.
136. Rogach, A.L., and Ogris, M. Near-infrared-emitting semiconductor quantum dots for tumor imaging and targeting. Curr Opin Mol Ther *12*, 331-339.
137. Hardman, R. (2006). A toxicologic review of quantum dots: toxicity depends on physicochemical and environmental factors. Environ Health Perspect *114*, 165-172.
138. Umezawa, K., Citterio, D., and Suzuki, K. (2008). Water-soluble NIR fluorescent probes based on squaraine and their application for protein labeling. Anal Sci *24*, 213-217.
139. Lisy, M.R., Goermar, A., Thomas, C., Pauli, J., Resch-Genger, U., Kaiser, W.A., and Hilger, I. (2008). In vivo near-infrared fluorescence imaging of carcinoembryonic antigen-expressing tumor cells in mice. Radiology *247*, 779-787.
140. Ghoroghchian, P.P., Therien, M.J., and Hammer, D.A. (2009). In vivo fluorescence imaging: a personal perspective. Wiley Interdiscip Rev Nanomed Nanobiotechnol *1*, 156-167.
141. Sun, Z., Ye, Q., Chi, C., and Wu, J. Low band gap polycyclic hydrocarbons: from closed-shell near infrared dyes and semiconductors to open-shell radicals. Chem Soc Rev *41*, 7857-7889.
142. Zhang, S., Metelev, V., Tabatadze, D., Zamecnik, P., and Bogdanov, A., Jr. (2008). Near-infrared fluorescent oligodeoxyribonucleotide reporters for sensing NF-kappaB DNA interactions in vitro. Oligonucleotides *18*, 235-243.
143. Chopra, A. (2004). Trastuzumab complexed to near-infrared fluorophore indocyanine green.
144. Bouteiller, C., Clave, G., Bernardin, A., Chipon, B., Massonneau, M., Renard, P.Y., and Romieu, A. (2007). Novel water-soluble near-infrared cyanine dyes: synthesis, spectral properties, and use in the preparation of internally quenched fluorescent probes. Bioconjug Chem *18*, 1303-1317.
145. Priem, T., Bouteiller, C., Camporese, D., Brune, X., Hardouin, J., Romieu, A., and Renard, P.Y. A novel sulfonated prosthetic group for [(18)F]-radiolabelling and imparting water solubility of biomolecules and cyanine fluorophores. Org Biomol Chem.

146. Bouit, P.A., Di Piazza, E., Rigaut, S., Le Guennic, B., Aronica, C., Toupet, L., Andraud, C., and Maury, O. (2008). Stable near-infrared anionic polymethine dyes: structure, photophysical, and redox properties. Org Lett *10*, 4159-4162.
147. Licha, K., Riefke, B., Ebert, B., and Grotzinger, C. (2002). Cyanine dyes as contrast agents in biomedical optical imaging. Acad Radiol *9 Suppl 2*, S320-322.
148. Choy, G., Choyke, P., and Libutti, S.K. (2003). Current advances in molecular imaging: noninvasive in vivo bioluminescent and fluorescent optical imaging in cancer research. Mol Imaging *2*, 303-312.
149. Nolting, D.D., Gore, J.C., and Pham, W. NEAR-INFRARED DYES: Probe Development and Applications in Optical Molecular Imaging. Curr Org Synth *8*, 521-534.
150. Reddington, M.V. (2007). Synthesis and properties of phosphonic acid containing cyanine and squaraine dyes for use as fluorescent labels. Bioconjug Chem *18*, 2178-2190.
151. Schuler, B., and Pannell, L.K. (2002). Specific labeling of polypeptides at amino-terminal cysteine residues using Cy5-benzyl thioester. Bioconjug Chem *13*, 1039-1043.
152. Tokuda, K., Zorumski, C.F., and Izumi, Y. (2009). Involvement of illumination in indocyanine green toxicity after its washout in the ex vivo rat retina. Retina *29*, 371-379.
153. Ricci, F., Missiroli, F., Regine, F., Grossi, M., and Dorin, G. (2009). Indocyanine green enhanced subthreshold diode-laser micropulse photocoagulation treatment of chronic central serous chorioretinopathy. Graefes Arch Clin Exp Ophthalmol *247*, 597-607.
154. Janssen, M.W., Druckrey-Fiskaaen, K.T., Omidi, L., Sliwinski, G., Thiele, C., Donaubauer, B., Polze, N., Kaisers, U.X., Thiery, J., Wittekind, C., Hauss, J.P., and Schon, M.R. Indocyanine green R15 ratio depends directly on liver perfusion flow rate. J Hepatobiliary Pancreat Sci *17*, 180-185.
155. Yong, K.T., Roy, I., Ding, H., Bergey, E.J., and Prasad, P.N. (2009). Biocompatible near-infrared quantum dots as ultrasensitive probes for long-term in vivo imaging applications. Small *5*, 1997-2004.
156. Shang, L., Yin, J., Li, J., Jin, L., and Dong, S. (2009). Gold nanoparticle-based near-infrared fluorescent detection of biological thiols in human plasma. Biosens Bioelectron *25*, 269-274.
157. Bwambok, D.K., El-Zahab, B., Challa, S.K., Li, M., Chandler, L., Baker, G.A., and Warner, I.M. (2009). Near-infrared fluorescent nanoGUMBOS for biomedical imaging. ACS Nano *3*, 3854-3860.
158. Puvanakrishnan, P., Park, J., Diagaradjane, P., Schwartz, J.A., Coleman, C.L., Gill-Sharp, K.L., Sang, K.L., Payne, J.D., Krishnan, S., and Tunnell, J.W. (2009). Near-infrared narrow-band imaging of gold/silica nanoshells in tumors. J Biomed Opt *14*, 024044.
159. Wang, M., Mi, C.C., Wang, W.X., Liu, C.H., Wu, Y.F., Xu, Z.R., Mao, C.B., and Xu, S.K. (2009). Immunolabeling and NIR-excited fluorescent imaging of HeLa cells by using NaYF(4):Yb,Er upconversion nanoparticles. ACS Nano *3*, 1580-1586.
160. Lee, C.M., Jeong, H.J., Cheong, S.J., Kim, E.M., Kim, D.W., Lim, S.T., and Sohn, M.H. Prostate cancer-targeted imaging using magnetofluorescent polymeric nanoparticles functionalized with bombesin. Pharm Res *27*, 712-721.
161. Leung, K. (2004). Quantum dot800-poly(ethylene glycol)-c(Arg-Gly-Asp-d-Tyr-Lys).
162. He, X., Chen, J., Wang, K., Qin, D., and Tan, W. (2007). Preparation of luminescent Cy5 doped core-shell SFNPs and its application as a near-infrared fluorescent marker. Talanta *72*, 1519-1526.

163. Santra, S., Liesenfeld, B., Dutta, D., Chatel, D., Batich, C.D., Tan, W., Moudgil, B.M., and Mericle, R.A. (2005). Folate conjugated fluorescent silica nanoparticles for labeling neoplastic cells. J Nanosci Nanotechnol *5*, 899-904.
164. Kester, M., Heakal, Y., Fox, T., Sharma, A., Robertson, G.P., Morgan, T.T., Altinoglu, E.I., Tabakovic, A., Parette, M.R., Rouse, S.M., Ruiz-Velasco, V., and Adair, J.H. (2008). Calcium phosphate nanocomposite particles for in vitro imaging and encapsulated chemotherapeutic drug delivery to cancer cells. Nano Lett *8*, 4116-4121.
165. Muddana, H.S., Morgan, T.T., Adair, J.H., and Butler, P.J. (2009). Photophysics of Cy3-encapsulated calcium phosphate nanoparticles. Nano Lett *9*, 1559-1566.
166. Li, H., Zhang, Z., Blessington, D., Nelson, D.S., Zhou, R., Lund-Katz, S., Chance, B., Glickson, J.D., and Zheng, G. (2004). Carbocyanine labeled LDL for optical imaging of tumors. Acad Radiol *11*, 669-677.
167. Yan, C., Tang, F., Li, L., Li, H., Huang, X., Chen, D., Meng, X., and Ren, J. (2009). Synthesis of Aqueous CdTe/CdS/ZnS Core/shell/shell Quantum Dots by a Chemical Aerosol Flow Method. Nanoscale Res Lett *5*, 189-194.
168. Xing, Y., and Rao, J. (2008). Quantum dot bioconjugates for in vitro diagnostics & in vivo imaging. Cancer Biomark *4*, 307-319.
169. Nagarajan, S., and Zhang, Y. Upconversion fluorescent nanoparticles as a potential tool for in-depth imaging. Nanotechnology *22*, 395101.
170. Wang, F., Banerjee, D., Liu, Y., Chen, X., and Liu, X. Upconversion nanoparticles in biological labeling, imaging, and therapy. Analyst *135*, 1839-1854.
171. Wang, K., Ruan, J., Qian, Q., Song, H., Bao, C., Zhang, X., Kong, Y., Zhang, C., Hu, G., Ni, J., and Cui, D. BRCAA1 monoclonal antibody conjugated fluorescent magnetic nanoparticles for in vivo targeted magnetofluorescent imaging of gastric cancer. J Nanobiotechnology *9*, 23.
172. Hun, X., Zhang, Z., and Tiao, L. (2008). Anti-Her-2 monoclonal antibody conjugated polymer fluorescent nanoparticles probe for ovarian cancer imaging. Anal Chim Acta *625*, 201-206.
173. Zhang, R., Xiong, C., Huang, M., Zhou, M., Huang, Q., Wen, X., Liang, D., and Li, C. Peptide-conjugated polymeric micellar nanoparticles for Dual SPECT and optical imaging of EphB4 receptors in prostate cancer xenografts. Biomaterials *32*, 5872-5879.
174. Saravanakumar, G., Jo, D.G., and Park, J.H. Polysaccharide-based nanoparticles: a versatile platform for drug delivery and biomedical imaging. Curr Med Chem *19*, 3212-3229.
175. Quan, B., Choi, K., Kim, Y.H., Kang, K.W., and Chung, D.S. Near infrared dye indocyanine green doped silica nanoparticles for biological imaging. Talanta *99*, 387-393.
176. Schaafsma, B.E., Mieog, J.S., Hutteman, M., van der Vorst, J.R., Kuppen, P.J., Lowik, C.W., Frangioni, J.V., van de Velde, C.J., and Vahrmeijer, A.L. The clinical use of indocyanine green as a near-infrared fluorescent contrast agent for image-guided oncologic surgery. J Surg Oncol *104*, 323-332.
177. Ma, Y., Sadoqi, M., and Shao, J. Biodistribution of indocyanine green-loaded nanoparticles with surface modifications of PEG and folic acid. Int J Pharm *436*, 25-31.
178. Saxena, V., Sadoqi, M., and Shao, J. (2006). Polymeric nanoparticulate delivery system for Indocyanine green: biodistribution in healthy mice. Int J Pharm *308*, 200-204.

179. Santra, S. Fluorescent silica nanoparticles for cancer imaging. Methods Mol Biol *624*, 151-162.
180. Friedman, R. Nano dot technology enters clinical trials. J Natl Cancer Inst *103*, 1428-1429.
181. Ruedas-Rama, M.J., Walters, J.D., Orte, A., and Hall, E.A. Fluorescent nanoparticles for intracellular sensing: a review. Anal Chim Acta *751*, 1-23.
182. Lapresta-Fernandez, A., Doussineau, T., Dutz, S., Steiniger, F., Moro, A.J., and Mohr, G.J. Magnetic and fluorescent core-shell nanoparticles for ratiometric pH sensing. Nanotechnology *22*, 415501.
183. Coto-Garcia, A.M., Sotelo-Gonzalez, E., Fernandez-Arguelles, M.T., Pereiro, R., Costa-Fernandez, J.M., and Sanz-Medel, A. Nanoparticles as fluorescent labels for optical imaging and sensing in genomics and proteomics. Anal Bioanal Chem *399*, 29-42.
184. Lee, H., Akers, W., Bhushan, K., Bloch, S., Sudlow, G., Tang, R., and Achilefu, S. Near-infrared pH-activatable fluorescent probes for imaging primary and metastatic breast tumors. Bioconjug Chem *22*, 777-784.
185. Lacivita, E., Leopoldo, M., Berardi, F., Colabufo, N.A., and Perrone, R. Activatable fluorescent probes: a new concept in optical molecular imaging. Curr Med Chem *19*, 4731-4741.
186. Tung, C.H., Bredow, S., Mahmood, U., and Weissleder, R. (1999). Preparation of a cathepsin D sensitive near-infrared fluorescence probe for imaging. Bioconjug Chem *10*, 892-896.
187. Bremer, C., Tung, C.H., and Weissleder, R. (2002). Molecular imaging of MMP expression and therapeutic MMP inhibition. Acad Radiol *9 Suppl 2*, S314-315.
188. Pham, W., Weissleder, R., and Tung, C.H. (2002). An azulene dimer as a near-infrared quencher. Angew Chem Int Ed Engl *41*, 3659-3662, 3519.
189. Jaffer, F.A., Tung, C.H., Gerszten, R.E., and Weissleder, R. (2002). In vivo imaging of thrombin activity in experimental thrombi with thrombin-sensitive near-infrared molecular probe. Arterioscler Thromb Vasc Biol *22*, 1929-1935.
190. Ryu, J.H., Lee, A., Chu, J.U., Koo, H., Ko, C.Y., Kim, H.S., Yoon, S.Y., Kim, B.S., Choi, K., Kwon, I.C., Kim, K., and Youn, I. Early diagnosis of arthritis in mice with collagen-induced arthritis, using a fluorogenic matrix metalloproteinase 3-specific polymeric probe. Arthritis Rheum *63*, 3824-3832.
191. Lee, S., Park, K., Lee, S.Y., Ryu, J.H., Park, J.W., Ahn, H.J., Kwon, I.C., Youn, I.C., Kim, K., and Choi, K. (2008). Dark quenched matrix metalloproteinase fluorogenic probe for imaging osteoarthritis development in vivo. Bioconjug Chem *19*, 1743-1747.
192. Dano, K., Andreasen, P.A., Grondahl-Hansen, J., Kristensen, P., Nielsen, L.S., and Skriver, L. (1985). Plasminogen activators, tissue degradation, and cancer. Adv Cancer Res *44*, 139-266.
193. Waltz, D.A., Natkin, L.R., Fujita, R.M., Wei, Y., and Chapman, H.A. (1997). Plasmin and plasminogen activator inhibitor type 1 promote cellular motility by regulating the interaction between the urokinase receptor and vitronectin. J Clin Invest *100*, 58-67.
194. Carmeliet, P., Moons, L., Lijnen, R., Baes, M., Lemaitre, V., Tipping, P., Drew, A., Eeckhout, Y., Shapiro, S., Lupu, F., and Collen, D. (1997). Urokinase-generated plasmin activates matrix metalloproteinases during aneurysm formation. Nat Genet *17*, 439-444.
195. Jenkins, G. (2008). The role of proteases in transforming growth factor-beta activation. Int J Biochem Cell Biol *40*, 1068-1078.

196. Annecke, K., Schmitt, M., Euler, U., Zerm, M., Paepke, D., Paepke, S., von Minckwitz, G., Thomssen, C., and Harbeck, N. (2008). uPA and PAI-1 in breast cancer: review of their clinical utility and current validation in the prospective NNBC-3 trial. Adv Clin Chem *45*, 31-45.
197. Look, M.P., van Putten, W.L., Duffy, M.J., Harbeck, N., Christensen, I.J., Thomssen, C., Kates, R., Spyratos, F., Ferno, M., Eppenberger-Castori, S., Sweep, C.G., Ulm, K., Peyrat, J.P., Martin, P.M., Magdelenat, H., Brunner, N., Duggan, C., Lisboa, B.W., Bendahl, P.O., Quillien, V., Daver, A., Ricolleau, G., Meijer-van Gelder, M.E., Manders, P., Fiets, W.E., Blankenstein, M.A., Broet, P., Romain, S., Daxenbichler, G., Windbichler, G., Cufer, T., Borstnar, S., Kueng, W., Beex, L.V., Klijn, J.G., O'Higgins, N., Eppenberger, U., Janicke, F., Schmitt, M., and Foekens, J.A. (2002). Pooled analysis of prognostic impact of urokinase-type plasminogen activator and its inhibitor PAI-1 in 8377 breast cancer patients. J Natl Cancer Inst *94*, 116-128.
198. Li, Z.B., Niu, G., Wang, H., He, L., Yang, L., Ploug, M., and Chen, X. (2008). Imaging of urokinase-type plasminogen activator receptor expression using a 64Cu-labeled linear peptide antagonist by microPET. Clin Cancer Res *14*, 4758-4766.
199. Sun, J., Zheng, Q., Wu, Y., Liu, Y., Guo, X., and Wu, W. Biocompatibility of KLD-12 peptide hydrogel as a scaffold in tissue engineering of intervertebral discs in rabbits. J Huazhong Univ Sci Technolog Med Sci *30*, 173-177.
200. Sieminski, A.L., Semino, C.E., Gong, H., and Kamm, R.D. (2008). Primary sequence of ionic self-assembling peptide gels affects endothelial cell adhesion and capillary morphogenesis. J Biomed Mater Res A *87*, 494-504.
201. Kisiday, J., Jin, M., Kurz, B., Hung, H., Semino, C., Zhang, S., and Grodzinsky, A.J. (2002). Self-assembling peptide hydrogel fosters chondrocyte extracellular matrix production and cell division: implications for cartilage tissue repair. Proc Natl Acad Sci U S A *99*, 9996-10001.
202. Ke, S.H., Coombs, G.S., Tachias, K., Corey, D.R., and Madison, E.L. (1997). Optimal subsite occupancy and design of a selective inhibitor of urokinase. J Biol Chem *272*, 20456-20462.
203. Gilmore, B.F., Carson, L., McShane, L.L., Quinn, D., Coulter, W.A., and Walker, B. (2006). Synthesis, kinetic evaluation, and utilization of a biotinylated dipeptide proline diphenyl phosphonate for the disclosure of dipeptidyl peptidase IV-like serine proteases. Biochem Biophys Res Commun *347*, 373-379.
204. Harbeck, N., Dettmar, P., Thomssen, C., Berger, U., Ulm, K., Kates, R., Hofler, H., Janicke, F., Graeff, H., and Schmitt, M. (1999). Risk-group discrimination in node-negative breast cancer using invasion and proliferation markers: 6-year median follow-up. Br J Cancer *80*, 419-426.
205. Chockalingam, K., Blenner, M., and Banta, S. (2007). Design and application of stimulus-responsive peptide systems. Protein Eng Des Sel *20*, 155-161.
206. Zhang, S., Marini, D.M., Hwang, W., and Santoso, S. (2002). Design of nanostructured biological materials through self-assembly of peptides and proteins. Curr Opin Chem Biol *6*, 865-871.
207. Zhang, S., Gelain, F., and Zhao, X. (2005). Designer self-assembling peptide nanofiber scaffolds for 3D tissue cell cultures. Semin Cancer Biol *15*, 413-420.
208. Segers, V.F., and Lee, R.T. (2007). Local delivery of proteins and the use of self-assembling peptides. Drug Discov Today *12*, 561-568.

209. Kisiday, J.D., Kopesky, P.W., Evans, C.H., Grodzinsky, A.J., McIlwraith, C.W., and Frisbie, D.D. (2008). Evaluation of adult equine bone marrow- and adipose-derived progenitor cell chondrogenesis in hydrogel cultures. J Orthop Res *26*, 322-331.
210. Bergstrom, R.C., Coombs, G.S., Ye, S., Madison, E.L., Goldsmith, E.J., and Corey, D.R. (2003). Binding of nonphysiological protein and peptide substrates to proteases: differences between urokinase-type plasminogen activator and trypsin and contributions to the evolution of regulated proteolysis. Biochemistry *42*, 5395-5402.
211. Mank, A.J., and Yeung, E.S. (1995). Diode laser-induced fluorescence detection in capillary electrophoresis after pre-column derivatization of amino acids and small peptides. J Chromatogr A *708*, 309-321.
212. Mujumdar, R.B., Ernst, L.A., Mujumdar, S.R., Lewis, C.J., and Waggoner, A.S. (1993). Cyanine dye labeling reagents: sulfoindocyanine succinimidyl esters. Bioconjug Chem *4*, 105-111.
213. Ruan, L., Zhang, H., Luo, H., Liu, J., Tang, F., Shi, Y.K., and Zhao, X. (2009). Designed amphiphilic peptide forms stable nanoweb, slowly releases encapsulated hydrophobic drug, and accelerates animal hemostasis. Proc Natl Acad Sci U S A *106*, 5105-5110.
214. Law, B., and Tung, C.H. (2008). Structural modification of protease inducible preprogrammed nanofiber precursor. Biomacromolecules *9*, 421-425.
215. Law, B., and Tung, C.H. (2009). Proteolysis: a biological process adapted in drug delivery, therapy, and imaging. Bioconjug Chem *20*, 1683-1695.
216. Kim, J.K., Anderson, J., Jun, H.W., Repka, M.A., and Jo, S. (2009). Self-assembling peptide amphiphile-based nanofiber gel for bioresponsive cisplatin delivery. Mol Pharm *6*, 978-985.
217. Atkinson, J.M., Siller, C.S., and Gill, J.H. (2008). Tumour endoproteases: the cutting edge of cancer drug delivery? Br J Pharmacol *153*, 1344-1352.
218. Chau, Y., Padera, R.F., Dang, N.M., and Langer, R. (2006). Antitumor efficacy of a novel polymer-peptide-drug conjugate in human tumor xenograft models. Int J Cancer *118*, 1519-1526.
219. Rooseboom, M., Commandeur, J.N., and Vermeulen, N.P. (2004). Enzyme-catalyzed activation of anticancer prodrugs. Pharmacol Rev *56*, 53-102.
220. Tauro, J.R., Lee, B.S., Lateef, S.S., and Gemeinhart, R.A. (2008). Matrix metalloprotease selective peptide substrates cleavage within hydrogel matrices for cancer chemotherapy activation. Peptides *29*, 1965-1973.
221. Pham, W., Choi, Y., Weissleder, R., and Tung, C.H. (2004). Developing a peptide-based near-infrared molecular probe for protease sensing. Bioconjug Chem *15*, 1403-1407.
222. Koutsopoulos, S., Unsworth, L.D., Nagai, Y., and Zhang, S. (2009). Controlled release of functional proteins through designer self-assembling peptide nanofiber hydrogel scaffold. Proc Natl Acad Sci U S A *106*, 4623-4628.
223. Hsiao, J.K., Law, B., Weissleder, R., and Tung, C.H. (2006). In-vivo imaging of tumor associated urokinase-type plasminogen activator activity. J Biomed Opt *11*, 34013.
224. Westphal, J.R., Van't Hullenaar, R., Geurts-Moespot, A., Sweep, F.C., Verheijen, J.H., Bussemakers, M.M., Askaa, J., Clemmensen, I., Eggermont, A.A., Ruiter, D.J., and De Waal, R.M. (2000). Angiostatin generation by human tumor cell lines: involvement of plasminogen activators. Int J Cancer *86*, 760-767.
225. Banerjee, J., Hanson, A.J., Gadam, B., Elegbede, A.I., Tobwala, S., Ganguly, B., Wagh, A.V., Muhonen, W.W., Law, B., Shabb, J.B., Srivastava, D.K., and Mallik, S. (2009).

Release of liposomal contents by cell-secreted matrix metalloproteinase-9. Bioconjug Chem *20*, 1332-1339.
226. Lee, S., Ryu, J.H., Park, K., Lee, A., Lee, S.Y., Youn, I.C., Ahn, C.H., Yoon, S.M., Myung, S.J., Moon, D.H., Chen, X., Choi, K., Kwon, I.C., and Kim, K. (2009). Polymeric nanoparticle-based activatable near-infrared nanosensor for protease determination in vivo. Nano Lett *9*, 4412-4416.
227. Zhao, X., and Zhang, S. (2007). Designer self-assembling peptide materials. Macromol Biosci *7*, 13-22.
228. Sun, J., and Zheng, Q. (2009). Experimental study on self-assembly of KLD-12 peptide hydrogel and 3-D culture of MSC encapsulated within hydrogel in vitro. J Huazhong Univ Sci Technolog Med Sci *29*, 512-516.
229. Zhang, S. (2003). Fabrication of novel biomaterials through molecular self-assembly. Nat Biotechnol *21*, 1171-1178.
230. Duffy, M.J. (1996). Proteases as prognostic markers in cancer. Clin Cancer Res *2*, 613-618.
231. Duffy, M.J., and Crown, J. (2008). A personalized approach to cancer treatment: how biomarkers can help. Clin Chem *54*, 1770-1779.
232. Jakobovits, A. (2008). Monoclonal antibody therapy for prostate cancer. Handb Exp Pharmacol, 237-256.
233. Warren, A., Langley, J.M., Thomas, W., and Scott, J. (2007). Optimizing the delivery and use of a new monoclonal antibody in children with congenital heart disease: a successful provincial respiratory syncytial virus prophylaxis program. Can J Cardiol *23*, 463-466.
234. Maneewatch, S., Sakolvaree, Y., Tapchaisri, P., Saengjaruk, P., Songserm, T., Wongratanachewin, S., Tongtawe, P., Srimanote, P., Chaisri, U., and Chaicumpa, W. (2009). Humanized-monoclonal antibody against heterologous Leptospira infection. Protein Eng Des Sel *22*, 305-312.
235. Tassev, D.V., and Cheung, N.K. (2009). Monoclonal antibody therapies for solid tumors. Expert Opin Biol Ther *9*, 341-353.
236. Yu, M.K., Park, J., and Jon, S. Targeting strategies for multifunctional nanoparticles in cancer imaging and therapy. Theranostics *2*, 3-44.
237. Ozzello, L., Blank, E.W., De Rosa, C.M., Ceriani, R.L., Tolo, H., Kauppinen, H.L., and Cantell, K. (1998). Conjugation of interferon alpha to a humanized monoclonal antibody (HuBrE-3vl) enhances the selective localization and antitumor effects of interferon in breast cancer xenografts. Breast Cancer Res Treat *48*, 135-147.
238. Mukai, T., Fujioka, Y., Arano, Y., and Saji, H. (2003). [Design of radiolabeled antibody fragments for tumor-selective radioactivity localization--brush border enzyme-sensitive bond to decrease renal accumulation of radioactivity]. Yakugaku Zasshi *123*, 647-652.
239. Argyriou, A.A., and Kalofonos, H.P. (2009). Recent advances relating to the clinical application of naked monoclonal antibodies in solid tumors. Mol Med *15*, 183-191.
240. Wang, Y., Keck, Z.Y., Saha, A., Xia, J., Conrad, F., Lou, J., Eckart, M., Marks, J.D., and Foung, S.K. Affinity maturation to improve human monoclonal antibody neutralization potency and breadth against hepatitis C virus. J Biol Chem *286*, 44218-44233.
241. Stein, R., Qu, Z., Chen, S., Solis, D., Hansen, H.J., and Goldenberg, D.M. (2006). Characterization of a humanized IgG4 anti-HLA-DR monoclonal antibody that lacks effector cell functions but retains direct antilymphoma activity and increases the potency of rituximab. Blood *108*, 2736-2744.

242. Zhang, T., and Herlyn, D. (2009). Combination of active specific immunotherapy or adoptive antibody or lymphocyte immunotherapy with chemotherapy in the treatment of cancer. Cancer Immunol Immunother *58*, 475-492.
243. Finkelstein, S.E., and Fishman, M. Clinical opportunities in combining immunotherapy with radiation therapy. Front Oncol *2*, 169.
244. El-Sayed, I.H., Huang, X., and El-Sayed, M.A. (2006). Selective laser photo-thermal therapy of epithelial carcinoma using anti-EGFR antibody conjugated gold nanoparticles. Cancer Lett *239*, 129-135.
245. Witters, L.M., Kumar, R., Chinchilli, V.M., and Lipton, A. (1997). Enhanced anti-proliferative activity of the combination of tamoxifen plus HER-2-neu antibody. Breast Cancer Res Treat *42*, 1-5.
246. Yuan, H.H., Han, Y., Bian, W.X., Liu, L., and Bai, Y.X. The effect of monoclonal antibody cetuximab (C225) in combination with tyrosine kinase inhibitor gefitinib (ZD1839) on colon cancer cell lines. Pathology *44*, 547-551.
247. Frazier, J.L., Han, J.E., Lim, M., and Olivi, A. Immunotherapy combined with chemotherapy in the treatment of tumors. Neurosurg Clin N Am *21*, 187-194.
248. Baxevanis, C.N., Perez, S.A., and Papamichail, M. (2009). Combinatorial treatments including vaccines, chemotherapy and monoclonal antibodies for cancer therapy. Cancer Immunol Immunother *58*, 317-324.
249. Law, L.Y. Dramatic response to trastuzumab and paclitaxel in a patient with human epidermal growth factor receptor 2-positive metastatic cholangiocarcinoma. J Clin Oncol *30*, e271-273.
250. Pegram, M.D. (2001). Docetaxel and herceptin: foundation for future strategies. Oncologist *6 Suppl 3*, 22-25.
251. O'Shaughnessy, J., Vukelja, S.J., Marsland, T., Kimmel, G., Ratnam, S., and Pippen, J. (2002). Phase II trial of gemcitabine plus trastuzumab in metastatic breast cancer patients previously treated with chemotherapy: preliminary results. Clin Breast Cancer *3 Suppl 1*, 17-20.
252. Bell, R. (2001). Ongoing trials with trastuzumab in metastatic breast cancer. Ann Oncol *12 Suppl 1*, S69-73.
253. Ropero, S., Menendez, J.A., Vazquez-Martin, A., Montero, S., Cortes-Funes, H., and Colomer, R. (2004). Trastuzumab plus tamoxifen: anti-proliferative and molecular interactions in breast carcinoma. Breast Cancer Res Treat *86*, 125-137.
254. Tiezzi, D.G., de Andrade, J.M., Marana, H.R., Garieri, A.P., and de Paula Philbert, P.M. (2009). Clinical criteria as predictive factors of response to primary hormone therapy in locally advanced breast cancer. Breast J *15*, 333-338.
255. Rastelli, F., and Crispino, S. (2008). Factors predictive of response to hormone therapy in breast cancer. Tumori *94*, 370-383.
256. Lim, E., Metzger-Filho, O., and Winer, E.P. The natural history of hormone receptor-positive breast cancer. Oncology (Williston Park) *26*, 688-694, 696.
257. Jones, A. (2003). Combining trastuzumab (Herceptin) with hormonal therapy in breast cancer: what can be expected and why? Ann Oncol *14*, 1697-1704.
258. Klinkenbijl, J.H., Jeekel, J., Sahmoud, T., van Pel, R., Couvreur, M.L., Veenhof, C.H., Arnaud, J.P., Gonzalez, D.G., de Wit, L.T., Hennipman, A., and Wils, J. (1999). Adjuvant radiotherapy and 5-fluorouracil after curative resection of cancer of the

pancreas and periampullary region: phase III trial of the EORTC gastrointestinal tract cancer cooperative group. Ann Surg *230*, 776-782; discussion 782-774.
259. Ross, G.M. (1999). Induction of cell death by radiotherapy. Endocr Relat Cancer *6*, 41-44.
260. Halyard, M.Y., Pisansky, T.M., Dueck, A.C., Suman, V., Pierce, L., Solin, L., Marks, L., Davidson, N., Martino, S., Kaufman, P., Kutteh, L., Dakhil, S.R., and Perez, E.A. (2009). Radiotherapy and adjuvant trastuzumab in operable breast cancer: tolerability and adverse event data from the NCCTG Phase III Trial N9831. J Clin Oncol *27*, 2638-2644.
261. Belkacemi, Y., Gligorov, J., Ozsahin, M., Marsiglia, H., De Lafontan, B., Laharie-Mineur, H., Aimard, L., Antoine, E.C., Cutuli, B., Namer, M., and Azria, D. (2008). Concurrent trastuzumab with adjuvant radiotherapy in HER2-positive breast cancer patients: acute toxicity analyses from the French multicentric study. Ann Oncol *19*, 1110-1116.
262. Sadana, A., and Vo-Dinh, T. (1997). Antibody-antigen binding kinetics. A model for multivalency antibodies for large antigen systems. Appl Biochem Biotechnol *67*, 1-22.
263. Houck, K.S., and Huang, L. (1987). The role of multivalency in antibody mediated liposome targeting. Biochem Biophys Res Commun *145*, 1205-1210.
264. Petronzelli, F., Pelliccia, A., Anastasi, A.M., D'Alessio, V., Albertoni, C., Rosi, A., Leoni, B., De Angelis, C., Paganelli, G., Palombo, G., Dani, M., Carminati, P., and De Santis, R. (2005). Improved tumor targeting by combined use of two antitenascin antibodies. Clin Cancer Res *11*, 7137s-7145s.
265. Albrecht, H., Denardo, G.L., and Denardo, S.J. (2006). Monospecific bivalent scFv-SH: effects of linker length and location of an engineered cysteine on production, antigen binding activity and free SH accessibility. J Immunol Methods *310*, 100-116.
266. Schoonooghe, S., Kaigorodov, V., Zawisza, M., Dumolyn, C., Haustraete, J., Grooten, J., and Mertens, N. (2009). Efficient production of human bivalent and trivalent anti-MUC1 Fab-scFv antibodies in Pichia pastoris. BMC Biotechnol *9*, 70.
267. Honegger, A. (2008). Engineering antibodies for stability and efficient folding. Handb Exp Pharmacol, 47-68.
268. Stavenhagen, J.B., Gorlatov, S., Tuaillon, N., Rankin, C.T., Li, H., Burke, S., Huang, L., Johnson, S., Koenig, S., and Bonvini, E. (2008). Enhancing the potency of therapeutic monoclonal antibodies via Fc optimization. Adv Enzyme Regul *48*, 152-164.
269. Teeling, J.L., French, R.R., Cragg, M.S., van den Brakel, J., Pluyter, M., Huang, H., Chan, C., Parren, P.W., Hack, C.E., Dechant, M., Valerius, T., van de Winkel, J.G., and Glennie, M.J. (2004). Characterization of new human CD20 monoclonal antibodies with potent cytolytic activity against non-Hodgkin lymphomas. Blood *104*, 1793-1800.
270. Michaelson, J.S., Demarest, S.J., Miller, B., Amatucci, A., Snyder, W.B., Wu, X., Huang, F., Phan, S., Gao, S., Doern, A., Farrington, G.K., Lugovskoy, A., Joseph, I., Bailly, V., Wang, X., Garber, E., Browning, J., and Glaser, S.M. (2009). Anti-tumor activity of stability-engineered IgG-like bispecific antibodies targeting TRAIL-R2 and LTbetaR. MAbs *1*, 128-141.
271. Casey, J.L., Pedley, R.B., King, D.J., Green, A.J., Yarranton, G.T., and Begent, R.H. (1999). Dosimetric evaluation and radioimmunotherapy of anti-tumour multivalent Fab' fragments. Br J Cancer *81*, 972-980.
272. Kipriyanov, S.M., Little, M., Kropshofer, H., Breitling, F., Gotter, S., and Dubel, S. (1996). Affinity enhancement of a recombinant antibody: formation of complexes with

multiple valency by a single-chain Fv fragment-core streptavidin fusion. Protein Eng *9*, 203-211.
273. Adams, G.P., McCartney, J.E., Tai, M.S., Oppermann, H., Huston, J.S., Stafford, W.F., 3rd, Bookman, M.A., Fand, I., Houston, L.L., and Weiner, L.M. (1993). Highly specific in vivo tumor targeting by monovalent and divalent forms of 741F8 anti-c-erbB-2 single-chain Fv. Cancer Res *53*, 4026-4034.
274. Shahied, L.S., Tang, Y., Alpaugh, R.K., Somer, R., Greenspon, D., and Weiner, L.M. (2004). Bispecific minibodies targeting HER2/neu and CD16 exhibit improved tumor lysis when placed in a divalent tumor antigen binding format. J Biol Chem *279*, 53907-53914.
275. Weiner, G.J. (2007). Monoclonal antibody mechanisms of action in cancer. Immunol Res *39*, 271-278.
276. Natsume, A., Niwa, R., and Satoh, M. (2009). Improving effector functions of antibodies for cancer treatment: Enhancing ADCC and CDC. Drug Des Devel Ther *3*, 7-16.
277. Oflazoglu, E., and Audoly, L.P. Evolution of anti-CD20 monoclonal antibody therapeutics in oncology. MAbs *2*, 14-19.
278. Glennie, M.J., French, R.R., Cragg, M.S., and Taylor, R.P. (2007). Mechanisms of killing by anti-CD20 monoclonal antibodies. Mol Immunol *44*, 3823-3837.
279. Sola, R.J., and Griebenow, K. (2009). Effects of glycosylation on the stability of protein pharmaceuticals. J Pharm Sci *98*, 1223-1245.
280. Sola, R.J., and Griebenow, K. Glycosylation of therapeutic proteins: an effective strategy to optimize efficacy. BioDrugs *24*, 9-21.
281. Yamane-Ohnuki, N., and Satoh, M. (2009). Production of therapeutic antibodies with controlled fucosylation. MAbs *1*, 230-236.
282. Shinkawa, T., Nakamura, K., Yamane, N., Shoji-Hosaka, E., Kanda, Y., Sakurada, M., Uchida, K., Anazawa, H., Satoh, M., Yamasaki, M., Hanai, N., and Shitara, K. (2003). The absence of fucose but not the presence of galactose or bisecting N-acetylglucosamine of human IgG1 complex-type oligosaccharides shows the critical role of enhancing antibody-dependent cellular cytotoxicity. J Biol Chem *278*, 3466-3473.
283. Taniguchi, N., Miyoshi, E., Gu, J., Honke, K., and Matsumoto, A. (2006). Decoding sugar functions by identifying target glycoproteins. Curr Opin Struct Biol *16*, 561-566.
284. Mirick, G.R., Bradt, B.M., Denardo, S.J., and Denardo, G.L. (2004). A review of human anti-globulin antibody (HAGA, HAMA, HACA, HAHA) responses to monoclonal antibodies. Not four letter words. Q J Nucl Med Mol Imaging *48*, 251-257.
285. Teicher, B.A., and Chari, R.V. Antibody conjugate therapeutics: challenges and potential. Clin Cancer Res *17*, 6389-6397.
286. Chari, R.V. (2008). Targeted cancer therapy: conferring specificity to cytotoxic drugs. Acc Chem Res *41*, 98-107.
287. Rowland, G.F., O'Neill, G.J., and Davies, D.A. (1975). Suppression of tumour growth in mice by a drug-antibody conjugate using a novel approach to linkage. Nature *255*, 487-488.
288. Senter, P.D. (1990). Activation of prodrugs by antibody-enzyme conjugates: a new approach to cancer therapy. Faseb J *4*, 188-193.
289. Sievers, E.L., and Senter, P.D. Antibody-Drug Conjugates in Cancer Therapy. Annu Rev Med.

290. Ritchie, M., Tchistiakova, L., and Scott, N. Implications of receptor-mediated endocytosis and intracellular trafficking dynamics in the development of antibody drug conjugates. MAbs *5*.
291. Wu, A.M., and Senter, P.D. (2005). Arming antibodies: prospects and challenges for immunoconjugates. Nat Biotechnol *23*, 1137-1146.
292. Dosio, F., Brusa, P., and Cattel, L. Immunotoxins and Anticancer Drug Conjugate Assemblies: The Role of the Linkage between Components. Toxins (Basel) *3*, 848-883.
293. Lopus, M. Antibody-DM1 conjugates as cancer therapeutics. Cancer Lett *307*, 113-118.
294. Hamann, P.R., Hinman, L.M., Hollander, I., Beyer, C.F., Lindh, D., Holcomb, R., Hallett, W., Tsou, H.R., Upeslacis, J., Shochat, D., Mountain, A., Flowers, D.A., and Bernstein, I. (2002). Gemtuzumab ozogamicin, a potent and selective anti-CD33 antibody-calicheamicin conjugate for treatment of acute myeloid leukemia. Bioconjug Chem *13*, 47-58.
295. Tolcher, A.W., Sugarman, S., Gelmon, K.A., Cohen, R., Saleh, M., Isaacs, C., Young, L., Healey, D., Onetto, N., and Slichenmyer, W. (1999). Randomized phase II study of BR96-doxorubicin conjugate in patients with metastatic breast cancer. J Clin Oncol *17*, 478-484.
296. McDonagh, C.F., Kim, K.M., Turcott, E., Brown, L.L., Westendorf, L., Feist, T., Sussman, D., Stone, I., Anderson, M., Miyamoto, J., Lyon, R., Alley, S.C., Gerber, H.P., and Carter, P.J. (2008). Engineered anti-CD70 antibody-drug conjugate with increased therapeutic index. Mol Cancer Ther *7*, 2913-2923.
297. Doronina, S.O., Toki, B.E., Torgov, M.Y., Mendelsohn, B.A., Cerveny, C.G., Chace, D.F., DeBlanc, R.L., Gearing, R.P., Bovee, T.D., Siegall, C.B., Francisco, J.A., Wahl, A.F., Meyer, D.L., and Senter, P.D. (2003). Development of potent monoclonal antibody auristatin conjugates for cancer therapy. Nat Biotechnol *21*, 778-784.
298. Hackbarth, M., Haas, N., Fotopoulou, C., Lichtenegger, W., and Sehouli, J. (2008). Chemotherapy-induced dermatological toxicity: frequencies and impact on quality of life in women's cancers. Results of a prospective study. Support Care Cancer *16*, 267-273.
299. Kayl, A.E., and Meyers, C.A. (2006). Side-effects of chemotherapy and quality of life in ovarian and breast cancer patients. Curr Opin Obstet Gynecol *18*, 24-28.
300. Wakankar, A.A., Feeney, M.B., Rivera, J., Chen, Y., Kim, M., Sharma, V.K., and Wang, Y.J. Physicochemical stability of the antibody-drug conjugate Trastuzumab-DM1: changes due to modification and conjugation processes. Bioconjug Chem *21*, 1588-1595.
301. Alley, S.C., Okeley, N.M., and Senter, P.D. Antibody-drug conjugates: targeted drug delivery for cancer. Curr Opin Chem Biol *14*, 529-537.
302. Erickson, H.K., Lewis Phillips, G.D., Leipold, D.D., Provenzano, C.A., Mai, E., Johnson, H.A., Gunter, B., Audette, C.A., Gupta, M., Pinkas, J., and Tibbitts, J. The effect of different linkers on target cell catabolism and pharmacokinetics/pharmacodynamics of trastuzumab maytansinoid conjugates. Mol Cancer Ther *11*, 1133-1142.
303. Ojima, I. (2008). Guided molecular missiles for tumor-targeting chemotherapy--case studies using the second-generation taxoids as warheads. Acc Chem Res *41*, 108-119.
304. Chari, R.V. (1998). Targeted delivery of chemotherapeutics: tumor-activated prodrug therapy. Adv Drug Deliv Rev *31*, 89-104.
305. Chen, S., Zhao, X., Chen, J., Kuznetsova, L., Wong, S.S., and Ojima, I. Mechanism-based tumor-targeting drug delivery system. Validation of efficient vitamin receptor-mediated endocytosis and drug release. Bioconjug Chem *21*, 979-987.

306. Gu, Y.J., Cheng, J., Jin, J., Cheng, S.H., and Wong, W.T. Development and evaluation of pH-responsive single-walled carbon nanotube-doxorubicin complexes in cancer cells. Int J Nanomedicine *6*, 2889-2898.
307. DeNardo, G.L., and DeNardo, S.J. (2004). Evaluation of a cathepsin-cleavable peptide linked radioimmunoconjugate of a panadenocarcinoma MAb, m170, in mice and patients. Cancer Biother Radiopharm *19*, 85-92.
308. Kukis, D.L., Novak-Hofer, I., and DeNardo, S.J. (2001). Cleavable linkers to enhance selectivity of antibody-targeted therapy of cancer. Cancer Biother Radiopharm *16*, 457-467.
309. Howard, M.D., Ponta, A., Eckman, A., Jay, M., and Bae, Y. Polymer micelles with hydrazone-ester dual linkers for tunable release of dexamethasone. Pharm Res *28*, 2435-2446.
310. Dubowchik, G.M., Firestone, R.A., Padilla, L., Willner, D., Hofstead, S.J., Mosure, K., Knipe, J.O., Lasch, S.J., and Trail, P.A. (2002). Cathepsin B-labile dipeptide linkers for lysosomal release of doxorubicin from internalizing immunoconjugates: model studies of enzymatic drug release and antigen-specific in vitro anticancer activity. Bioconjug Chem *13*, 855-869.
311. Sanderson, R.J., Hering, M.A., James, S.F., Sun, M.M., Doronina, S.O., Siadak, A.W., Senter, P.D., and Wahl, A.F. (2005). In vivo drug-linker stability of an anti-CD30 dipeptide-linked auristatin immunoconjugate. Clin Cancer Res *11*, 843-852.
312. Greco, F., and Vicent, M.J. (2008). Polymer-drug conjugates: current status and future trends. Front Biosci *13*, 2744-2756.
313. Kopecek, J. Polymer-drug conjugates: Origins, progress to date and future directions. Adv Drug Deliv Rev.
314. Atalay, G., Cardoso, F., Awada, A., and Piccart, M.J. (2003). Novel therapeutic strategies targeting the epidermal growth factor receptor (EGFR) family and its downstream effectors in breast cancer. Ann Oncol *14*, 1346-1363.
315. Marques, M.M., Martinez, N., Rodriguez-Garcia, I., and Alonso, A. (1999). EGFR family-mediated signal transduction in the human keratinocyte cell line HaCaT. Exp Cell Res *252*, 432-438.
316. Patel, R., and Leung, H.Y. Targeting the EGFR-family for therapy: biological challenges and clinical perspective. Curr Pharm Des *18*, 2672-2679.
317. Higashiyama, S., Iwabuki, H., Morimoto, C., Hieda, M., Inoue, H., and Matsushita, N. (2008). Membrane-anchored growth factors, the epidermal growth factor family: beyond receptor ligands. Cancer Sci *99*, 214-220.
318. Jorissen, R.N., Walker, F., Pouliot, N., Garrett, T.P., Ward, C.W., and Burgess, A.W. (2003). Epidermal growth factor receptor: mechanisms of activation and signalling. Exp Cell Res *284*, 31-53.
319. Rodrigues, G.A., Falasca, M., Zhang, Z., Ong, S.H., and Schlessinger, J. (2000). A novel positive feedback loop mediated by the docking protein Gab1 and phosphatidylinositol 3-kinase in epidermal growth factor receptor signaling. Mol Cell Biol *20*, 1448-1459.
320. Sasaoka, T., Langlois, W.J., Leitner, J.W., Draznin, B., and Olefsky, J.M. (1994). The signaling pathway coupling epidermal growth factor receptors to activation of p21ras. J Biol Chem *269*, 32621-32625.
321. de Graeff, P., Crijns, A.P., Ten Hoor, K.A., Klip, H.G., Hollema, H., Oien, K., Bartlett, J.M., Wisman, G.B., de Bock, G.H., de Vries, E.G., de Jong, S., and van der Zee, A.G.

(2008). The ErbB signalling pathway: protein expression and prognostic value in epithelial ovarian cancer. Br J Cancer *99*, 341-349.
322. Meert, A.P., Martin, B., Delmotte, P., Berghmans, T., Lafitte, J.J., Mascaux, C., Paesmans, M., Steels, E., Verdebout, J.M., and Sculier, J.P. (2002). The role of EGF-R expression on patient survival in lung cancer: a systematic review with meta-analysis. Eur Respir J *20*, 975-981.
323. Hechtman, J.F., and Polydorides, A.D. HER2/neu gene amplification and protein overexpression in gastric and gastroesophageal junction adenocarcinoma: a review of histopathology, diagnostic testing, and clinical implications. Arch Pathol Lab Med *136*, 691-697.
324. Albanell, J., and Baselga, J. (1999). Trastuzumab, a humanized anti-HER2 monoclonal antibody, for the treatment of breast cancer. Drugs Today (Barc) *35*, 931-946.
325. Ismael, G., Hegg, R., Muehlbauer, S., Heinzmann, D., Lum, B., Kim, S.B., Pienkowski, T., Lichinitser, M., Semiglazov, V., Melichar, B., and Jackisch, C. Subcutaneous versus intravenous administration of (neo)adjuvant trastuzumab in patients with HER2-positive, clinical stage I-III breast cancer (HannaH study): a phase 3, open-label, multicentre, randomised trial. Lancet Oncol *13*, 869-878.
326. Gianni, L., Dafni, U., Gelber, R.D., Azambuja, E., Muehlbauer, S., Goldhirsch, A., Untch, M., Smith, I., Baselga, J., Jackisch, C., Cameron, D., Mano, M., Pedrini, J.L., Veronesi, A., Mendiola, C., Pluzanska, A., Semiglazov, V., Vrdoljak, E., Eckart, M.J., Shen, Z., Skiadopoulos, G., Procter, M., Pritchard, K.I., Piccart-Gebhart, M.J., and Bell, R. Treatment with trastuzumab for 1 year after adjuvant chemotherapy in patients with HER2-positive early breast cancer: a 4-year follow-up of a randomised controlled trial. Lancet Oncol *12*, 236-244.
327. Vogel, C.L., Cobleigh, M.A., Tripathy, D., Gutheil, J.C., Harris, L.N., Fehrenbacher, L., Slamon, D.J., Murphy, M., Novotny, W.F., Burchmore, M., Shak, S., Stewart, S.J., and Press, M. (2002). Efficacy and safety of trastuzumab as a single agent in first-line treatment of HER2-overexpressing metastatic breast cancer. J Clin Oncol *20*, 719-726.
328. Montemurro, F., Choa, G., Faggiuolo, R., Donadio, M., Minischetti, M., Durando, A., Capaldi, A., Vietti-Ramus, G., Alabiso, O., and Aglietta, M. (2004). A phase II study of three-weekly docetaxel and weekly trastuzumab in HER2-overexpressing advanced breast cancer. Oncology *66*, 38-45.
329. O'Shaughnessy, J.A., Vukelja, S., Marsland, T., Kimmel, G., Ratnam, S., and Pippen, J.E. (2004). Phase II study of trastuzumab plus gemcitabine in chemotherapy-pretreated patients with metastatic breast cancer. Clin Breast Cancer *5*, 142-147.
330. De Maio, E., Pacilio, C., Gravina, A., Morabito, A., Di Rella, F., Labonia, V., Landi, G., Nuzzo, F., Rossi, E., Silvestro, P., Botti, G., Di Bonito, M., Curcio, M.P., Formichelli, F., La Vecchia, F., Staiano, M., Maurea, N., D'Aiuto, G., D'Aiuto, M., Thomas, R., Signoriello, G., Perrone, F., and de Matteis, A. (2007). Vinorelbine plus 3-weekly trastuzumab in metastatic breast cancer: a single-centre phase 2 trial. BMC Cancer *7*, 50.
331. Chopra, A. (2004). 111In-(Diethylenetriamine pentaacetic acid)n-trastuzumab-(IRDye 800CW)m.
332. Germershaus, O., Neu, M., Behe, M., and Kissel, T. (2008). HER2 targeted polyplexes: the effect of polyplex composition and conjugation chemistry on in vitro and in vivo characteristics. Bioconjug Chem *19*, 244-253.

333. Sun, B., and Feng, S.S. (2009). Trastuzumab-functionalized nanoparticles of biodegradable copolymers for targeted delivery of docetaxel. Nanomedicine (Lond) *4*, 431-445.
334. Vu, T., and Claret, F.X. Trastuzumab: updated mechanisms of action and resistance in breast cancer. Front Oncol *2*, 62.
335. Miller, T.W., Rexer, B.N., Garrett, J.T., and Arteaga, C.L. Mutations in the phosphatidylinositol 3-kinase pathway: role in tumor progression and therapeutic implications in breast cancer. Breast Cancer Res *13*, 224.
336. Albanell, J., Codony, J., Rovira, A., Mellado, B., and Gascon, P. (2003). Mechanism of action of anti-HER2 monoclonal antibodies: scientific update on trastuzumab and 2C4. Adv Exp Med Biol *532*, 253-268.
337. Yakes, F.M., Chinratanalab, W., Ritter, C.A., King, W., Seelig, S., and Arteaga, C.L. (2002). Herceptin-induced inhibition of phosphatidylinositol-3 kinase and Akt Is required for antibody-mediated effects on p27, cyclin D1, and antitumor action. Cancer Res *62*, 4132-4141.
338. Nagata, Y., Lan, K.H., Zhou, X., Tan, M., Esteva, F.J., Sahin, A.A., Klos, K.S., Li, P., Monia, B.P., Nguyen, N.T., Hortobagyi, G.N., Hung, M.C., and Yu, D. (2004). PTEN activation contributes to tumor inhibition by trastuzumab, and loss of PTEN predicts trastuzumab resistance in patients. Cancer Cell *6*, 117-127.
339. Ribatti, D., Nico, B., Crivellato, E., and Vacca, A. (2007). The structure of the vascular network of tumors. Cancer Lett *248*, 18-23.
340. Aird, W.C. (2009). Molecular heterogeneity of tumor endothelium. Cell Tissue Res *335*, 271-281.
341. Kerbel, R.S., Viloria-Petit, A., Klement, G., and Rak, J. (2000). 'Accidental' anti-angiogenic drugs. anti-oncogene directed signal transduction inhibitors and conventional chemotherapeutic agents as examples. Eur J Cancer *36*, 1248-1257.
342. Izumi, Y., Xu, L., di Tomaso, E., Fukumura, D., and Jain, R.K. (2002). Tumour biology: herceptin acts as an anti-angiogenic cocktail. Nature *416*, 279-280.
343. Klos, K.S., Zhou, X., Lee, S., Zhang, L., Yang, W., Nagata, Y., and Yu, D. (2003). Combined trastuzumab and paclitaxel treatment better inhibits ErbB-2-mediated angiogenesis in breast carcinoma through a more effective inhibition of Akt than either treatment alone. Cancer *98*, 1377-1385.
344. Nakamura, A., Akiyama, K., and Takai, T. (2005). Fc receptor targeting in the treatment of allergy, autoimmune diseases and cancer. Expert Opin Ther Targets *9*, 169-190.
345. Clynes, R.A., Towers, T.L., Presta, L.G., and Ravetch, J.V. (2000). Inhibitory Fc receptors modulate in vivo cytotoxicity against tumor targets. Nat Med *6*, 443-446.
346. Marmor, M.D., and Yarden, Y. (2004). Role of protein ubiquitylation in regulating endocytosis of receptor tyrosine kinases. Oncogene *23*, 2057-2070.
347. Li, X., Shen, L., Zhang, J., Su, J., Liu, X., Han, H., Han, W., and Yao, L. (2007). Degradation of HER2 by Cbl-based chimeric ubiquitin ligases. Cancer Res *67*, 8716-8724.
348. Christianson, T.A., Doherty, J.K., Lin, Y.J., Ramsey, E.E., Holmes, R., Keenan, E.J., and Clinton, G.M. (1998). NH2-terminally truncated HER-2/neu protein: relationship with shedding of the extracellular domain and with prognostic factors in breast cancer. Cancer Res *58*, 5123-5129.

349. Molina, M.A., Codony-Servat, J., Albanell, J., Rojo, F., Arribas, J., and Baselga, J. (2001). Trastuzumab (herceptin), a humanized anti-Her2 receptor monoclonal antibody, inhibits basal and activated Her2 ectodomain cleavage in breast cancer cells. Cancer Res *61*, 4744-4749.
350. Ewer, S.M., and Ewer, M.S. (2008). Cardiotoxicity profile of trastuzumab. Drug Saf *31*, 459-467.
351. Keefe, D.L. (2002). Trastuzumab-associated cardiotoxicity. Cancer *95*, 1592-1600.
352. Chien, A.J., and Rugo, H.S. The cardiac safety of trastuzumab in the treatment of breast cancer. Expert Opin Drug Saf *9*, 335-346.
353. Gianni, L., Salvatorelli, E., and Minotti, G. (2007). Anthracycline cardiotoxicity in breast cancer patients: synergism with trastuzumab and taxanes. Cardiovasc Toxicol *7*, 67-71.
354. Gajria, D., and Chandarlapaty, S. HER2-amplified breast cancer: mechanisms of trastuzumab resistance and novel targeted therapies. Expert Rev Anticancer Ther *11*, 263-275.
355. Nahta, R., and Esteva, F.J. (2006). Herceptin: mechanisms of action and resistance. Cancer Lett *232*, 123-138.
356. Bedard, P.L., de Azambuja, E., and Cardoso, F. (2009). Beyond trastuzumab: overcoming resistance to targeted HER-2 therapy in breast cancer. Curr Cancer Drug Targets *9*, 148-162.
357. Baselga, J., Cortes, J., Kim, S.B., Im, S.A., Hegg, R., Im, Y.H., Roman, L., Pedrini, J.L., Pienkowski, T., Knott, A., Clark, E., Benyunes, M.C., Ross, G., and Swain, S.M. Pertuzumab plus trastuzumab plus docetaxel for metastatic breast cancer. N Engl J Med *366*, 109-119.
358. Baselga, J., and Swain, S.M. CLEOPATRA: a phase III evaluation of pertuzumab and trastuzumab for HER2-positive metastatic breast cancer. Clin Breast Cancer *10*, 489-491.
359. Lu, C.H., Wyszomierski, S.L., Tseng, L.M., Sun, M.H., Lan, K.H., Neal, C.L., Mills, G.B., Hortobagyi, G.N., Esteva, F.J., and Yu, D. (2007). Preclinical testing of clinically applicable strategies for overcoming trastuzumab resistance caused by PTEN deficiency. Clin Cancer Res *13*, 5883-5888.
360. Johnston, S.R., Martin, L.A., Leary, A., Head, J., and Dowsett, M. (2007). Clinical strategies for rationale combinations of aromatase inhibitors with novel therapies for breast cancer. J Steroid Biochem Mol Biol *106*, 180-186.
361. LoRusso, P.M., Weiss, D., Guardino, E., Girish, S., and Sliwkowski, M.X. Trastuzumab emtansine: a unique antibody-drug conjugate in development for human epidermal growth factor receptor 2-positive cancer. Clin Cancer Res *17*, 6437-6447.
362. Martin, M., Makhson, A., Gligorov, J., Lichinitser, M., Lluch, A., Semiglazov, V., Scotto, N., Mitchell, L., and Tjulandin, S. Phase II study of bevacizumab in combination with trastuzumab and capecitabine as first-line treatment for HER-2-positive locally recurrent or metastatic breast cancer. Oncologist *17*, 469-475.
363. Sternberg, C.N., Davis, I.D., Mardiak, J., Szczylik, C., Lee, E., Wagstaff, J., Barrios, C.H., Salman, P., Gladkov, O.A., Kavina, A., Zarba, J.J., Chen, M., McCann, L., Pandite, L., Roychowdhury, D.F., and Hawkins, R.E. Pazopanib in locally advanced or metastatic renal cell carcinoma: results of a randomized phase III trial. J Clin Oncol *28*, 1061-1068.
364. Burstein, H.J., Sun, Y., Dirix, L.Y., Jiang, Z., Paridaens, R., Tan, A.R., Awada, A., Ranade, A., Jiao, S., Schwartz, G., Abbas, R., Powell, C., Turnbull, K., Vermette, J., Zacharchuk, C., and Badwe, R. Neratinib, an irreversible ErbB receptor tyrosine kinase

inhibitor, in patients with advanced ErbB2-positive breast cancer. J Clin Oncol *28*, 1301-1307.
365. Narayan, M., Wilken, J.A., Harris, L.N., Baron, A.T., Kimbler, K.D., and Maihle, N.J. (2009). Trastuzumab-induced HER reprogramming in "resistant" breast carcinoma cells. Cancer Res *69*, 2191-2194.
366. Medina, P.J., and Goodin, S. (2008). Lapatinib: a dual inhibitor of human epidermal growth factor receptor tyrosine kinases. Clin Ther *30*, 1426-1447.
367. Baselga, J., Bradbury, I., Eidtmann, H., Di Cosimo, S., de Azambuja, E., Aura, C., Gomez, H., Dinh, P., Fauria, K., Van Dooren, V., Aktan, G., Goldhirsch, A., Chang, T.W., Horvath, Z., Coccia-Portugal, M., Domont, J., Tseng, L.M., Kunz, G., Sohn, J.H., Semiglazov, V., Lerzo, G., Palacova, M., Probachai, V., Pusztai, L., Untch, M., Gelber, R.D., and Piccart-Gebhart, M. Lapatinib with trastuzumab for HER2-positive early breast cancer (NeoALTTO): a randomised, open-label, multicentre, phase 3 trial. Lancet *379*, 633-640.
368. Lee, J.H., Yigit, M.V., Mazumdar, D., and Lu, Y. Molecular diagnostic and drug delivery agents based on aptamer-nanomaterial conjugates. Adv Drug Deliv Rev *62*, 592-605.
369. Patra, C.R., Jing, Y., Xu, Y.H., Bhattacharya, R., Mukhopadhyay, D., Glockner, J.F., Wang, J.P., and Mukherjee, P. A core-shell nanomaterial with endogenous therapeutic and diagnostic functions. Cancer Nanotechnol *1*, 13-18.
370. Biddlestone-Thorpe, L., Marchi, N., Guo, K., Ghosh, C., Janigro, D., Valerie, K., and Yang, H. Nanomaterial-mediated CNS delivery of diagnostic and therapeutic agents. Adv Drug Deliv Rev *64*, 605-613.
371. Jokerst, J.V., and Gambhir, S.S. Molecular imaging with theranostic nanoparticles. Acc Chem Res *44*, 1050-1060.
372. Jiang, W., Kim, B.Y., Rutka, J.T., and Chan, W.C. (2008). Nanoparticle-mediated cellular response is size-dependent. Nat Nanotechnol *3*, 145-150.
373. Pan, Y., Neuss, S., Leifert, A., Fischler, M., Wen, F., Simon, U., Schmid, G., Brandau, W., and Jahnen-Dechent, W. (2007). Size-dependent cytotoxicity of gold nanoparticles. Small *3*, 1941-1949.
374. Chithrani, B.D., Ghazani, A.A., and Chan, W.C. (2006). Determining the size and shape dependence of gold nanoparticle uptake into mammalian cells. Nano Lett *6*, 662-668.
375. Zhang, S., Li, J., Lykotrafitis, G., Bao, G., and Suresh, S. (2009). Size-Dependent Endocytosis of Nanoparticles. Adv Mater *21*, 419-424.
376. Gullotti, E., and Yeo, Y. (2009). Extracellularly activated nanocarriers: a new paradigm of tumor targeted drug delivery. Mol Pharm *6*, 1041-1051.
377. You, S., and Li, W. (2008). Administration of nanodrugs in proper menstrual stage for maximal drug retention in breast cancer. Med Hypotheses *71*, 141-147.
378. Chandran, S.S., Banerjee, S.R., Mease, R.C., Pomper, M.G., and Denmeade, S.R. (2008). Characterization of a targeted nanoparticle functionalized with a urea-based inhibitor of prostate-specific membrane antigen (PSMA). Cancer Biol Ther *7*, 974-982.
379. Maeda, H., Wu, J., Sawa, T., Matsumura, Y., and Hori, K. (2000). Tumor vascular permeability and the EPR effect in macromolecular therapeutics: a review. J Control Release *65*, 271-284.
380. Owens, D.E., 3rd, and Peppas, N.A. (2006). Opsonization, biodistribution, and pharmacokinetics of polymeric nanoparticles. Int J Pharm *307*, 93-102.

381. Hobbs, S.K., Monsky, W.L., Yuan, F., Roberts, W.G., Griffith, L., Torchilin, V.P., and Jain, R.K. (1998). Regulation of transport pathways in tumor vessels: role of tumor type and microenvironment. Proc Natl Acad Sci U S A *95*, 4607-4612.
382. Heldin, C.H., Rubin, K., Pietras, K., and Ostman, A. (2004). High interstitial fluid pressure - an obstacle in cancer therapy. Nat Rev Cancer *4*, 806-813.
383. Phillips, M.A., Gran, M.L., and Peppas, N.A. Targeted Nanodelivery of Drugs and Diagnostics. Nano Today *5*, 143-159.
384. Pearce, T.R., Shroff, K., and Kokkoli, E. Peptide targeted lipid nanoparticles for anticancer drug delivery. Adv Mater *24*, 3803-3822, 3710.
385. Fay, F., and Scott, C.J. Antibody-targeted nanoparticles for cancer therapy. Immunotherapy *3*, 381-394.
386. Lemarchand, C., Gref, R., and Couvreur, P. (2004). Polysaccharide-decorated nanoparticles. Eur J Pharm Biopharm *58*, 327-341.
387. Jin, S., Leach, J.C., and Ye, K. (2009). Nanoparticle-mediated gene delivery. Methods Mol Biol *544*, 547-557.
388. Patil, Y.B., Swaminathan, S.K., Sadhukha, T., Ma, L., and Panyam, J. The use of nanoparticle-mediated targeted gene silencing and drug delivery to overcome tumor drug resistance. Biomaterials *31*, 358-365.
389. Elbayoumi, T.A., and Torchilin, V.P. (2009). Tumor-specific anti-nucleosome antibody improves therapeutic efficacy of doxorubicin-loaded long-circulating liposomes against primary and metastatic tumor in mice. Mol Pharm *6*, 246-254.
390. Anhorn, M.G., Wagner, S., Kreuter, J., Langer, K., and von Briesen, H. (2008). Specific targeting of HER2 overexpressing breast cancer cells with doxorubicin-loaded trastuzumab-modified human serum albumin nanoparticles. Bioconjug Chem *19*, 2321-2331.
391. Gupta, B., and Torchilin, V.P. (2007). Monoclonal antibody 2C5-modified doxorubicin-loaded liposomes with significantly enhanced therapeutic activity against intracranial human brain U-87 MG tumor xenografts in nude mice. Cancer Immunol Immunother *56*, 1215-1223.
392. Fujita, M., Lee, B.S., Khazenzon, N.M., Penichet, M.L., Wawrowsky, K.A., Patil, R., Ding, H., Holler, E., Black, K.L., and Ljubimova, J.Y. (2007). Brain tumor tandem targeting using a combination of monoclonal antibodies attached to biopoly(beta-L-malic acid). J Control Release *122*, 356-363.
393. Steinhauser, I., Spankuch, B., Strebhardt, K., and Langer, K. (2006). Trastuzumab-modified nanoparticles: optimisation of preparation and uptake in cancer cells. Biomaterials *27*, 4975-4983.
394. Moghimi, S.M., Hunter, A.C., and Murray, J.C. (2001). Long-circulating and target-specific nanoparticles: theory to practice. Pharmacol Rev *53*, 283-318.
395. Murphy, E.A., Majeti, B.K., Barnes, L.A., Makale, M., Weis, S.M., Lutu-Fuga, K., Wrasidlo, W., and Cheresh, D.A. (2008). Nanoparticle-mediated drug delivery to tumor vasculature suppresses metastasis. Proc Natl Acad Sci U S A *105*, 9343-9348.
396. Li, L., Wang, R., Wilcox, D., Zhao, X., Song, J., Lin, X., Kohlbrenner, W.M., Fesik, S.W., and Shen, Y. Tumor vasculature is a key determinant for the efficiency of nanoparticle-mediated siRNA delivery. Gene Ther *19*, 775-780.

397. Zhou, M., Smith, A.M., Das, A.K., Hodson, N.W., Collins, R.F., Ulijn, R.V., and Gough, J.E. (2009). Self-assembled peptide-based hydrogels as scaffolds for anchorage-dependent cells. Biomaterials *30*, 2523-2530.
398. Li, H., Zhang, F., Zhang, Y., Ye, M., Zhou, B., Tang, Y.Z., Yang, H.J., Xie, M.Y., Chen, S.F., He, J.H., Fang, H.P., and Hu, J. (2009). Peptide diffusion and self-assembly in ambient water nanofilm on mica surface. J Phys Chem B *113*, 8795-8799.
399. Law, B., Weissleder, R., and Tung, C.H. (2006). Peptide-based biomaterials for protease-enhanced drug delivery. Biomacromolecules *7*, 1261-1265.
400. Zou, Z., Zheng, Q., Wu, Y., Guo, X., Yang, S., Li, J., and Pan, H. Biocompatibility and bioactivity of designer self-assembling nanofiber scaffold containing FGL motif for rat dorsal root ganglion neurons. J Biomed Mater Res A *95*, 1125-1131.
401. Panda, J.J., Kaul, A., Alam, S., Babbar, A.K., Mishra, A.K., and Chauhan, V.S. Designed peptides as model self-assembling nanosystems: characterization and potential biomedical applications. Ther Deliv *2*, 193-204.
402. Cui, H., Webber, M.J., and Stupp, S.I. Self-assembly of peptide amphiphiles: from molecules to nanostructures to biomaterials. Biopolymers *94*, 1-18.
403. Zhao, X., Pan, F., Xu, H., Yaseen, M., Shan, H., Hauser, C.A., Zhang, S., and Lu, J.R. Molecular self-assembly and applications of designer peptide amphiphiles. Chem Soc Rev *39*, 3480-3498.
404. Edwin, N.J., Hammer, R.P., McCarley, R.L., and Russo, P.S. Reversibility of beta-amyloid self-assembly: effects of pH and added salts assessed by fluorescence photobleaching recovery. Biomacromolecules *11*, 341-347.
405. Qin, S.Y., Xu, S.S., Zhuo, R.X., and Zhang, X.Z. Morphology transformation via pH-triggered self-assembly of peptides. Langmuir *28*, 2083-2090.
406. Gelain, F., Bottai, D., Vescovi, A., and Zhang, S. (2006). Designer self-assembling peptide nanofiber scaffolds for adult mouse neural stem cell 3-dimensional cultures. PLoS One *1*, e119.
407. Hsieh, P.C., MacGillivray, C., Gannon, J., Cruz, F.U., and Lee, R.T. (2006). Local controlled intramyocardial delivery of platelet-derived growth factor improves postinfarction ventricular function without pulmonary toxicity. Circulation *114*, 637-644.
408. Wu, M., Ye, Z., Liu, Y., Liu, B., and Zhao, X. Release of hydrophobic anticancer drug from a newly designed self-assembling peptide. Mol Biosyst *7*, 2040-2047.
409. Matson, J.B., and Stupp, S.I. Drug release from hydrazone-containing peptide amphiphiles. Chem Commun (Camb) *47*, 7962-7964.
410. Accardo, A., Tesauro, D., Mangiapia, G., Pedone, C., and Morelli, G. (2007). Nanostructures by self-assembling peptide amphiphile as potential selective drug carriers. Biopolymers *88*, 115-121.
411. Webber, M.J., Tongers, J., Newcomb, C.J., Marquardt, K.T., Bauersachs, J., Losordo, D.W., and Stupp, S.I. Supramolecular nanostructures that mimic VEGF as a strategy for ischemic tissue repair. Proc Natl Acad Sci U S A *108*, 13438-13443.
412. Horii, A., Wang, X., Gelain, F., and Zhang, S. (2007). Biological designer self-assembling peptide nanofiber scaffolds significantly enhance osteoblast proliferation, differentiation and 3-D migration. PLoS One *2*, e190.
413. Rajangam, K., Behanna, H.A., Hui, M.J., Han, X., Hulvat, J.F., Lomasney, J.W., and Stupp, S.I. (2006). Heparin binding nanostructures to promote growth of blood vessels. Nano Lett *6*, 2086-2090.

414. Patel, S., Kurpinski, K., Quigley, R., Gao, H., Hsiao, B.S., Poo, M.M., and Li, S. (2007). Bioactive nanofibers: synergistic effects of nanotopography and chemical signaling on cell guidance. Nano Lett *7*, 2122-2128.
415. Lim, Y.B., Moon, K.S., and Lee, M. (2009). Recent advances in functional supramolecular nanostructures assembled from bioactive building blocks. Chem Soc Rev *38*, 925-934.
416. Safenkova, I.V., Zherdev, A.V., and Dzantiev, B.B. Correlation between the composition of multivalent antibody conjugates with colloidal gold nanoparticles and their affinity. J Immunol Methods *357*, 17-25.
417. Liu, H.Y., and Gao, X. Engineering monovalent quantum dot-antibody bioconjugates with a hybrid gel system. Bioconjug Chem *22*, 510-517.
418. Haun, J.B., Devaraj, N.K., Hilderbrand, S.A., Lee, H., and Weissleder, R. Bioorthogonal chemistry amplifies nanoparticle binding and enhances the sensitivity of cell detection. Nat Nanotechnol *5*, 660-665.
419. Chiu, G.N., Edwards, L.A., Kapanen, A.I., Malinen, M.M., Dragowska, W.H., Warburton, C., Chikh, G.G., Fang, K.Y., Tan, S., Sy, J., Tucker, C., Waterhouse, D.N., Klasa, R., and Bally, M.B. (2007). Modulation of cancer cell survival pathways using multivalent liposomal therapeutic antibody constructs. Mol Cancer Ther *6*, 844-855.
420. Shuvaev, V.V., Ilies, M.A., Simone, E., Zaitsev, S., Kim, Y., Cai, S., Mahmud, A., Dziubla, T., Muro, S., Discher, D.E., and Muzykantov, V.R. Endothelial targeting of antibody-decorated polymeric filomicelles. ACS Nano *5*, 6991-6999.
421. Wangler, C., Moldenhauer, G., Eisenhut, M., Haberkorn, U., and Mier, W. (2008). Antibody-dendrimer conjugates: the number, not the size of the dendrimers, determines the immunoreactivity. Bioconjug Chem *19*, 813-820.
422. Muro, S., Dziubla, T., Qiu, W., Leferovich, J., Cui, X., Berk, E., and Muzykantov, V.R. (2006). Endothelial targeting of high-affinity multivalent polymer nanocarriers directed to intercellular adhesion molecule 1. J Pharmacol Exp Ther *317*, 1161-1169.
423. Khan, J.A., Kudgus, R.A., Szabolcs, A., Dutta, S., Wang, E., Cao, S., Curran, G.L., Shah, V., Curley, S., Mukhopadhyay, D., Robertson, J.D., Bhattacharya, R., and Mukherjee, P. Designing nanoconjugates to effectively target pancreatic cancer cells in vitro and in vivo. PLoS One *6*, e20347.
424. Stendahl, J.C., Wang, L.J., Chow, L.W., Kaufman, D.B., and Stupp, S.I. (2008). Growth factor delivery from self-assembling nanofibers to facilitate islet transplantation. Transplantation *86*, 478-481.
425. Hsieh, P.C., Davis, M.E., Gannon, J., MacGillivray, C., and Lee, R.T. (2006). Controlled delivery of PDGF-BB for myocardial protection using injectable self-assembling peptide nanofibers. J Clin Invest *116*, 237-248.
426. Nishimura, A., Hayakawa, T., Yamamoto, Y., Hamori, M., Tabata, K., Seto, K., and Shibata, N. Controlled release of insulin from self-assembling nanofiber hydrogel, PuraMatrix: application for the subcutaneous injection in rats. Eur J Pharm Sci *45*, 1-7.
427. Davis, M.E., Hsieh, P.C., Takahashi, T., Song, Q., Zhang, S., Kamm, R.D., Grodzinsky, A.J., Anversa, P., and Lee, R.T. (2006). Local myocardial insulin-like growth factor 1 (IGF-1) delivery with biotinylated peptide nanofibers improves cell therapy for myocardial infarction. Proc Natl Acad Sci U S A *103*, 8155-8160.

428. Sadatmousavi, P., Mamo, T., and Chen, P. Diethylene glycol functionalized self-assembling peptide nanofibers and their hydrophobic drug delivery potential. Acta Biomater *8*, 3241-3250.
429. Liu, J., Zhang, L., Yang, Z., and Zhao, X. Controlled release of paclitaxel from a self-assembling peptide hydrogel formed in situ and antitumor study in vitro. Int J Nanomedicine *6*, 2143-2153.
430. Soukasene, S., Toft, D.J., Moyer, T.J., Lu, H., Lee, H.K., Standley, S.M., Cryns, V.L., and Stupp, S.I. Antitumor activity of peptide amphiphile nanofiber-encapsulated camptothecin. ACS Nano *5*, 9113-9121.
431. Webber, M.J., Matson, J.B., Tamboli, V.K., and Stupp, S.I. Controlled release of dexamethasone from peptide nanofiber gels to modulate inflammatory response. Biomaterials *33*, 6823-6832.
432. Wang, H., Wei, J., Yang, C., Zhao, H., Li, D., Yin, Z., and Yang, Z. The inhibition of tumor growth and metastasis by self-assembled nanofibers of taxol. Biomaterials *33*, 5848-5853.
433. Hosseinkhani, H., Hosseinkhani, M., Khademhosseini, A., and Kobayashi, H. (2007). Bone regeneration through controlled release of bone morphogenetic protein-2 from 3-D tissue engineered nano-scaffold. J Control Release *117*, 380-386.
434. Meng, H., Chen, L., Ye, Z., Wang, S., and Zhao, X. (2009). The effect of a self-assembling peptide nanofiber scaffold (peptide) when used as a wound dressing for the treatment of deep second degree burns in rats. J Biomed Mater Res B Appl Biomater *89*, 379-391.
435. Schneider, A., Garlick, J.A., and Egles, C. (2008). Self-assembling peptide nanofiber scaffolds accelerate wound healing. PLoS One *3*, e1410.
436. Vicent, M.J., and Duncan, R. (2006). Polymer conjugates: nanosized medicines for treating cancer. Trends Biotechnol *24*, 39-47.
437. Duncan, R. (2006). Polymer conjugates as anticancer nanomedicines. Nat Rev Cancer *6*, 688-701.
438. Luo, Z., Zhao, X., and Zhang, S. (2008). Self-organization of a chiral D-EAK16 designer peptide into a 3D nanofiber scaffold. Macromol Biosci *8*, 785-791.
439. Wiltzius, J.J., Landau, M., Nelson, R., Sawaya, M.R., Apostol, M.I., Goldschmidt, L., Soriaga, A.B., Cascio, D., Rajashankar, K., and Eisenberg, D. (2009). Molecular mechanisms for protein-encoded inheritance. Nat Struct Mol Biol *16*, 973-978.
440. Snyder, S.L., and Sobocinski, P.Z. (1975). An improved 2,4,6-trinitrobenzenesulfonic acid method for the determination of amines. Anal Biochem *64*, 284-288.
441. Husain, M., and Bieniarz, C. (1994). Fc site-specific labeling of immunoglobulins with calf intestinal alkaline phosphatase. Bioconjug Chem *5*, 482-490.
442. Abraham, R., Moller, D., Gabel, D., Senter, P., Hellstrom, I., and Hellstrom, K.E. (1991). The influence of periodate oxidation on monoclonal antibody avidity and immunoreactivity. J Immunol Methods *144*, 77-86.
443. Hage, D.S. (2000). Periodate oxidation of antibodies for site-selective immobilization in immunoaffinity chromatography. Methods Mol Biol *147*, 69-82.
444. Wiechelman, K.J., Braun, R.D., and Fitzpatrick, J.D. (1988). Investigation of the bicinchoninic acid protein assay: identification of the groups responsible for color formation. Anal Biochem *175*, 231-237.

445. Papp, I., Sieben, C., Sisson, A.L., Kostka, J., Bottcher, C., Ludwig, K., Herrmann, A., and Haag, R. Inhibition of influenza virus activity by multivalent glycoarchitectures with matched sizes. Chembiochem *12*, 887-895.
446. Sung, M., Poon, G.M., and Gariepy, J. (2006). The importance of valency in enhancing the import and cell routing potential of protein transduction domain-containing molecules. Biochim Biophys Acta *1758*, 355-363.
447. Zhao, J., Mi, Y., Liu, Y., and Feng, S.S. Quantitative control of targeting effect of anticancer drugs formulated by ligand-conjugated nanoparticles of biodegradable copolymer blend. Biomaterials *33*, 1948-1958.
448. Gao, H., Shi, W., and Freund, L.B. (2005). Mechanics of receptor-mediated endocytosis. Proc Natl Acad Sci U S A *102*, 9469-9474.
449. Gao, H., Shi, W., and Freund, L.B. (2005). Mechanics of receptor-mediated endocytosis. Proc. Natl. Acad. Sci. U S A. *102*, 9469-9474.
450. Zhao, F., Zhao, Y., Liu, Y., Chang, X., and Chen, C. (2011). Cellular uptake, intracellular trafficking, and cytotoxicity of nanomaterials. Small *7*, 1322-1337.
451. Gratton, S.E., Ropp, P.A., Pohlhaus, P.D., Luft, J.C., Madden, V.J., Napier, M.E., and DeSimone, J.M. (2008). The effect of particle design on cellular internalization pathways. Proc. Natl.Acad.Sci.U S A. *105*, 11613-11618.
452. Wang, J., Tian, S., Petros, R.A., Napier, M.E., and Desimone, J.M. (2010). The complex role of multivalency in nanoparticles targeting the transferrin receptor for cancer therapies. J. Am. Chem. Soc. *132*, 11306-11313.
453. Ben-Kasus, T., Schechter, B., Sela, M., and Yarden, Y. (2007). Cancer therapeutic antibodies come of age: targeting minimal residual disease. Mol Oncol *1*, 42-54.
454. Muro, S., Cui, X., Gajewski, C., Murciano, J.C., Muzykantov, V.R., and Koval, M. (2003). Slow intracellular trafficking of catalase nanoparticles targeted to ICAM-1 protects endothelial cells from oxidative stress. Am J Physiol Cell Physiol *285*, C1339-1347.
455. Hennessy, B.T., Smith, D.L., Ram, P.T., Lu, Y., and Mills, G.B. (2005). Exploiting the PI3K/AKT pathway for cancer drug discovery. Nat Rev Drug Discov *4*, 988-1004.
456. Pohlmann, P.R., Mayer, I.A., and Mernaugh, R. (2009). Resistance to Trastuzumab in Breast Cancer. Clin Cancer Res *15*, 7479-7491.
457. Ben-Kasus, T., Schechter, B., Lavi, S., Yarden, Y., and Sela, M. (2009). Persistent elimination of ErbB-2/HER2-overexpressing tumors using combinations of monoclonal antibodies: relevance of receptor endocytosis. Proc Natl Acad Sci U S A *106*, 3294-3299.
458. Miller, K., Wang, M., Gralow, J., Dickler, M., Cobleigh, M., Perez, E.A., Shenkier, T., Cella, D., and Davidson, N.E. (2007). Paclitaxel plus bevacizumab versus paclitaxel alone for metastatic breast cancer. N Engl J Med *357*, 2666-2676.
459. Hughes, B. Antibody-drug conjugates for cancer: poised to deliver? Nat Rev Drug Discov *9*, 665-667.
460. Jefferis, R. (2009). Glycosylation as a strategy to improve antibody-based therapeutics. Nat Rev Drug Discov *8*, 226-234.
461. Kisiday, J.D., Kurz, B., DiMicco, M.A., and Grodzinsky, A.J. (2005). Evaluation of medium supplemented with insulin-transferrin-selenium for culture of primary bovine calf chondrocytes in three-dimensional hydrogel scaffolds. Tissue Eng *11*, 141-151.

462. Baade, P.D., Youlden, D.R., and Krnjacki, L.J. (2009). International epidemiology of prostate cancer: geographical distribution and secular trends. Mol Nutr Food Res *53*, 171-184.
463. Siegel, R., Ward, E., Brawley, O., and Jemal, A. Cancer statistics, 2011: the impact of eliminating socioeconomic and racial disparities on premature cancer deaths. CA Cancer J Clin *61*, 212-236.
464. Swinnen, J.V., Roskams, T., Joniau, S., Van Poppel, H., Oyen, R., Baert, L., Heyns, W., and Verhoeven, G. (2002). Overexpression of fatty acid synthase is an early and common event in the development of prostate cancer. Int J Cancer *98*, 19-22.
465. Swinnen, J.V., Vanderhoydonc, F., Elgamal, A.A., Eelen, M., Vercaeren, I., Joniau, S., Van Poppel, H., Baert, L., Goossens, K., Heyns, W., and Verhoeven, G. (2000). Selective activation of the fatty acid synthesis pathway in human prostate cancer. Int J Cancer *88*, 176-179.
466. Hoffman, R.M., Gilliland, F.D., Eley, J.W., Harlan, L.C., Stephenson, R.A., Stanford, J.L., Albertson, P.C., Hamilton, A.S., Hunt, W.C., and Potosky, A.L. (2001). Racial and ethnic differences in advanced-stage prostate cancer: the Prostate Cancer Outcomes Study. J Natl Cancer Inst *93*, 388-395.
467. Chavarro, J.E., Stampfer, M.J., Li, H., Campos, H., Kurth, T., and Ma, J. (2007). A prospective study of polyunsaturated fatty acid levels in blood and prostate cancer risk. Cancer Epidemiol Biomarkers Prev *16*, 1364-1370.
468. Benatti, P., Peluso, G., Nicolai, R., and Calvani, M. (2004). Polyunsaturated fatty acids: biochemical, nutritional and epigenetic properties. J Am Coll Nutr *23*, 281-302.
469. Vedtofte, M.S., Jakobsen, M.U., Lauritzen, L., and Heitmann, B.L. The role of essential fatty acids in the control of coronary heart disease. Curr Opin Clin Nutr Metab Care *15*, 592-596.
470. Baum, S.J. EPA and DHA: distinct yet essential n-3 fatty acids. J Clin Lipidol *6*, 477; author reply 477-479.
471. Zhou, L., and Nilsson, A. (2001). Sources of eicosanoid precursor fatty acid pools in tissues. J Lipid Res *42*, 1521-1542.
472. Simopoulos, A.P. (1991). Omega-3 fatty acids in health and disease and in growth and development. Am J Clin Nutr *54*, 438-463.
473. Simopoulos, A.P. (2003). Importance of the ratio of omega-6/omega-3 essential fatty acids: evolutionary aspects. World Rev Nutr Diet *92*, 1-22.
474. Sampath, H., and Ntambi, J.M. (2005). Polyunsaturated fatty acid regulation of genes of lipid metabolism. Annu Rev Nutr *25*, 317-340.
475. Murff, H.J., Shu, X.O., Li, H., Yang, G., Wu, X., Cai, H., Wen, W., Gao, Y.T., and Zheng, W. Dietary polyunsaturated fatty acids and breast cancer risk in Chinese women: a prospective cohort study. Int J Cancer *128*, 1434-1441.
476. Astorg, P. (2004). Dietary N-6 and N-3 polyunsaturated fatty acids and prostate cancer risk: a review of epidemiological and experimental evidence. Cancer Causes Control *15*, 367-386.
477. Azrad, M., and Demark-Wahnefried, W. Dietary omega-6 and omega-3 fatty acids and prostate cancer - letter. Cancer Prev Res (Phila) *5*, 798; author reply 799.
478. Silva Jde, A., Trindade, E.B., Fabre, M.E., Menegotto, V.M., Gevaerd, S., Buss Zda, S., and Frode, T.S. Fish oil supplement alters markers of inflammatory and nutritional status in colorectal cancer patients. Nutr Cancer *64*, 267-273.

479. Murff, H.J., Shrubsole, M.J., Cai, Q., Smalley, W.E., Dai, Q., Milne, G.L., Ness, R.M., and Zheng, W. Dietary intake of PUFAs and colorectal polyp risk. Am J Clin Nutr *95*, 703-712.
480. Serini, S., Piccioni, E., and Calviello, G. (2009). Dietary n-3 PUFA vascular targeting and the prevention of tumor growth and age-related macular degeneration. Curr Med Chem *16*, 4511-4526.
481. Gerber, M. Omega-3 fatty acids and cancers: a systematic update review of epidemiological studies. Br J Nutr *107 Suppl 2*, S228-239.
482. Begin, M.E., Das, U.N., Ells, G., and Horrobin, D.F. (1985). Selective killing of human cancer cells by polyunsaturated fatty acids. Prostaglandins Leukot Med *19*, 177-186.
483. Begin, M.E., Ells, G., Das, U.N., and Horrobin, D.F. (1986). Differential killing of human carcinoma cells supplemented with n-3 and n-6 polyunsaturated fatty acids. J Natl Cancer Inst *77*, 1053-1062.
484. Begin, M.E. (1989). Tumor cytotoxicity of essential fatty acids. Nutrition *5*, 258-260.
485. Begin, M.E., Ells, G., and Horrobin, D.F. (1988). Polyunsaturated fatty acid-induced cytotoxicity against tumor cells and its relationship to lipid peroxidation. J Natl Cancer Inst *80*, 188-194.
486. Cantrill, R.C., Ells, G.W., DeMarco, A.C., and Horrobin, D.F. (1997). Mechanisms of the selective cytotoxic actions of certain essential fatty acids. Adv Exp Med Biol *400A*, 539-544.
487. Llaverias, G., Danilo, C., Wang, Y., Witkiewicz, A.K., Daumer, K., Lisanti, M.P., and Frank, P.G. A Western-type diet accelerates tumor progression in an autochthonous mouse model of prostate cancer. Am J Pathol *177*, 3180-3191.
488. Fulda, S., Gorman, A.M., Hori, O., and Samali, A. Cellular stress responses: cell survival and cell death. Int J Cell Biol *2010*, 214074.
489. Kuhn, H., Saam, J., Eibach, S., Holzhutter, H.G., Ivanov, I., and Walther, M. (2005). Structural biology of mammalian lipoxygenases: enzymatic consequences of targeted alterations of the protein structure. Biochem Biophys Res Commun *338*, 93-101.
490. Higuchi, T., Shirai, N., Saito, M., Suzuki, H., and Kagawa, Y. (2008). Levels of plasma insulin, leptin and adiponectin, and activities of key enzymes in carbohydrate metabolism in skeletal muscle and liver in fasted ICR mice fed dietary n-3 polyunsaturated fatty acids. J Nutr Biochem *19*, 577-586.
491. Poulsen, R.C., Moughan, P.J., and Kruger, M.C. (2007). Long-chain polyunsaturated fatty acids and the regulation of bone metabolism. Exp Biol Med (Maywood) *232*, 1275-1288.
492. Ricciotti, E., and FitzGerald, G.A. Prostaglandins and inflammation. Arterioscler Thromb Vasc Biol *31*, 986-1000.
493. Brash, A.R. (1999). Lipoxygenases: occurrence, functions, catalysis, and acquisition of substrate. J Biol Chem *274*, 23679-23682.
494. Chawengsub, Y., Gauthier, K.M., and Campbell, W.B. (2009). Role of arachidonic acid lipoxygenase metabolites in the regulation of vascular tone. Am J Physiol Heart Circ Physiol *297*, H495-507.
495. Haeggstrom, J.Z., and Funk, C.D. Lipoxygenase and leukotriene pathways: biochemistry, biology, and roles in disease. Chem Rev *111*, 5866-5898.

496. Yuan, H., Li, M.Y., Ma, L.T., Hsin, M.K., Mok, T.S., Underwood, M.J., and Chen, G.G. 15-Lipoxygenases and its metabolites 15(S)-HETE and 13(S)-HODE in the development of non-small cell lung cancer. Thorax *65*, 321-326.
497. Zhang, B., Wang, C.L., Zhao, W.H., Lv, M., Wang, C.Y., Zhong, W.X., Zhou, W.Y., Yu, W.S., Zhang, Y., and Li, S. (2008). Effect of 5-LOX/COX-2 common inhibitor DHDMBF30 on pancreatic cancer cell Capan2. World J Gastroenterol *14*, 2494-2500.
498. Thum, T., and Borlak, J. (2008). LOX-1 receptor blockade abrogates oxLDL-induced oxidative DNA damage and prevents activation of the transcriptional repressor Oct-1 in human coronary arterial endothelium. J Biol Chem *283*, 19456-19464.
499. Kuhn, H., and Brash, A.R. (1990). Occurrence of lipoxygenase products in membranes of rabbit reticulocytes. Evidence for a role of the reticulocyte lipoxygenase in the maturation of red cells. J Biol Chem *265*, 1454-1458.
500. Feltenmark, S., Gautam, N., Brunnstrom, A., Griffiths, W., Backman, L., Edenius, C., Lindbom, L., Bjorkholm, M., and Claesson, H.E. (2008). Eoxins are proinflammatory arachidonic acid metabolites produced via the 15-lipoxygenase-1 pathway in human eosinophils and mast cells. Proc Natl Acad Sci U S A *105*, 680-685.
501. Stachowska, E., Dziedziejko, V., Safranow, K., Jakubowska, K., Olszewska, M., Machalinski, B., and Chlubek, D. (2007). Effect of conjugated linoleic acids on the activity and mRNA expression of 5- and 15-lipoxygenases in human macrophages. J Agric Food Chem *55*, 5335-5342.
502. Gulliksson, M., Brunnstrom, A., Johannesson, M., Backman, L., Nilsson, G., Harvima, I., Dahlen, B., Kumlin, M., and Claesson, H.E. (2007). Expression of 15-lipoxygenase type-1 in human mast cells. Biochim Biophys Acta *1771*, 1156-1165.
503. Hunter, J.A., Finkbeiner, W.E., Nadel, J.A., Goetzl, E.J., and Holtzman, M.J. (1985). Predominant generation of 15-lipoxygenase metabolites of arachidonic acid by epithelial cells from human trachea. Proc Natl Acad Sci U S A *82*, 4633-4637.
504. Oliw, E.H., Fabiani, R., Johansson, L., and Ronquist, G. (1993). Arachidonic acid 15-lipoxygenase and traces of E prostaglandins in purified human prostasomes. J Reprod Fertil *99*, 195-199.
505. Liminga, M., Fagerholm, P., and Oliw, E.H. (1994). Lipoxygenases in corneal epithelia of man and cynomolgus monkey. Exp Eye Res *59*, 313-321.
506. Brash, A.R., Boeglin, W.E., and Chang, M.S. (1997). Discovery of a second 15S-lipoxygenase in humans. Proc Natl Acad Sci U S A *94*, 6148-6152.
507. Baer, A.N., Costello, P.B., and Green, F.A. (1990). Free and esterified 13(R,S)-hydroxyoctadecadienoic acids: principal oxygenase products in psoriatic skin scales. J Lipid Res *31*, 125-130.
508. Claesson, H.E. (2009). On the biosynthesis and biological role of eoxins and 15-lipoxygenase-1 in airway inflammation and Hodgkin lymphoma. Prostaglandins Other Lipid Mediat *89*, 120-125.
509. Kuhn, H., and O'Donnell, V.B. (2006). Inflammation and immune regulation by 12/15-lipoxygenases. Prog Lipid Res *45*, 334-356.
510. Shannon, V.R., Chanez, P., Bousquet, J., and Holtzman, M.J. (1993). Histochemical evidence for induction of arachidonate 15-lipoxygenase in airway disease. Am Rev Respir Dis *147*, 1024-1028.
511. Funk, C.D. (2006). Lipoxygenase pathways as mediators of early inflammatory events in atherosclerosis. Arterioscler Thromb Vasc Biol *26*, 1204-1206.

512. Mochizuki, N., and Kwon, Y.G. (2008). 15-lipoxygenase-1 in the vasculature: expanding roles in angiogenesis. Circ Res *102*, 143-145.
513. Kerjaschki, D., Bago-Horvath, Z., Rudas, M., Sexl, V., Schneckenleithner, C., Wolbank, S., Bartel, G., Krieger, S., Kalt, R., Hantusch, B., Keller, T., Nagy-Bojarszky, K., Huttary, N., Raab, I., Lackner, K., Krautgasser, K., Schachner, H., Kaserer, K., Rezar, S., Madlener, S., Vonach, C., Davidovits, A., Nosaka, H., Hammerle, M., Viola, K., Dolznig, H., Schreiber, M., Nader, A., Mikulits, W., Gnant, M., Hirakawa, S., Detmar, M., Alitalo, K., Nijman, S., Offner, F., Maier, T.J., Steinhilber, D., and Krupitza, G. Lipoxygenase mediates invasion of intrametastatic lymphatic vessels and propagates lymph node metastasis of human mammary carcinoma xenografts in mouse. J Clin Invest *121*, 2000-2012.
514. Claesson, H.E., Griffiths, W.J., Brunnstrom, A., Schain, F., Andersson, E., Feltenmark, S., Johnson, H.A., Porwit, A., Sjoberg, J., and Bjorkholm, M. (2008). Hodgkin Reed-Sternberg cells express 15-lipoxygenase-1 and are putative producers of eoxins in vivo: novel insight into the inflammatory features of classical Hodgkin lymphoma. FEBS J *275*, 4222-4234.
515. Reddy, N., Everhart, A., Eling, T., and Glasgow, W. (1997). Characterization of a 15-lipoxygenase in human breast carcinoma BT-20 cells: stimulation of 13-HODE formation by TGF alpha/EGF. Biochem Biophys Res Commun *231*, 111-116.
516. Kelavkar, U.P., Cohen, C., Kamitani, H., Eling, T.E., and Badr, K.F. (2000). Concordant induction of 15-lipoxygenase-1 and mutant p53 expression in human prostate adenocarcinoma: correlation with Gleason staging. Carcinogenesis *21*, 1777-1787.
517. Cimen, I., Tuncay, S., and Banerjee, S. (2009). 15-Lipoxygenase-1 expression suppresses the invasive properties of colorectal carcinoma cell lines HCT-116 and HT-29. Cancer Sci *100*, 2283-2291.
518. Zuo, X., Morris, J.S., Broaddus, R., and Shureiqi, I. (2009). 15-LOX-1 transcription suppression through the NuRD complex in colon cancer cells. Oncogene *28*, 1496-1505.
519. Shureiqi, I., Jiang, W., Zuo, X., Wu, Y., Stimmel, J.B., Leesnitzer, L.M., Morris, J.S., Fan, H.Z., Fischer, S.M., and Lippman, S.M. (2003). The 15-lipoxygenase-1 product 13-S-hydroxyoctadecadienoic acid down-regulates PPAR-delta to induce apoptosis in colorectal cancer cells. Proc Natl Acad Sci U S A *100*, 9968-9973.
520. Shureiqi, I., Chen, D., Lee, J.J., Yang, P., Newman, R.A., Brenner, D.E., Lotan, R., Fischer, S.M., and Lippman, S.M. (2000). 15-LOX-1: a novel molecular target of nonsteroidal anti-inflammatory drug-induced apoptosis in colorectal cancer cells. J Natl Cancer Inst *92*, 1136-1142.
521. Shureiqi, I., Wu, Y., Chen, D., Yang, X.L., Guan, B., Morris, J.S., Yang, P., Newman, R.A., Broaddus, R., Hamilton, S.R., Lynch, P., Levin, B., Fischer, S.M., and Lippman, S.M. (2005). The critical role of 15-lipoxygenase-1 in colorectal epithelial cell terminal differentiation and tumorigenesis. Cancer Res *65*, 11486-11492.
522. Zhu, H., Glasgow, W., George, M.D., Chrysovergis, K., Olden, K., Roberts, J.D., and Eling, T. (2008). 15-lipoxygenase-1 activates tumor suppressor p53 independent of enzymatic activity. Int J Cancer *123*, 2741-2749.
523. Shureiqi, I., Xu, X., Chen, D., Lotan, R., Morris, J.S., Fischer, S.M., and Lippman, S.M. (2001). Nonsteroidal anti-inflammatory drugs induce apoptosis in esophageal cancer cells by restoring 15-lipoxygenase-1 expression. Cancer Res *61*, 4879-4884.

524. Wu, J., Xia, H.H., Tu, S.P., Fan, D.M., Lin, M.C., Kung, H.F., Lam, S.K., and Wong, B.C. (2003). 15-Lipoxygenase-1 mediates cyclooxygenase-2 inhibitor-induced apoptosis in gastric cancer. Carcinogenesis *24*, 243-247.
525. Philips, B.J., Dhir, R., Hutzley, J., Sen, M., and Kelavkar, U.P. (2008). Polyunsaturated fatty acid metabolizing 15-Lipoxygenase-1 (15-LO-1) expression in normal and tumorigenic human bladder tissues. Appl Immunohistochem Mol Morphol *16*, 159-164.
526. Hennig, R., Kehl, T., Noor, S., Ding, X.Z., Rao, S.M., Bergmann, F., Furstenberger, G., Buchler, M.W., Friess, H., Krieg, P., and Adrian, T.E. (2007). 15-lipoxygenase-1 production is lost in pancreatic cancer and overexpression of the gene inhibits tumor cell growth. Neoplasia *9*, 917-926.
527. Jiang, W.G., Watkins, G., Douglas-Jones, A., and Mansel, R.E. (2006). Reduction of isoforms of 15-lipoxygenase (15-LOX)-1 and 15-LOX-2 in human breast cancer. Prostaglandins Leukot Essent Fatty Acids *74*, 235-245.
528. Viita, H., Pacholska, A., Ahmad, F., Tietavainen, J., Naarala, J., Hyvarinen, A., Wirth, T., and Yla-Herttuala, S. 15-lipoxygenase-1 induces lipid peroxidation and apoptosis, and improves survival in rat malignant glioma. In Vivo *26*, 1-8.
529. Spraggon, G., Phillips, C., Nowak, U.K., Ponting, C.P., Saunders, D., Dobson, C.M., Stuart, D.I., and Jones, E.Y. (1995). The crystal structure of the catalytic domain of human urokinase-type plasminogen activator. Structure *3*, 681-691.
530. McColl, B.K., Baldwin, M.E., Roufail, S., Freeman, C., Moritz, R.L., Simpson, R.J., Alitalo, K., Stacker, S.A., and Achen, M.G. (2003). Plasmin activates the lymphangiogenic growth factors VEGF-C and VEGF-D. J Exp Med *198*, 863-868.
531. Li, Q., Laumonnier, Y., Syrovets, T., and Simmet, T. (2007). Plasmin triggers cytokine induction in human monocyte-derived macrophages. Arterioscler Thromb Vasc Biol *27*, 1383-1389.
532. Deryugina, E.I., and Quigley, J.P. Cell surface remodeling by plasmin: a new function for an old enzyme. J Biomed Biotechnol *2012*, 564259.
533. Wolberg, A.S. Determinants of fibrin formation, structure, and function. Curr Opin Hematol *19*, 349-356.
534. Sahores, M., Prinetti, A., Chiabrando, G., Blasi, F., and Sonnino, S. (2008). uPA binding increases UPAR localization to lipid rafts and modifies the receptor microdomain composition. Biochim Biophys Acta *1778*, 250-259.
535. Myohanen, H., and Vaheri, A. (2004). Regulation and interactions in the activation of cell-associated plasminogen. Cell Mol Life Sci *61*, 2840-2858.
536. Chorostowska-Wynimko, J., Skrzypczak-Jankun, E., and Jankun, J. (2004). Plasminogen activator inhibitor type-1: its structure, biological activity and role in tumorigenesis (Review). Int J Mol Med *13*, 759-766.
537. Milella, M., Kornblau, S.M., Estrov, Z., Carter, B.Z., Lapillonne, H., Harris, D., Konopleva, M., Zhao, S., Estey, E., and Andreeff, M. (2001). Therapeutic targeting of the MEK/MAPK signal transduction module in acute myeloid leukemia. J Clin Invest *108*, 851-859.
538. Stepan, V., Pausawasdi, N., Ramamoorthy, S., and Todisco, A. (2004). The Akt and MAPK signal-transduction pathways regulate growth factor actions in isolated gastric parietal cells. Gastroenterology *127*, 1150-1161.
539. Johnson, G.L., and Lapadat, R. (2002). Mitogen-activated protein kinase pathways mediated by ERK, JNK, and p38 protein kinases. Science *298*, 1911-1912.

540. Cargnello, M., and Roux, P.P. Activation and function of the MAPKs and their substrates, the MAPK-activated protein kinases. Microbiol Mol Biol Rev *75*, 50-83.
541. Santarpia, L., Lippman, S.M., and El-Naggar, A.K. Targeting the MAPK-RAS-RAF signaling pathway in cancer therapy. Expert Opin Ther Targets *16*, 103-119.
542. Zhu, C., Qi, X., Chen, Y., Sun, B., Dai, Y., and Gu, Y. PI3K/Akt and MAPK/ERK1/2 signaling pathways are involved in IGF-1-induced VEGF-C upregulation in breast cancer. J Cancer Res Clin Oncol *137*, 1587-1594.
543. Roberts, P.J., and Der, C.J. (2007). Targeting the Raf-MEK-ERK mitogen-activated protein kinase cascade for the treatment of cancer. Oncogene *26*, 3291-3310.
544. Sabapathy, K. Role of the JNK pathway in human diseases. Prog Mol Biol Transl Sci *106*, 145-169.
545. Bradham, C., and McClay, D.R. (2006). p38 MAPK in development and cancer. Cell Cycle *5*, 824-828.
546. Wagner, E.F., and Nebreda, A.R. (2009). Signal integration by JNK and p38 MAPK pathways in cancer development. Nat Rev Cancer *9*, 537-549.
547. Friday, B.B., and Adjei, A.A. (2008). Advances in targeting the Ras/Raf/MEK/Erk mitogen-activated protein kinase cascade with MEK inhibitors for cancer therapy. Clin Cancer Res *14*, 342-346.
548. Zhou, S., Liu, R., Yuan, K., Yi, T., Zhao, X., Huang, C., and Wei, Y. Proteomics analysis of tumor microenvironment: Implications of metabolic and oxidative stresses in tumorigenesis. Mass Spectrom Rev.
549. Gupta, S.C., Hevia, D., Patchva, S., Park, B., Koh, W., and Aggarwal, B.B. Upsides and downsides of reactive oxygen species for cancer: the roles of reactive oxygen species in tumorigenesis, prevention, and therapy. Antioxid Redox Signal *16*, 1295-1322.
550. Kiguchi, T., Niiya, K., Shibakura, M., Miyazono, T., Shinagawa, K., Ishimaru, F., Kiura, K., Ikeda, K., Nakata, Y., and Harada, M. (2001). Induction of urokinase-type plasminogen activator by the anthracycline antibiotic in human RC-K8 lymphoma and H69 lung-carcinoma cells. Int J Cancer *93*, 792-797.
551. Valko, M., Rhodes, C.J., Moncol, J., Izakovic, M., and Mazur, M. (2006). Free radicals, metals and antioxidants in oxidative stress-induced cancer. Chem Biol Interact *160*, 1-40.
552. Cecchi, F., Rabe, D.C., and Bottaro, D.P. Targeting the HGF/Met signaling pathway in cancer therapy. Expert Opin Ther Targets *16*, 553-572.
553. Lee, K.H., and Kim, J.R. (2009). Reactive oxygen species regulate the generation of urokinase plasminogen activator in human hepatoma cells via MAPK pathways after treatment with hepatocyte growth factor. Exp Mol Med *41*, 180-188.
554. Choong, P.F., and Nadesapillai, A.P. (2003). Urokinase plasminogen activator system: a multifunctional role in tumor progression and metastasis. Clin Orthop Relat Res, S46-58.
555. Li, Y., and Cozzi, P.J. (2007). Targeting uPA/uPAR in prostate cancer. Cancer Treat Rev *33*, 521-527.
556. Blecha, J.E., Anderson, M.O., Chow, J.M., Guevarra, C.C., Pender, C., Penaranda, C., Zavodovskaya, M., Youngren, J.F., and Berkman, C.E. (2007). Inhibition of IGF-1R and lipoxygenase by nordihydroguaiaretic acid (NDGA) analogs. Bioorg Med Chem Lett *17*, 4026-4029.
557. Stavniichuk, R., Shevalye, H., Hirooka, H., Nadler, J.L., and Obrosova, I.G. Interplay of sorbitol pathway of glucose metabolism, 12/15-lipoxygenase, and mitogen-activated

protein kinases in the pathogenesis of diabetic peripheral neuropathy. Biochem Pharmacol *83*, 932-940.
558. Kelavkar, U.P., and Cohen, C. (2004). 15-lipoxygenase-1 expression upregulates and activates insulin-like growth factor-1 receptor in prostate cancer cells. Neoplasia *6*, 41-52.
559. Lee, K.H., Kim, S.W., and Kim, J.R. (2009). Reactive oxygen species regulate urokinase plasminogen activator expression and cell invasion via mitogen-activated protein kinase pathways after treatment with hepatocyte growth factor in stomach cancer cells. J Exp Clin Cancer Res *28*, 73.
560. Kyriakis, J.M., and Avruch, J. Mammalian MAPK signal transduction pathways activated by stress and inflammation: a 10-year update. Physiol Rev *92*, 689-737.
561. Yun, M.R., Park, H.M., Seo, K.W., Lee, S.J., Im, D.S., and Kim, C.D. 5-Lipoxygenase plays an essential role in 4-HNE-enhanced ROS production in murine macrophages via activation of NADPH oxidase. Free Radic Res *44*, 742-750.
562. Amir, M., Liu, K., Zhao, E., and Czaja, M.J. Distinct functions of JNK and C-Jun in oxidant-induced hepatocyte death. J Cell Biochem.
563. Hung, S.H., Shen, K.H., Wu, C.H., Liu, C.L., and Shih, Y.W. (2009). Alpha-mangostin suppresses PC-3 human prostate carcinoma cell metastasis by inhibiting matrix metalloproteinase-2/9 and urokinase-plasminogen expression through the JNK signaling pathway. J Agric Food Chem *57*, 1291-1298.
564. Nie, D., Nemeth, J., Qiao, Y., Zacharek, A., Li, L., Hanna, K., Tang, K., Hillman, G.G., Cher, M.L., Grignon, D.J., and Honn, K.V. (2003). Increased metastatic potential in human prostate carcinoma cells by overexpression of arachidonate 12-lipoxygenase. Clin Exp Metastasis *20*, 657-663.
565. Lu, J.M., Nurko, J., Weakley, S.M., Jiang, J., Kougias, P., Lin, P.H., Yao, Q., and Chen, C. Molecular mechanisms and clinical applications of nordihydroguaiaretic acid (NDGA) and its derivatives: an update. Med Sci Monit *16*, RA93-100.
566. Bocan, T.M., Rosebury, W.S., Mueller, S.B., Kuchera, S., Welch, K., Daugherty, A., and Cornicelli, J.A. (1998). A specific 15-lipoxygenase inhibitor limits the progression and monocyte-macrophage enrichment of hypercholesterolemia-induced atherosclerosis in the rabbit. Atherosclerosis *136*, 203-216.